

**ASSESSMENT OF HYDRO-MORPHOLOGICAL RESPONSE OF SELECTED
REACH OF THE JAMUNA RIVER DUE TO STRUCTURAL INTERVENTION
USING DELFT3D MODEL**

MD. ZAKIR HASAN

Student No.: 0412162004P



DEPARTMENT OF WATER RESOURCES ENGINEERING
BANGLADESH UNIVERSITY OF ENGINEERING AND TECHNOLOGY
(BUET)

Dhaka, Bangladesh

September, 2018

**ASSESSMENT OF HYDRO-MORPHOLOGICAL RESPONSE OF SELECTED
REACH OF THE JAMUNA RIVER DUE TO STRUCTURAL INTERVENTION
USING DELFT3D MODEL**



A THESIS SUBMITTED TO THE DEPARTMENT OF WATER RESOURCES
ENGINEERING IN PARTIAL FULFILLMENT OF THE REQUIREMENTS FOR THE
DEGREE OF **MASTER OF SCIENCE IN WATER RESOURCES ENGINEERING**

SUBMITTED BY

MD. ZAKIR HASAN

DEPARTMENT OF WATER RESOURCES ENGINEERING
BANGLADESH UNIVERSITY OF ENGINEERING AND TECHNOLOGY
(BUET)

Dhaka, Bangladesh

September, 2018

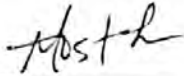
CERTIFICATION OF APPROVAL

We hereby recommended that the M.Sc. Engg. Research work presented by Md. Zakir Hasan, Roll No. 0412162004 (P), Session: April 2012, entitled “**Assessment of Hydro-Morphological Response of Selected Reach of the Jamuna River due to Structural Intervention Using Delft3D Model**” has been accepted as satisfactory in partial fulfillment of the requirements for the degree Master of Science in Water Resources Engineering on 30th September 2018.



Dr. Md. Abdul Matin
Professor
Department of Water Resources Engineering, BUET
Dhaka-1000, Bangladesh

Chairman of the Committee
(Supervisor)



Dr. Md. Mostofa Ali
Professor & Head
Department of Water Resources Engineering, BUET
Dhaka-1000, Bangladesh

Member



Dr. A.T.M Hasan Zobeyer
Associate Professor
Department of Water Resources Engineering, BUET
Dhaka-1000, Bangladesh

Member



Dr. Faruq Ahmed Mohiuddin
Senior Water Resources Specialist
Institute of Water Modelling (IWM)
Dhaka-1206, Bangladesh

Member
(External)

DECLARATION

This is to certify that this project entitled “**Assessment of Hydro-Morphological Response of Selected Reach of the Jamuna River due to Structural Intervention using Delft3d Model**” has been done by me under the supervision of Dr. Md. Abdul Matin, Professor, Department of Water Resources Engineering, Bangladesh University of Engineering and Technology, Dhaka. I do hereby declare that this project or any part of it has not been accepted elsewhere for the award of any degree or diploma from any other institution.

Signature of the candidate

Zakir Hasan

Md. Zakir Hasan

TABLE OF CONTENTS

	<i>Page No.</i>
<i>Certification of Approval</i>	<i>i</i>
<i>Declaration</i>	<i>ii</i>
<i>Table of Contents</i>	<i>iii</i>
<i>List of Figures</i>	<i>vii</i>
<i>List of Tables</i>	<i>x</i>
<i>List of Symbols</i>	<i>xi</i>
<i>List of Abbreviation</i>	<i>xii</i>
<i>Acknowledgement</i>	<i>xiii</i>
<i>Abstract</i>	<i>xiv</i>
CHAPTER 1: INTRODUCTION	1
1.1 General	1
1.2 Background of the Study	1
1.3 Objectives of the Study	3
1.4 Structure of the Thesis	3
CHAPTER 2: LITERATURE REVIEW	4
2.1 General	4
2.2 River Bank Erosion	4
2.3 Sediment Transport	5
2.4 Previous Studies on Hydro-Morphology of the Jamuna River	5
2.5 Previous Studies on Structural Intervention in a River	10
2.6 Previous Studies on Mathematical Modelling	11
2.7 Previous Studies on Delft3D Model	13
2.8 Study Area	15
2.8.1 The Jamuna River System	17
2.8.2 Source and Course of the River	17
2.8.3 Catchment Characteristics	18
2.8.4 Topography of the Catchment Area	19
2.8.5 Sediment Characteristics	20
2.8.6 Hydraulic Characteristics of the Jamuna	20

CHAPTER 3: THEORETICAL BACKGROUND	22
3.1 General	22
3.2 Hydrodynamics of a River	22
3.3 Morphology of a River	23
3.4 Structural Intervention in a River	24
3.4.1 Marginal Embankments/Levees	24
3.4.2 Guide Bank	25
3.4.3 Revetments	25
3.4.4 Groynes/Spurs	26
3.4.4.1 Length of Groynes/Spurs (L_g)	27
3.4.4.2 Spacing between Groynes/Spurs (S_g)	27
3.5 Structural Intervention in the Jamuna River	28
3.5.1 Groynes/Spurs	28
3.5.2 Revetments and Hard points	29
3.6 River Response	32
3.6.1 River Responses Type	32
3.6.2 Qualitative Response	33
3.7 Mathematical Modeling	34
3.8 Delft3D Model	35
3.8.1 Numerical Aspects of Delft3D-FLOW	35
3.8.1.1 Staggered grid	36
3.8.1.2 Definition of model boundaries	37
3.8.2 Hydrodynamic equations	38
3.8.2.1 The σ co-ordinate system	39
3.8.2.2 Cartesian co-ordinate system in the vertical (Z-model)	40
3.8.2.3 Continuity equation	41
3.8.2.4 Momentum equations in horizontal direction	42
3.8.2.5 Vertical velocities	43
3.8.3 Transport equations	43
CHAPTER 4: DATA COLLECTION AND METHODOLOGY	46
4.1 General	46
4.2 Work Analysis and Preparing Work Plan	46
4.3 Data Collection	48

4.3.1 Hydrometric Data	48
4.3.2 Bathymetric Data	50
4.3.3 Satellite Image	51
4.3.4 Sediment Data	51
4.3.5 Field Visit and Bed Sample Collection	52
4.4 Methodology	54
4.5 Model Setup	54
4.5.1 RGFGRID	56
4.5.2 QUICKIN	56
4.5.3 QUICKPLOT	57
4.5.4 Dry Points	58
4.5.5 Thin Dams	58
4.5.6 Modeling Framework	59
4.5.7 Space and Time Variation	60
4.5.8 Model Stability Check, Calibration and Validation	60
4.5.9 Different Option Simulation	61
4.5.10 Data Extraction	62
CHAPTER 5: MODEL SET UP FOR SELECTED REACH OF THE JAMUNA RIVER	63
5.1 General	63
5.2 Model Setup for Selected Reach of the Jamuna River	63
5.2.1 Grid Generation	64
5.2.2 Bathymetry	64
5.2.3 Boundary Conditions	65
5.2.4 Additional Parameters	68
5.2.5 Model Calibration	68
5.2.6 Model Validation	70
5.2.7 Morphological Calibration of the Model	71
5.2.8 Comparison of Simulated Water Level between MIKE21C and Delft3D	74
5.2.9 Model Stability Analysis	75
5.3 Model Simulation with Different Options	75
CHAPTER 6: RESULTS AND DISCUSSIONS	86
6.1 General	86
6.2 Observation of Hydrodynamic Parameters	86

6.2.1 Velocity Vectors	88
6.2.2 Depth Averaged Velocity	93
6.2.2.1 Bank Line Velocity	98
6.2.3 Bed Shear Stress	99
6.2.3.1 Bank Line Bed Shear Stress	101
6.3 Observation of Morphologic parameters	102
6.3.1 Cumulative Erosion/Deposition Curves	103
6.3.2 Bed Level Variation at Different Locations	106
6.3.2.1 Bed Level Variation across the River for Option 2	108
6.3.2.2 Bed Level Variation along the River for Option 2	110
6.3.2.3 Bed Level Variation across the River for Option 4 and Option 6	112
6.3.2.4 Bed Level Variation along the River for Option 4 and Option 6	113
6.4 Summary of the Results	115
CHAPTER 7: CONCLUSIONS AND RECOMMENDATIONS	119
7.1 General	119
7.2 Conclusions	119
7.3 Recommendations for Further Study	120
REFERENCES	121
APPENDIX-A: Model output for different parameters	
APPENDIX-B: Model simulated cross-sections at different locations	
APPENDIX-C: Model output in tabular forms for various option simulations	

LIST OF FIGURES

Figure 2.1: Study area along the Jamuna River (Source: CEGIS, 2012)	16
Figure 2.2: Brahmaputra-Jamuna River System within Bangladesh Territory	19
Figure 3.1: River Classification by Brice	24
Figure 3.2: Typical cross-sections of levees for different heights	25
Figure 3.3: Components of a revetment on riverbank	26
Figure 3.4: Types of groynes based on alignment	27
Figure 3.5: Permeable groune for Jamuna Bank protection At Kamarjani (FAP21/22)	29
Figure 3.6: Permeable groune for Jamuna Bank protection At Kamarjani	30
Figure 3.7: Lane’s balance (Source: Sarker, 2008)	34
Figure 3.8: Example of a grid in Delft3D-FLOW	36
Figure 3.9: Mapping of physical space to computational space	36
Figure 3.10: Grid staggering, 3D view (left) and top view (right)	37
Figure 3.11: Example of Delft3D model area	38
Figure 3.12: Definition of water level (ζ), depth (h) and total depth (H)	40
Figure 3.13: Example of σ - and Z -grid	41
Figure 4.1: Flow chart showing the entire methodology	47
Figure 4.2: Historical water level data at Sirajganj hard point	49
Figure 4.3: Historical discharge hydrographs at Bahadurabad station	50
Figure 4.4: Bathymetric data of 50 km reach of the Jamuna River	51
Figure 4.5: Grain size distribution of sample 1	52
Figure 4.6: Grain size distribution of sample 2	52
Figure 4.7: Hjulströms diagram (Hjulström, 1935)	53
Figure 4.8: Title window of Delft3D	55
Figure 4.9: Graphic User Interface (GUI) of Delft3D	55
Figure 4.10: RGFGRID and QUICKIN window	57
Figure 4.11: Structure of Delft3D	57
Figure 4.12: Sub-data group Dry points	58
Figure 4.13: Equivalence of v-type thin dams (left) and u-type thin dams (right) with the same grid indices, (M 1 to M+1, N)	59
Figure 5.1: Computational Grid cell of Jamuna River in the study area	64
Figure 5.2: Model bathymetry of Jamuna River in the study area	65
Figure 5.3: Upstream and downstream boundaries of the model	66
Figure 5.4: Flow conditions applied at upstream boundary of the model	67
Figure 5.5: Downstream water level boundary for the model	67
Figure 5.6: Comparison of model simulated and observed water levels of Jamuna River at Sirajganj for different ‘n’.	69
Figure 5.7: Comparison of model simulated and observed water levels of Jamuna River at Sirajganj for the monsoon of 2012	69
Figure 5.8: Calibration of the model at Bangabandhu Bridge site for water level	70
Figure 5.9: Validation of the model simulated and observed water level data at Sirajganj for the year 2013	71
Figure 5.10: Flow discharge vs. observed sediment discharge graph at Bahadurabad	72
Figure 5.11: Flow discharge vs. simulated sediment discharge graph at Sirajganj	72
Figure 5.12: Comparison of cross-sections at SHP for pre-monsoon 2011 with diffusivity 1	73
Figure 5.13: Comparison of cross-sections at SHP for pre-monsoon 2011 with diffusivity 5	73
Figure 5.14: Comparison of cross-sections at SHP for pre-monsoon 2011 with diffusivity 10	73

Figure 5.15: Comparison of simulated WL data between MIKE21C and Delft3D in 2012 at Sirajganj	74
Figure 5.16: Erosion prone areas at the right bank of the Jamuna River	76
Figure 5.17: Base (without any structure)	78
Figure 5.18: Option 1 (Single groyne)	79
Figure 5.19: Option 2 (2 groynes with S/L ratio 1.0)	80
Figure 5.20: Option 3 (2 groynes with S/L ratio 1.5)	81
Figure 5.21: Option 4 (2 groyne with S/L ratio 2.0)	82
Figure 5.22: Option 5 (3 groyne with S/L ratio 1.0)	83
Figure 5.23: Option 6 (3 groyne with S/L ratio 1.5)	84
Figure 5.24: Option 7 (3 groyne with S/L ratio 2.0)	85
Figure 6.1: Water level at different dates for 2 groynes with S/L = 1.5	86
Figure 6.2: Depth averaged velocities at different dates for 2 groynes with S/L = 1.5	87
Figure 6.3: Bed shear stress at different dates for 2 groynes with S/L = 1.5	87
Figure 6.4: Velocity vectors from model output for (a) Base, (b) Option 1, (c) Option 2, (d) Option 3, (e) option 4, (f) Option 5, (g) Option 6 and (h) Option 7	92
Figure 6.5: Relative comparison of velocity variation at groyne u/s for different options	94
Figure 6.6: Relative comparison of velocity variation at groyne d/s for different options	94
Figure 6.7: Relative comparison of velocity variation at groyne SHP for different options	95
Figure 6.8: Relative comparison of velocity variation at groyne BBS for different options	95
Figure 6.9: Comparison of velocity with base at the u/s of 1 st groyne for option 2	96
Figure 6.10: Comparison of velocity with base at the d/s of 1 st groyne for option 2	96
Figure 6.11: Comparison of velocity with base at the u/s of 2 nd groyne for option 2	97
Figure 6.12: Comparison of velocity with base at the d/s of 2 nd groyne for option 2	97
Figure 6.13: Comparison of bank line velocities for different spacing of groynes	98
Figure 6.14: Relative comparison of bed shear stress at groyne u/s for different options	99
Figure 6.15: Relative comparison of bed shear stress at groyne d/s for different options	99
Figure 6.16: Relative comparison of bed shear stress at groyne SHP for different options	100
Figure 6.17: Relative comparison of bed shear stress at groyne BBS for different options	100
Figure 6.18: Comparison of bed shear stress along the bank line for different spacing of groynes	101
Figure 6.19: Cum. erosion/sedimentation at different dates for 2 groynes with S/L = 1.5	102
Figure 6.20: Total transport at different dates for 2 groynes with S/L = 1.5	102
Figure 6.21: Relative comparison of cum. erosion/deposition at groyne u/s for different options	104
Figure 6.22: Relative comparison of cum. erosion/deposition at groyne d/s for different options	104
Figure 6.23: Relative comparison of cum. erosion/deposition at groyne SHP for different options	105
Figure 6.24: Relative comparison of cum. erosion/deposition at groyne BBS for different options	105
Figure 6.25: Cross-section locations to observe bed level variation across and along the river for option 2	106
Figure 6.26: Cross-section locations to observe bed level variation across and along the river for option 4 and 6	107
Figure 6.27: Bed level variation along the 1 st groyne with respect to base for option 2 (Section a-a)	108
Figure 6.28: Bed level variation along the 2 nd groyne with respect to base for option 2 (Section c-c)	109
Figure 6.29: Bed level variation between the 1 st and 2 nd groyne with respect to base for option 2, option 3 and option 4 (Section b-b)	109
Figure 6.30: Bed level variation along the river in front of the nose of the groynes with respect to base for Option 2 (S/L = 1.0) (Section 1-1)	110
Figure 6.31: Bed level variation along the river in front of the nose of the groynes with respect to base for Option 4 (S/L=2.0) (Section 1-1)	111

Figure 6.32: Bed level variation between the 1 st and 2 nd groyne with respect to base for option 4 (Section a-a)	112
Figure 6.33: Bed level variation between the 2 nd and 3 rd groyne with respect to base for option 6 (Section a-a)	112
Figure 6.34: Bed level variation along the river in front of the nose of the groynes with respect to base for Option 4 (2 groynes with S/L = 2.0) (Section 1-1)	113
Figure 6.35: Bed level variation along the river along the nose of the groynes with respect to base for Option 6 (3 groynes with S/L = 1.5) (Section 1-1)	113
Figure 6.36: Bed level variation along the river in front of the nose of the groynes with respect to base for Option 6 (3 groynes with S/L = 1.5) (Section 1-1)	114

LIST OF TABLES

Table 2.1: Summary of hydraulic characteristics of the Jamuna River	21
Table 3.1: List of various structural intervention in Brahmaputra/Jumna and the present status	31
Table 4.1: Available Water Level & Discharge Data	48
Table 4.2: Status of collected sediment data of the Jamuna River	51
Table 4.3: Simulation of the model with different options	61
Table 5.1: Summary of the parameters used for the model of Jamuna River	68
Table 5.2: Stability analysis results of the model	75
Table 5.3: Description of the simulation options	77
Table 6.1: Change of parameters with respect to base condition at u/s for various options (July)	116
Table 6.2: Change of parameters with respect to base condition at d/s for various options (July)	116
Table 6.3: Change of parameters with respect to base condition at SHP for various options (July)	117
Table 6.4: Change of parameters with respect to base condition at BBS for various options (July)	117
Table 6.5: Monthly variation of cum. erosion/deposition at different locations for all the options	118

LIST OF SYMBOLS

d_{50}	Size of bed material load
F_x	Horizontal stress
F_y	Vertical stress
g	Acceleration due to gravity
H	Water level
HFL	High flood level
h	Water depth
i	Channel slope
L	Length of groyne
n	Manning's roughness coefficient
P_x	Horizontal pressure
P_y	Vertical pressure
Q	Discharge
Q_s	Sediment discharge
S	Spacing of groynes
SHW	Shallow water
U	Horizontal component of velocity
V	Vertical component of velocity
x, y	Cartesian coordinate system
z	Bed level
ρ	Density of water
ν_v	Eddy viscosity

LIST OF ABBREVIATIONS

ADCP	Acoustic Doppler Current Profiler
BBS	Bangabandhu Bridge Site
BIWTA	Bangladesh Inland Water transport Authority
BWDB	Bangladesh Water Development Board
CEGIS	Center for Environment and Geographic Information Services
Delft 3D	Three-dimensional model developed by Delft hydraulics
DHI	Danish Hydraulic Institute
D/S	Downstream
FAP	Flood Action Plan
GBM	Ganges Brahmaputra Meghna
GUI	Graphic User Interface
HEC-RAS	Hydraulic Engineering Center- River Analysis System
IWM	Institute of Water Modelling
MIKE 21C	Two-dimensional One Layer Curvilinear Model Develop by MIKE ABBOTT
PWD	Public Works Department
SHP	Sirajganj Hard Point
U/S	Upstream
WARPO	Water Resources Planning Organization

ACKNOWLEDGEMENT

All praises are due to the Almighty Allah who has provided me with the opportunity to complete this research.

The author acknowledges his deepest gratitude to his supervisor Dr. Md. Abdul Matin, Professor, Department of Water Resources Engineering, BUET for providing me such an interesting idea for the thesis work and encouraging working with it. His cordial supervision, valuable suggestion and unfailing eagerness made the study to a successful work.

The author is also grateful to Dr. Mostofa Ali, Professor & Head, Department of Water Resources Engineering, BUET, Dr. A.T.M Hasan Zobeyer, Associate Professor, Department of Water Resources Engineering, BUET and Dr. Faruq Ahmed Mohiuddin, Senior Water Resources Specialist, IWM, who were the members of the board of examiners. Their valuable comments on this thesis are duly acknowledged.

The author would like to thank his family members for their encouragement and inspiration. The author is grateful for their guidance and blessings. Without their help and support and sacrifice the author wouldn't have finished his M.Sc. Engg.

The author is very much thankful to Mr. Tanvir Ahmed, M.Sc. student, IHE, Netherlands for his help and support to do this work. The author is pleased to Md. Musfequzzaman, Associate Specialist, IWM and Shampa, PhD student, Kyoto University, Japan for their inspiration and support.

The author is indebted to Institute of Water Modelling (IWM), Center for Environmental and Geographic Information Services (CEGIS) and officials of Bangladesh Water Development Board (BWDB) Sirajganj, for providing necessary information and data to carry out this research work.

Md. Zakir Hasan
September 2018

ABSTRACT

In this study, an attempt has been made to analyze the hydro-morphological responses of the Jamuna River due to structural intervention in a selected reach by preparing a morphological model. The study reach covers from 30 km upstream of Bangabandhu Bridge (BB) to 20 km downstream of this bridge. A two-dimensional mathematical model has been developed using Delft3D and studied various options with structural intervention of groyne(s) along a selected reach in the right bank of the Jamuna River at the upstream of Sirajganj Hard Point (SHP). The model has been calibrated and validated against the data for the year 2012 and 2013 respectively. Then simulations have been done with seven different options consist of groynes with various number and spacing. The length of the groynes have been selected as about one-fourth of the channel width. The spacing and length ratio (S/L) of the groynes have been set as 1.0, 1.5 and 2.0 respectively for the option simulations. In order to quantify the response of the river hydrodynamics and morphology for various options at different locations, model results for the month of July have been assessed. All the model output have been presented and discussed. For the purpose of discussion and interpretation of model output, four points as the upstream of the structure (u/s), downstream of the structure (d/s), Sirajganj Hard Point (SHP) and Bangabandhu Bridge Site (BBS) have been taken into consideration. Model results show that at the upstream of the selected intervention, water level increases about 10.84% and for the downstream is 6.72%. This rise of water level may be for the afflux effect due to the structural intervention(s). The velocity and bed shear stress show decreasing tendency around the structures which indicates the attainment of siltation zone. The effects are considerable at the upstream and downstream of the groyne(s) and for the other two points (e.g. Sirajganj Hard Point and Bangabandhu Bridge Site) the effect is very little due to the long distance. From the velocity vectors and bank line velocities as well as bed shear stress, it can be decided that for this specific reach of the river, the maximum allowable spacing between the groynes is 2.0 times of its length. Otherwise the bank will be in vulnerable condition due to erosion. The bed level variation surrounding the groynes is considerable. The effect of groyne extends up to 1 km inside the river and 2 km laterally

from either nose of the groyne. The maximum erosion is -5.25 m and deposition is +3.70 m along the length of the groyne. In case of lateral section (along the river) the values are -6.0 m and +4.0 m respectively.

For the structures, the near bank velocity and bed shear stress become very small with the increasing number of intervention. Thus it can be said that to prevent the bank erosion, this types of structures with increasing numbers and different spacing provides satisfactory results. Overall, the model results show that it has the capacity to assess the hydro-morphological river responses for various options particularly at the vicinity of the interventions.

CHAPTER 1

INTRODUCTION

1.1 General

Structural intervention in a river is a major part of river training and bank protection. Being one of the most vital rivers in Bangladesh, the Jamuna experiences severe bed and bank erosion every year. Sometimes, steps are taken to prevent such type of troubles but in many cases the projects fail for the unpredictable behavior of the Jamuna River. To address the problems two-dimensional hydrodynamic and morphological model is being used as a functional tool now a days. Delft3D is such type of modeling software to analyze river responses at different conditions. In this study, analysis of the selected erosion prone reach of the Jamuna River has been done with structural intervention like groynes and compare the results with the free flow condition. Thus relationship among different hydrodynamic and morphological parameters have been established for different conditions that might help the planners, engineers and implementing authorities in future to work on the Jamuna River.

1.2 Background of the Study

The Jamuna River in Bangladesh is one of the world's largest and most geomorphologically active braided alluvial rivers (Mosselman, 2006). The length of the Jamuna is about 2900 km originated from the Himalayas and has a drainage area of 573,500 km². The length of the river is almost 240 km inside of Bangladesh. The overall width of the River varies spatially and temporally, from 6 to 14 km. There exists different types of channel within the overall width of the river (Rahman, Mahmud and Uddin, 2012). Movement of bars and branches (Schuurman, Kleinhans and Middelkoop, 2016), river bank erosion, bank lines shifting in the scale of several hundred meters to a few kilometers in a year is common in the river (Ahmed and Hasan, 2011). Main channels in this river shift from one side to another thus experience bed level changes over the period. The bed level changes over a year can be several meters locally. On the other hand, main stream flows along the river bank in many locations that generates excess near bank velocity, which causes seasonal bank erosion for particular locations (Musfequzzaman, 2012). Bank erosion in the Jamuna River is one of the major problems in Bangladesh. Thousands of people become homeless every year and they lose their

homestead and croplands. Mosques, schools, hospitals and other infrastructures are damaged due to erosion into the mighty Jamuna River (Urmilaz, 2012). The west bank of the Jamuna River commonly known as Brahmaputra Right Embankment (BRE) is most vulnerable to this kind of problem. Moreover, Bangabandhu multipurpose bridge, the most vital bridge in Bangladesh is situated in the Jamuna River. In addition, Sirajganj district town with some industrial area is situated beside the Jamuna River. So the vulnerability of the bank of the Jamuna River is a major concern in the country as it is related to different social and economic activities of great worth. That's why training of the Jamuna River always gets priority to the implementing authority like Bangladesh Water Development Board (BWDB), Bangladesh Inland Water Transport Authority (BIWTA) to protect the river banks and river bed also. Many river training structures like gabions, submerged vanes, hard points and groynes have been used to protect the river banks especially at river bends (FAP21/22, 2001; Abbas, B. G., Mojtaba, 2009). Different pre and post studies and analyses have been done to sustain the right bank of the Jamuna. Various types of physical and mathematical model studies have been being done in relation to academic and professional purposes.

In the recent years, mathematical models have been increasingly used including hydrodynamics, sediment transport and morphological processes in different types of rivers (Dargahi, 2004; Nicholas, 2013; Yang, Lin and Zhou, 2015) since the physical model study is expensive and time consuming also. Several researches like assessment of river hydrodynamics and morphology (Urmilaz, 2012; Roy, 2015), impact of river dredging (Musfequzzaman, 2012; Alam and Matin, 2013) have been done using the modeling tool. However, study on river analysis with structural intervention using model is limited.

In this study, assessment has been done for change in the hydrometric parameters as well as morphologic scenarios for the selected reach of the Jamuna River due to transverse structures (groynes/cross bars) using a two-dimensional hydrodynamic model. Single and series of transverse structures have been placed in the erosion prone areas at different spacing along the right bank of the Jamuna River and model has been simulated using Delft3D model to observe the impact at bed and bank of the river as well as the adjacent Sirajganj town.

1.3 Objectives of the Study

The objectives of the study are as follows:

- i. To set up a two-dimensional hydrodynamic model with Delft3D for 50 km reach of the Jamuna River
- ii. To assess the hydrodynamic response of the river for different inflow conditions for structural interventions (groynes/cross bars) in right bank of the river
- iii. To analyze the response of river bed under study due to structural intervention (groynes/cross bars)

1.4 Structure of the Thesis

The thesis has been organized under seven chapters. Chapter 1 describes the background and objectives of the study. Chapter 2 describes different definition of relevant topics, literatures, previous studies related to this study. Chapter 3 describes theoretical background of tools used in this thesis work. Chapter 4 describes the data collection and its processing followed by data analysis and also methodology of the thesis. Chapter 5 illustrates the model set up for the study area. Chapter 6 presents the results of the study from different points of view and few discussions of these results are also discussed. Chapter 7 states the concluding points and recommendations for further study.

CHAPTER 2

LITERATURE REVIEW

2.1 General

Bangladesh is dominated by three great rivers – the Brahmaputra-Jamuna, the Ganges and the Meghna – that combine to feed sediment into one of the World’s largest deltas in the Bay of Bengal (Best *et al.*, 2007). The Brahmaputra, one of the largest braided rivers in the world, originates from the Himalayas and enters Bangladesh at Kurigram as Jamuna. Though the history of the Jamuna is not more than 250 years, it shows severe changes in its course due to natural and anthropogenic influences (Urmilaz, 2012). Due to the unpredictability, training of this river for mankind is so tough. That’s why, a lot of studies and researches have been done related to the Jamuna River for different purposes. The summaries of different works and studies relevant to this study as well as some related terminologies has been discussed in the following articles.

2.2 River Bank Erosion

Riverbank erosion is an endemic and recurrent natural hazard. When rivers enter the mature stage they become sluggish and meander or braid. These oscillations cause massive riverbank erosion. The intensity of bank erosion varies widely from river to river as it depends on such characteristics as bank material, water level variations, nearbank flow velocities, planform of the river and the supply of water, sediment into the river and so on. For example, loosely packed, recently deposited bank materials, consisting of silt and fine sand, are highly susceptible to erosion. Rapid recession of floods accelerates the rates of bank erosion in such materials. Rivers belong to dynamic systems as they are continuously changing their way. Erosion and accretion is a natural process for any river. Though, sometimes erosion exceeds accretion and cause havoc in lives and livelihoods, mostly the poor society become the worst casualty. Riverbank erosion occurs both naturally and through human interference. The natural riverbank erosion process can produce favorable outcomes such as the formation of productive floodplains and alluvial terraces. Even stable rivers may have some amount of erosion. However, unstable rivers and the erosion that take place beyond normal range on

either bank is a serious concern. Environmental refugees are one of the most burning issues at this time all over the world (Hoque Mollah and Ferdaush, 2015).

2.3 Sediment Transport

Sediment transport is the movement of solid particles, typically due to a combination of the gravity force acting on the sediment, and/or the movement of the fluid in which the sediment is entrained. An understanding of sediment transport is typically used in natural systems, where the particles are clastic rocks (sand, gravel, boulders, etc.), mud, or clay. The fluid is air, water, or ice; and the force of gravity acts to move the particles due to the sloping surface on which they are resting. Sediment transport due to fluid motion occurs in rivers, the oceans, lakes, seas, and other water bodies, due to currents and tides; in glaciers as they flow, and on terrestrial surfaces under the influence of wind (Urmilaz, 2012). The ability of the channel to entrain and transport sediment depends on the balance between gravitational forces acting to settle particles on the bed and drag forces that act to either suspend them in the flow or shove them along downstream.

The dynamic problems of liquid-solid interaction are greatly influenced by the sediment properties. The description of the latter, however, is exceedingly complex and one is forced to make many simplifying assumptions. The first of which is the subdivision into cohesive and non-cohesive sediments. In cohesive sediments the resistance to erosion depends on the strength of the cohesive bond between the particles which may far outweigh the influence of the physical characteristics of individual particles. The problem of erosion resistance of cohesive soils is a very complex one and at present our understanding of the physics of it is very incomplete. The non-cohesive soils generally consist of larger discrete particles than cohesive soils and the movement of these particles depends on the physical properties of the individual particles, such as size, shape and density (Hassanzadeh, 2012).

2.4 Previous Studies on Hydro-Morphology of the Jamuna River

(Uddin and Rahman, 2012) Investigated the flow processes into the scour hole near a bank protection work. A revetment-like structure (hard point) was selected in the Jamuna River for that study. Acoustic Doppler Current Profiler (ADCP) was used to measure the hydraulic data into the scour hole. The measured hydraulic data was analyzed and represented by velocity vectors.

(Best *et al.*, 2003) worked with the three-dimensional subsurface alluvial architecture of a large (approximately 3 km long, 1 km wide, 12 m high), mid-channel sand braid bar in the Jamuna River, Bangladesh. Evolution of the bar and its depositional characteristics were assessed from a unique combination of ground-penetrating radar surveys, vibracoring, and trenching that were allied to a series of bathymetric surveys taken during growth of the bar over a 29-month period. The methodology permitted identification of the formative processes of different packages of braid-bar sedimentation and provided a facies model for deposition within the entire bar. Finally the authors suggested a scale invariance in several aspects of mid-channel bar sedimentation in sand-bed rivers and proposes a model of braid-bar sedimentation that may be applied widely within studies of braided alluvial architecture.

(Musfequzaman, 2012) investigated the river responses due to dredging on a selected reach of the Jamuna River by preparing a morphological model of this river. The study reaches was from 30 km upstream of Bangabandhu Bridge to 20 km downstream of this bridge. At first the two idealized test channels i.e. straight and meandering channels were modeled and the results were explored for better understanding the theoretical response of river due to dredging. The both idealized test channels were 15 km long and 1 km wide. The conveyance areas of these channels were kept similar to the channel in front of Sirajganj Hard Point. To setup these morphological models, MIKE21C, an advanced two-dimensional mathematical modelling software developed by DHI, was applied and numbers of simulations were conducted for different dredging conditions to fulfill the study objectives. From analyses, the author found in idealized test channels that with the increasing of dredging depth as well as with the dredging width, dimensionless velocity increases along the dredged channel and decreases along the bank. Similar incidences were observed also in Jamuna model that along the dredged channel the dimensionless velocity increases with the increase of relative dredging depth. It was also observed comparing the model results with Shield diagram that the bed materials along bank remain at the boundary of erosive and non-erosive zone during average velocity of Jamuna. With higher dredging depth condition, the velocity along bank decreases in such an amount so that it becomes lower than the critical velocity and the bank becomes non erosive zone. In Jamuna River, bed scour near Sirajganj Hardpoint decreases maximum 33.4% for 7 m of dredging depth and average rate of decreasing of bed scour is 5.5 % per meter of dredging depth. However, if dredging executed near Sirajganj Hardpoint, the channel became wider as the dredging depth increases. Finally, it was found that the bank erosion decreases

with the increasing of dredging depth. In some point the bank erosion decreases about 50m due to dredging.

(Urmilaz, 2012) Simulated the sediment transport rate at the river Jamuna and variation of bed level along the river using a two dimensional morphological model. Non-cohesive sediment transport module of Delft 3D Flow was used for the simulation. The upstream boundary of the model was taken at 30 km upstream of Bangabandhu Bridge and downstream boundary was taken at 20 km downstream of Bangabandhu Bridge. Simulation period was taken from April 2010 to December 2012. Simulation was carried out for hydrodynamic calibration and for sediment transport rates. The cross-sections were taken at the locations that are vulnerable, such as Subaghacha, Sirajganj, Jamuna Bridge and also in the upstream near Kazipur and downstream near Chauhali etc. In the Morphology tab, the morphological scale factor was set to 8.25 which extend the 121 days hydrodynamics to about 1000 days of morphological change. Calibration and validation were carried out against field observations (water level) of 2010 and 2011 respectively. Comparisons between simulated and observed water level were taken at the Sirajganj station. The results showed satisfactory agreement with observed values. For hydrodynamic and morphological computation, a time series discharge data was used at the upstream boundary and water level data as downstream boundary. Observed and simulated bed level elevation of 2010 was compared and the comparison showed a very good agreement. After calibration of the model, the net amount of erosion and deposition along the river reach was computed. Finally, cross-sectional variation of bottom level during the monsoon seasons from 2010 to 2012 was observed. Results revealed that erosion takes place in the channel bed and the deposition mainly takes place to the adjacent char areas and increased its width and area. It was also evident that the channel has been shifted westwards of the reach due to shifting of the bank line of the river. Many tributary and distributaries were appeared due to progressive erosion. In Sirajganj, the sediment transport capacity seemed to be the highest due to higher velocity of flow. The zones of higher velocity has higher sediment transport capacities therefore occurs more erosion.

(Ahmed and Hasan, 2011) observed the flow pattern around the Sirajganj Hard point setting up a 2D hydrodynamic model of 50 km river reach of the Jamuna (30 km upstream and 20 km downstream of Jamuna Bridge). The model was expanded to determine the scenario of inundation depth, inundation area and velocity of flood flow also. Satellite image analysis was also performed to determine plan form and bank line shifting of

the river. There was a continuous shifting of bank line and the formation of embayment at the upstream of the hard point. The flow attacked the hard point at an oblique direction. Bed shear stress at the front of falling apron was found much higher than the critical bed shear stress. Again the flow was slightly converged along the hard point. So scour hole were formed in front of the falling apron. Though it did not exceed the design scour depth, some flow slides occurred during the fast scouring process due to excessive mica content which has low relative density. The apron material could not get sufficient time for its settlement on the quickly developed scour hole resulting in the failure of the hard point. The main cause of flood around Sirajganj town was the formation of breaches in Brahmaputra Right Embankment (BRE). As the topography of Sirajganj town is lower than the peak flood level of the Jamuna, failure of BRE caused flooding in Sirajganj town and the area around it and damaged to lives and properties. In 2007 flood events, The average inundation depth was 0.6-1.0 m. Maximum inundation depth in few areas of town was around 2.0 m. average velocity of flood water in town area was 0.3-0.4 m/s.

(Ali, 2004) Conducted a morphological analysis of the Jamuna River using finite element method. RMA2, a hydrodynamic model and SED2D, a sediment transport model, were used to simulate the morphology of the Jamuna. Models had been applied using SMS (Surface-water Modeling System) environment, which gave the pre and post-processing options for input and output data. The finite element mesh was developed using LANDSAT image of the 17th November 2000. Initial bed elevations for the nodes of the mesh had been composed from the scattered survey data of April 2001 by BIWTA. Once the mesh and bathymetry had been obtained, the models were ready thereby to incorporate boundary conditions, initial conditions and material properties. The hydrodynamic model developed in the study was satisfactorily calibrated and validated against the observed water surface elevations at Aricha for 2001 and 2002, respectively. Sediment model had also been calibrated using measured bathymetry by BIWTA with the simulated bathymetry of 23rd August 2001. The model was validated with the measured bathymetry of November 2002 and November 2003. Sediment rates at Baruria had been generated from the SED2D model and compared with the FAP-24 data (FAP, 1996). Results revealed that erosion took place in the outer bend of the meandering Eastern anabranch. In Western anabranch, severe deposition was observed near the confluence due to backwater effect of Jamuna-Ganges flow. Velocity reduction in the confluence significantly diminished their sediment transport capacity, and hence inducing deposition. Three morphological years showed much similar type of erosion/deposition patterns, which occurred

mainly in August and September of each year. An investigation, using surveyed bathymetries from 1996 to 2003, showed that the 1998 flood initiates drastic changes in its Western anabranch near Nagarbari, which indeed may have an impact on the shifting of flow more towards left bank at Naradaha. These observations of measured data were further substantiated by the results obtained from the simulation of models. To find a suitable location for ferry ghat and also for a sustainable navigable channel, three options were investigated. Existence of a deep pocket near Naradaha motivated the study to take those options and among them Option 2, which was a dredging option in the upstream channel connecting upper segment of the deep pocket, was appear to show very little deposition compared to other options. Thus the option in question presented a prospective alternative for developing a sustainable ferry route.

(Pal, Rahman and Yunus, 2017) inspected the hydro-morphodynamic changes of Jamuna River using HEC-RAS 1D model and historical data analysis. Data was sorted, analyzed and plotted for the investigation of variation of various parameters during pre-monsoon, monsoon and post-monsoon seasons for a 80 Km reach of Jamuna River. The model was calibrated (in 2004) and validated (in 2008) at Kazipur station by using manning's n 0.025 for which the correlation factor (r), NSE and RSR were respectively 0.9889, 0.9144 and 0.2926 that indicated the performance of the used model was very good. Results revealed that between 1980 to 2014 during monsoon period discharge, water level, sediment transport rate and velocity significantly increased than pre-monsoon and post-monsoon period. From analyses, maximum discharge, water level, velocity and sediment transport rate were found as 103129 m³/s, 15.11 m, 2.84 m/s and 32662117 tons/day respectively in 8th September 1998, 30th August 1988, 29th August 2005 and 9th October 2013 in monsoon. During this time, discharge, water level and sediment transport rate decreased in pre-monsoon and post-monsoon period respectively 66%, 70%; 38%, 40% and 87%, 72% with comparative to monsoon. The analysis also showed that velocity in monsoon increased about 45% to 75% than pre-monsoon and post-monsoon period. Velocity, flow area, top width and water surface elevation were found to be decreased about 35%, 50%; 61%, 70%; 55%, 66% and 29%, 36% during pre-monsoon and post-monsoon period with respect to monsoon period.

2.5 Previous Studies on Structural Intervention in a River

(Dani *et al.*, 2013) constructed a physical model of a typical sinusoidal South African river in the Hydraulics Laboratory at the University of Stellenbosch. The model consisted of two successive 90° bends to best simulate erosion patterns. Different layout designs for a series of groynes were tested to determine the optimal design for the given situation in terms of the projection lengths of the groynes, the spacing between the groynes as a factor of the projection length, and the orientation of the groynes with regard to the oncoming flow. An integrated software package that was developed at the National Centre for Computational Hydroscience and Engineering, at the University of Mississippi, named CCHE2D was used to simulate the physical model numerically. The model was calibrated and validated by combining the physical and mathematical model. The author concluded the study with a decision that groynes with a perpendicular orientation to the direction of the oncoming flow were optimal in comparison with the attracting and repelling type.

Another research about the morphological stabilization of lowland rivers using a series of groynes was conducted by (Alauddin, 2011) with RIC-Nays, a two-dimensional model for flow and morphology, upon confirmation through the detailed experimental data. The flow model was based on the depth-averaged shallow-water equations; the equations expressed in general coordinate system discretized by finite-difference method were solved on the boundary-fitted structured grids for the unknown nodal values by an iterative process. Morphological computation involved a combination of flow fields, sediment transports, and channel-bottom changes along with bankline migration. Streamwise bed load was calculated by Ashida and Michiue formula; the effect of cross-gradient and the influence of secondary flow were then taken into account in accordance with Hasegawa and Engelund, respectively. In considering suspended sediment, an exponential profile of concentration was assumed. Itakura and Kishi's formula was utilized to calculate the entrainment rate, and the 2D advection-diffusion equations were used for planar distribution of depth-averaged concentration. Finally the bed deformation was determined using the 2D sediment continuity equation. In treating the bankline migration: when computations showed that due to currents and scour, the cross-sectional slope angle of the riverbank exceeded the angle of repose, the sediment was assumed to be momentarily eroded up to the point of this angle, and bank erosion would progress. It was then included in the computation of the channel bed evolution as a supply of sediments from the banks.

Construction of a single groyne had only local effect on the flow and the river system. Therefore, the series of groynes were considered in this study to achieve better effect in both bank protection and navigation point of view; hence to increase the efficiency and enlarge the improved river stretch to be useful in engineering practices. To explore the most suitable design of groynes for lowland rivers, first, numerical investigations were made to examine the influence of various orientations and alignments of groynes. Schematized channel and flow parameters based on one of the sub-channels of Jamuna were considered in the study. The channel responses from four different orientations and three different modified alignments were investigated to identify the most effective alignment.

Groynes were modified with various combinations of permeability for some selected alignments, and detailed laboratory experiments were conducted under clear-water scour condition to investigate the fluvial responses influenced by the structures. Including straight conventional design of groynes five different alternative configurations were investigated to find the most effective one. The experimental investigations indicated that the functions of groynes were improved due to both alignment and permeability in the modified designs through minimizing separation of flow, hence minimizing local scour; maintaining bank-parallel flow as well as thalweg for navigation.

Utilizing the 2D numerical model, formation processes of alternate and multiple bars at experiment scale were studied first to verify the simulation results. The effects of initial and boundary conditions on the bar formation processes, and the cause of reduction of bar mode observed in experiments were also clarified. The multiple bar patterns present in the natural rivers were well reproduced by the numerical computation, where the evolution of bars is apparent with a pool-bar complex. As to their interactions with groynes, computation results revealed that accelerating flow due to intrusion of groynes triggers the sediment movement in the main channel, moves the bars reducing their scale, and finally disappears from the straight schematized channels. Thus, the groyne-system is useful to avoid the complexity in lowland rivers due to formation of bars, too.

2.6 Previous Studies on Mathematical Modelling

(Schiavi, E.Flower, A.C., Diaz, J. I., Munoz, 2008) studied about overland flow of water over an erodible sediment that led to a coupled model describing the evolution of the topographic elevation and the depth of the overland water film. The spatially uniform solution of this model was unstable, and this instability corresponded to the formation of rills, which in reality then

grow and coalesce to form large-scale river channels. In this paper the deduction and mathematical analysis of a deterministic model had been considered describing river channel formation and the evolution of its depth. The model involved a degenerate nonlinear parabolic equation (satisfied on the interior of the support of the solution) with a super-linear source term and a prescribed constant mass. The authors proposed a global formulation of the problem (formulated in the whole space, beyond the support of the solution) which allowed to show the existence of a solution and led to a suitable numerical scheme for its approximation. A particular novelty of the model was that the evolving channel self-determines its own width, without the need to pose any extra conditions at the channel margin.

(Churuksaeva and Starchenko, 2015) used depth averaged shallow water equations to model flows where water depth was much less than the horizontal dimension of the computational area and the free surface greatly influenced the flow. The research work was focused on developing the mathematical model, applying the unsteady 2D shallow water equations, and constructing a numerical method for computing the river flow in extensive spatial areas. A finite volume solver for turbulent shallow water equations was presented. Some computational examples were carried out to investigate the applicability of the model. The comparison between the numerical solution and experimental results shows that the depth averaged model correctly represents flow patterns in the cases described and nonlinear effects in a river flow.

(Ivanova and Ivanov, 2016) observed that according to the monitoring data number of floods in habitat areas was constantly growing. Thus, it was required to develop tools for flood prediction and prevention. This paper presented a research of 1-D mathematical modeling of flood wave propagation application in Krasnodar region of Russian Federation. The modelling was based on the Saint-Venant equations. The modeling had been processed in MIKE 11 by DHI software. The results of the modeling proved a series of actions that have to be identified and realized in order to eliminate floods and flood aftermaths. The results of the modelling had proved that constant reservoir bed clearing but not liquidation of the reservoir is necessary.

(Saleh I.Khassaf, Awad, 2015) Studied about the river flow predictions in open channels is an important issue in hydrology and hydraulics. Consequently, this paper was concerned with studying the unsteady flow that may exist in open channel , and its mathematically governed by the Saint Venant equation using a four-point implicit finite difference scheme. From many hydrologic software, HEC-RAS (Hydrologic Engineering Center – River Analysis System) is a good choice to develop the hydraulic model of

a given river system in the south of Iraq represented by Al- Kahlaa River by a network of main channel and three reach and a total of 57 cross sections with 3 boundary sections for one of the applications . The model was calibrated using the observed weekly stage and flow data . The results showed that a good agreement is achieved between the model predicted and the observed data using the values Manning's n (0.04) for over bank with the values of Manning's n (0.027) for main channel and also with using time weighting factor (θ) equal one . Lastly , the AL- Kahlaa River HEC-RAS model has been applied to analyze flows of Al Huwayza marsh feeding rivers (Al Kahlaa River and its main branches), evaluation of their hydraulic performance under two hydraulic model scenarios .The results demonstrate that in case of high flow discharge it is found that cross sections flooded and inadequate for such flows. While, flows are remained within cross section extents during drought season .

2.7 Previous Studies on Delft3D Model

(Elias *et al.*, 2001) conducted a measurement campaign in the framework of the Coast3D Project at Egmond, The Netherlands, during the spring of 1998. The site has been selected as representative for an alongshore relatively uniform coast. The instrumental layout was chosen to allow for validation of numerical models for the near shore. Not only a dense spatial coverage of the modelling area is available, but also detailed measurements of boundary conditions, like wind field, deep water wave height and water levels. In this study, the Coast3D dataset is used to validate the hydrodynamic performance of Delft3D. Evaluation of the model results, acquired by using default process parameter settings, shows a good approximation of measured long shore and cross-shore currents.

(Ali, Mynett and Azam, 2007) carried out a depth integrated two-dimensional numerical modeling to study the sediment dynamics within the Meghnaestuary. The sediment–water dynamics within this estuary are very complex due to its irregular shape, wide seasonal variation, and the changing role of the tide. Both cohesive and non-cohesive sediment transport formulations were used to estimate the total transport. An interactive morphological computation was also used to verify the bed level changes over 2 years. Sediment transports of both monsoon and dry seasons the two most hydrologically pronounced periods in this region were modeled, and a large seasonal variation in sedimenttransport pattern was

observed. Land reclamation dams were tested by the model and found to be effective in enhancing the accretion in its vicinity.

The modeling of bar dynamics is crucial for understanding coastal dynamics and shoreface nourishment evolution. Due to the complexity and variability of the physical processes involved, the formulations developed within the process-based numerical modelling system Delft3D for representing the forcing of the morphodynamic processes (waves, currents, sand transport) contain a high number of calibration parameters. Therefore, the setting up of any Delft3D computation requires a tedious calibration work, usually carried out manually and therefore by definition subjective. (Briere, Giardino and Van der Werf, 2011) set up an automated and objective calibration procedure for Delft3D morphodynamic computations. A number of calibration parameters had been identified based on a careful sensitivity analysis. The calibration method named DUD (Does not Use Derivatives) was selected and coupled to a alongshore uniform Delft3D model. The validity of the implementation was shown based on synthetic tests (twin experiments). The validation test was carried out using field data collected at Egmond-aan-Zee (The Netherlands). The analysis showed that the tool can be successfully used to calibrate Delft3D. However, the author suggested that further research is especially required to understand whether the computed parameters settings only simulate the best morphodynamic evolution of the bars or also describe properly the underlying physical processes.

(Alam and Matin, 2012) studied about the application of 2D model to assess different hydrodynamic characteristics of the Karnafuli river mainly in the case of navigability. The model had been set with the Delft3D modeling system using the necessary bathymetry data collected from Chittagong Port Authorities (CPA) hydrography division. The river reach between Kalurghat and Khal no-18 has been selected for model set up. The model used a curvilinear orthogonal grid with variable dimensions of grid cells starting from 58 m up to 166 m. Calibration and validation were done against the water level data for the year 2009. Model simulation result included flow (velocity) field, bed shear stress etc. had been analyzed to know the hydrodynamic behavior of the river.

(Urmi Laz and Navera, 2018) analyzed different hydrodynamic characteristics of the selected reach of the Jamuna river by applying a 2D model using Delft3D. The study reaches covered from 30 km upstream of Bangabandhu Bridge to 20 km downstream of the Bangabandhu

bridge. Boundary conditions for upstream and downstream were defined by discharge and water level data respectively. The model was developed with the bathymetry data collected from Bangladesh Water Development Board (BWDB). The model was calibrated with the available observed data for the period of April to July 2010 and validated onto the period of April to August, 2011. The hydrodynamics of the selected area was simulated by solving two-dimensional depth integrated momentum and continuity equations numerically with finite difference method. The author expected that the knowledge developed herein might be useful in providing an opportunity in assessing improvement in future prediction and also to suggest the effect of possible development work to be implemented in this river.

2.8 Study Area

The study area covers the reach of Jamuna River from 30 km upstream of Bangabandhu Bridge to 20 km downstream of that bridge, shown in Figure 2.1. In this study area, various important hydraulic structures like East Guide Bund and West Guide Bund of Bangabandhu Bridge, Sirajganj Hard Point and Bhuapur Hard Point are situated. Among all these location the prime concern of this study is the upstream of Sirajganj Hard Point area. From various previous studies, different features of study area is tried to focus in the following paragraph.

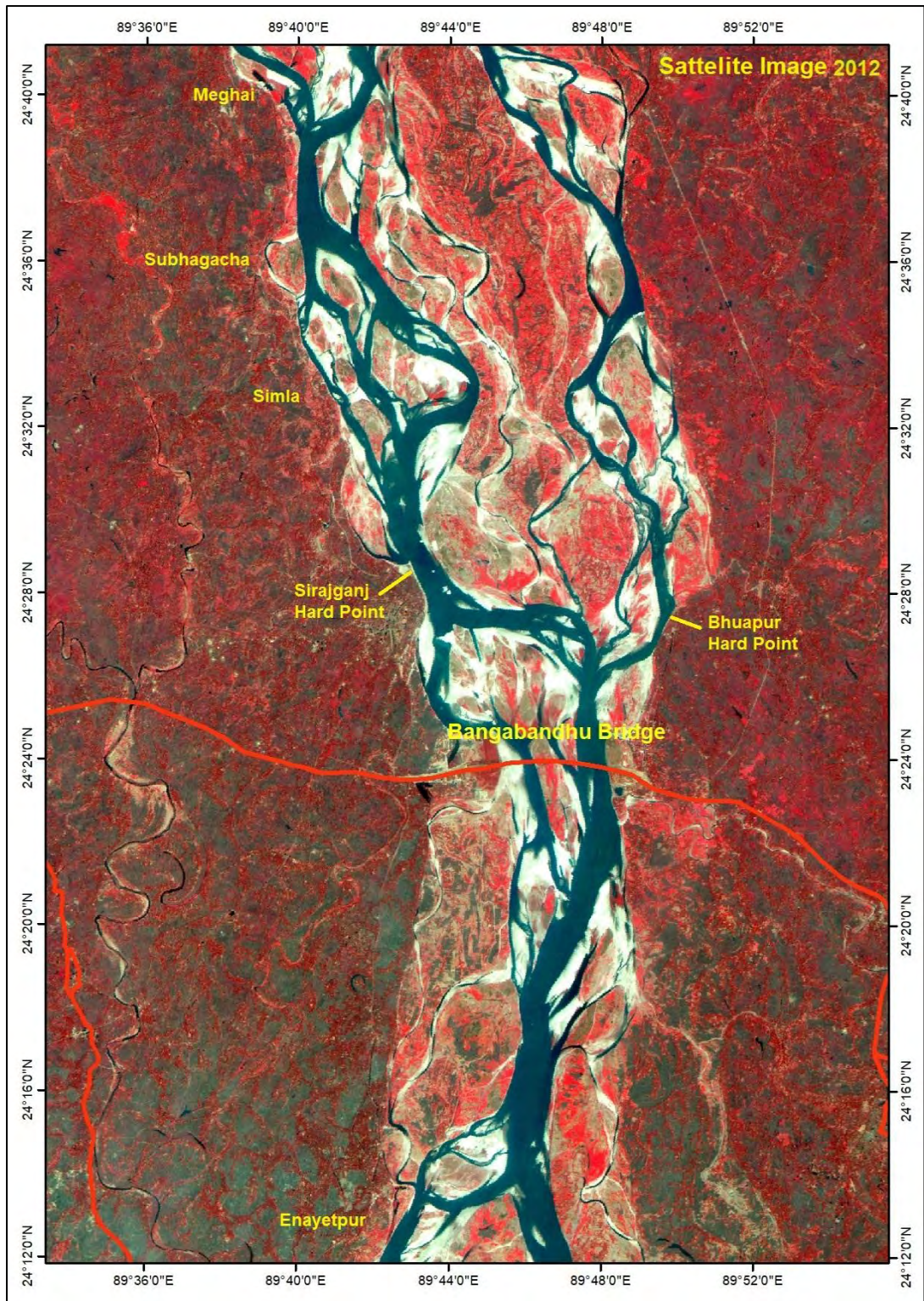


Figure 2.1: Study area along the Jamuna River (Source: CEGIS, 2012)

2.8.1 The Jamuna River System

The Jamuna River draining the northern and eastern slopes of the Himalayas has several right bank tributaries such as the Teesta, the Dharla, the Dudhkumar, etc. and two left bank distributaries, the Old Brahmaputra and the Dhaleswari Rivers. It is a wandering braided river with an average bankfull width of about 11 km. The channel has been widening, increasing from an average of 6.2 km in 1834 to 10.6 km in 1992. Having an average annual discharge of 19,600 m³/sec, the river drains an estimated 620×10⁹ m³ of water annually to the Bay of Bengal. The discharge varies from a minimum of 3,000 m³/sec to a maximum of 100,000 m³/sec, with a bankfull discharge of approximately 48,000 m³/sec. The average water surface slope is 7 cm/km. The range of variation of Brice braiding index of the Jamuna River is 4 to 6 (FAP21/22, 2001).

2.8.2 Source and Course of the River

The Brahmaputra flows through a narrow valley, which is known as the Brahmaputra valley in about east-west direction for 640km with a very low gradient. In this valley it is joined by several tributaries from both sides. On the west the valley is open and beyond Assam it widens into a broad low lying deltaic plain of Bangladesh. The Brahmaputra, after traversing the spurs of the Meghalaya plateau, turns south and enters Bangladesh with the name of Jamuna. The total length of the river from its source in southwestern Tibet to the mouth in the Bay of Bengal is about 2,850 km (including Padma and Meghna up to the mouth). Within Bangladesh territory, Jamuna is 240 km long (upto Aricha). The Jamuna enters Bangladesh east of Bhabanipur (India) and northeast of Kurigram district. Originally, the Jamuna (Brahmaputra) flowed southeast across Mymensing district where it received the Surma River and united with the Meghna. By the beginning of the 19th century its bed had risen due to tectonic movement of the Madhupur Tract and it found an outlet farther west along its present course (Coleman, 1969). It has four major tributaries: the Dudhkumar, Dharla, Teesta and the Baral-Gumani-Hurasagar system. The first three rivers are flashy in nature, rising from the steep catchment on the southern side of the Himalayas. The main distributaries of the Jamuna River are the Old Brahmaputra River, which leaves the left bank of the Brahmaputra River 20 km north of Bahadurabad, and the New haleswari River just south of the Bangabandhu Bridge (Figure 2.1).

2.8.3 Catchment Characteristics

The Brahmaputra-Jamuna drains the northern and eastern slopes of the Himalayas, and has a catchment area of 5, 83,000 sq.km. 50.5 percent of which lie in China, 33.6 percent in India, 8.1 percent in Bangladesh and 7.8 percent in Bhutan. The catchment area of Jamuna River in Bangladesh is about 47,000 sq. km. The average annual discharge is about 19,200 m³/sec, which is nearly twice that of the Ganges. The Brahmaputra River is characterized by high intensity flood flows during the monsoon season, June through September. There is considerable variation in the spatio-temporal distribution of rainfall with marked seasonality. Precipitation varies from as low as 120 cm in parts of Nagaland to above 600 cm in the southern slopes of the Himalayas. In Bangladesh territory rainfall varies from 280 cm at Kurigram to 180 cm at Ganges-Brahmaputra confluence (FAP2, 1992). Monsoon rains from June to September accounts for 60-70% of the annual rainfall. These rains that contribute a large portion of the runoff in the Brahmaputra and its tributaries are primarily controlled by the position of a belt of depressions called the monsoon trough extending from northwest India to the head of the Bay of Bengal. Deforestation in the Jamuna watershed has resulted in increased siltation levels, flash floods, and soil erosion. Occasionally, massive flooding causes huge losses to crops, life and property. Periodic flooding is a natural phenomenon which is ecologically important because it helps maintain the lowland grasslands and associated wildlife. Periodic floods also deposit fresh alluvium replenishing the fertile soil of the Jamuna River valley.

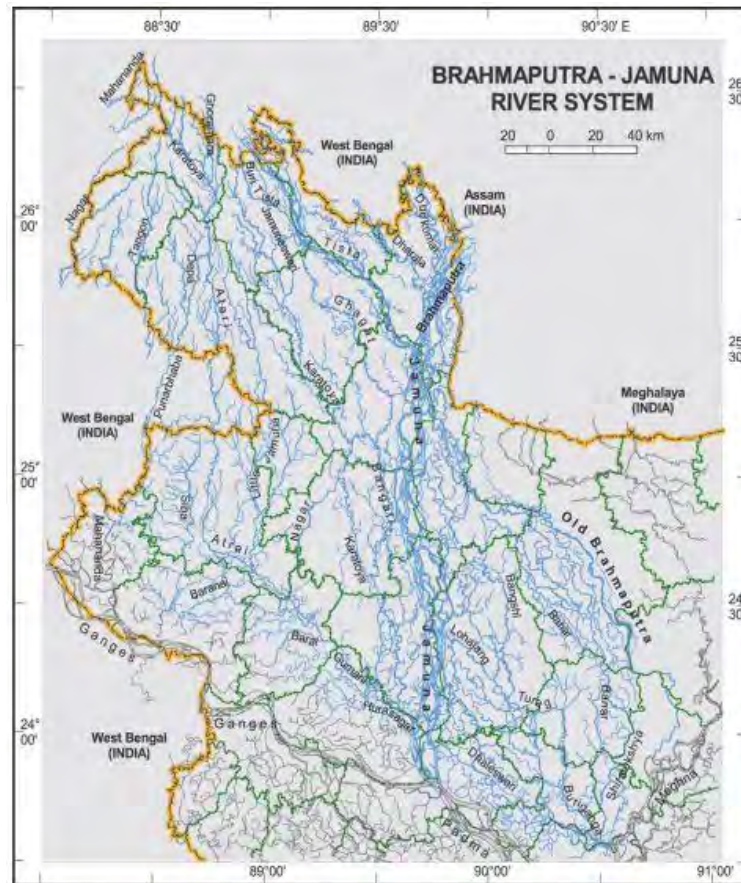


Figure 2.2: Brahmaputra-Jamuna River System within Bangladesh Territory
(Source: IWM, 2012)

2.8.4 Topography of the Catchment Area

Topographically, the study area is part of alluvial plains (low land) formed by the sediments of river and its tributaries and distributaries. In the context of physiography, the study area belongs to region: floodplains and sub-region: Jamuna floodplain. The sub-region can be again subdivided into the Bangali-Karatoya floodplain, Jamuna-Dhaleshwari floodplain, and diyaras and chars. The soil and topography of chars and diyaras vary considerably. Some of the largest ones have point bars. The elevation between the lowest and highest points of these accretions may be as much as 5m. The difference between them and the higher levees on either bank can be up to 6m. Some of the ridges are shallowly flooded but most of the ridges and all the basins of this floodplain region are flooded more than 0.91m deep for about four months (mid-June to mid-October) during the monsoon. Land elevation of the study area varies from 13mPWD to 18 mPWD.

2.8.5 Sediment Characteristics

The Jamuna River catchment supplies enormous quantities of sediment from the actively uplifting mountains in the Himalayas, the erosive foothills of the Himalayan Foredeep and the great alluvial deposits stored in the Assam Valley. Consequently, the Jamuna River carries a heavy sediment load, estimated to be over 650 million tonnes annually (Coleman, 1969). Most of this is in the silt size class (suspended load) but around 15 to 25 percent is sand (bed load). This sand is deposited along the course of the river and the clay fraction is transported to the delta region. The banks of the Jamuna River consist of fine cohesion less silty sand. The composition of the bank materials is remarkably uniform. For the Jamuna River the angle of internal friction is approximately 30°. It is however dependent on the mica contents. Because of the varying location of the river branches, much of the sediment has been eroded and accreted many times. The sand size sediment is relatively uniformly graded. The range of d_{50} values vary between 0.14 mm and 0.21 mm.

2.8.6 Hydraulic Characteristics of the Jamuna

The Jamuna is the lowest reach of the Brahmaputra River in Bangladesh. It is a large braided sand-bed river; the number of braids (during low flows) varies between 2 to 3. The average discharge during floods is about 50,000 m³/s and the maximum width during floods is more than 15km. The bed material is quite uniform. The valley slope in Bangladesh decreases gradually from 0.10 to 0.06 m/km (FAP24, 1996). The width of the river varies from 3 km to 18 km but the average width is about 10 km. Width/depth ratios for individual channels vary from 50:1 to 500:1. The gradient of the river in Bangladesh is 0.000085, decreasing to 0.00006 near the confluence with the Ganges. The river has a total annual sediment flow of about 650 million tons. The characteristics of the Jamuna River have been summarized in Table 2.1. According to an extensive sampling carried out by (FAP1, 1991), bank material seems to be quite uniform and consists of fine sand. The little variation in bank material composition in downstream direction is due to old clayey deposits.

Table 2.1: Summary of hydraulic characteristics of the Jamuna River

(Source: IWM, 2012)

Description	Parameter
Maximum total discharge	100,000 m ³ /s
Dominant discharge	38,000 m ³ /s
Average depth (main channel)	8 m
Average depth above chars during floods	1-2 m
Chezy Coefficient (average)	70 m ^{1/2} /s
Chezy Coefficient (floods)	90 m ^{1/2} /s
Average velocity during floods	2 m/s

CHAPTER 3

THEORETICAL BACKGROUND

3.1 General

The hydrodynamic and morphological characteristics of a braided river in alluvial flood plain like the Jamuna are very complicated and unpredictable. Different experiments and researches have been done to deal with these characteristics. Especially river training works is a common scenario to control and train the river for mankind. In this case, structural intervention in the river plays a vital role. In this chapter, theories on hydro-morphological characteristics of a river with its response along with the structural intervention has been discussed. In addition, theories related to mathematical modeling specially Delft3D model has been discussed with its processes.

3.2 Hydrodynamics of a River

The river hydrodynamics deal with the characteristics of the fluids and their ability to transport substances and physical properties. Science that studies the physical behavior of a fluid consisting of water and the materials it contains. This is an application of hydrodynamics to streams; it is a branch of fluid mechanics. It helps to understand the stream evolutionary process: action of the fluid on bed materials, flow characteristics, dissipation of the stream energy when transporting these materials.

The quantification of the movements of fluids is a complex task, and when considering natural flows, occurring in large scales as like rivers, lakes, oceans, this complexity is evidenced. Different types of parameters are associated with the hydrodynamics of a river. Flow velocity is one of the major hydrodynamic parameters. Dynamic behavior mostly depends upon the velocity of the river water. From the velocity distribution profile, it is found that the maximum velocity occurs at the mid channel section and decreases towards the river banks. In case of vertical section, the magnitude of the flow velocity increases to the upper portion and in the lower portion velocity tends to zero at the bed level. Flow velocity is directly proportional to the discharge. Another relationship between the flow velocity and depth of flow is inversely proportional. Bed shear stress is another parameter that belongs to hydrodynamic behavior. There is a strong relationship between the hydrodynamics and morphology of a river.

Depending upon the dynamicity, the transportation of sediment occurs from one place to another.

3.3 Morphology of a River

River morphology refers to the field of science dealing with changes of river planform and cross-section shape due to erosion, transportation and sedimentation processes. In this field the dynamics of flow and sediment transport are principal elements. Practically all rivers are subject to morphological processes. Sediment loads are classified into bed load and suspended load. In contact with a river bed, bed load consisting of material of larger diameter than fine sand, is brought to the lower reaches. Fine materials such as clay and silt are held in suspension in stream water and are carried without contact with the river bed. The three main channel patterns in alluvial plains are: braided, meandering and straight. Channels on an alluvial fan show a braided pattern, and their depth is shallow. The river bed is composed of gravelly deposits. Channels in a flood plain meander and have a river bed composed of sand. Channels bifurcate in a delta, and bifurcated channels have muddy river beds and tend to be straight. The movement of water and the kinds of sediment load affect the depth and width of a channel (Matsuda, 2004).

The classification by Brice (1983) is based on four major planform properties that are most readily observed on aerial photographs: sinuosity, point bars, braiding, and anabranching. Four major river types, each of which consists of commonly occurring association of planform properties, are illustrated in Fig. 3.1, in the direction of increasing slope. Sinuous canaliform rivers have a flat slope characterized by narrow crescent-shaped point bars, a notably uniform width, a lack of braiding, and a moderate to high sinuosity. The channel is relatively narrow and deep, with greatest lateral stability and high silt-clay content for the banks.

Sinuuous point bar rivers are steeper and have more rapid rates of lateral migration at bends, although straight reaches may remain stable for long period of time. Such rivers tend to have greater width at bend apexes; they also tend to have prominent point bars that are typically scrolled and visible at normal stage. Sinuous braided rivers are steeper and wider than sinuous point bar rivers with the same discharge, featured by rapid rates of lateral migration and rapid shifts in the position of the thalweg. Such rivers have fairly heavy bed-material load but less silt-clay content. Point bars are more irregular as the braiding increases. Non-sinuuous braided rivers without point bars exist on steep slopes with heavy bed-

material load and low silt-clay content. Such rivers are highly braided and have moderate rates of lateral migration at random places where one of the multiple branches impinges against a bank. The branch channels shift at random within the banklines (Hongwei, Xuehua and Bao'an, 2009).

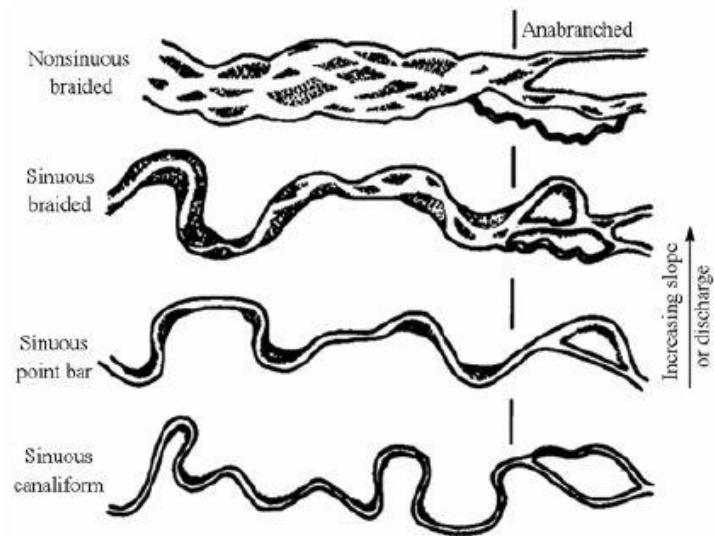


Figure 3.1: River Classification by Brice

3.4 Structural Intervention in a River

River training is a major part of river engineering. Control and training of the rivers are done for different purposes like navigation, flood management, transportation, fisheries and so on. In case of river training, different types of structures are inserted into the river. These structures play important roles in river hydrodynamics and also in morphology. Some examples of the structural intervention in rivers are described below:

3.4.1 Marginal Embankments/Levees

Marginal embankments are generally earthen embankments running parallel to the river at some suitable distance from it. They may be constructed on both sides of the river or only one side, for some suitable river length where the river is passing through towns or cities or any other places of importance. These embankment-walls retain the flood water and thus preventing it from spreading into the nearby lands and towns. A levee or dyke is mainly used for flood protection by controlling the river only.

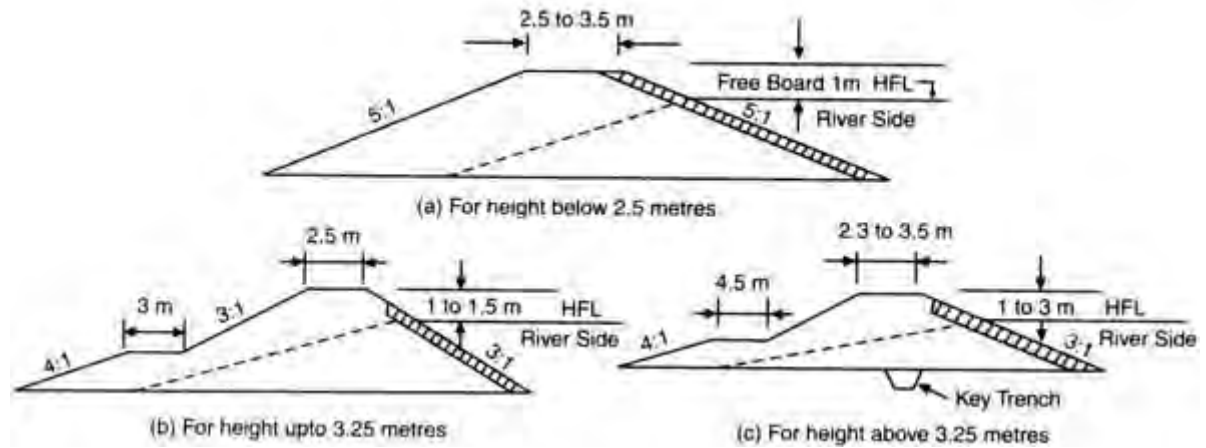


Figure 3.2: Typical cross-sections of levees for different heights

3.4.2 Guide Bank

Guide Banks are earthen embankments with stone pitching in the slopes facing water, to guide the river through the barrage or bridge. These river training works are provided for rivers flowing in planes, upstream and downstream of the hydraulic structures or bridges built on the river. Guide banks guide the river water flow through the barrage. Guide banks force the river into restricted channel, to ensure almost axial flow near the weir site.

A structure such as weir or a barrage or a bridge etc. is extended in a smaller width of the river and river water is trained to flow almost axially through this trough without out-flanking the structure. The river is normally trained for this purpose with the help of a pair of guide banks. The guide banks are generally provided in pairs, symmetrical in plan and may either be kept parallel or may diverge slightly upstream of the works (Garg, 2005).

3.4.3 Revetments

Revetment is artificial roughing of the bank slope with erosion-resistant materials. A revetment mainly consists of a cover layer, and a filter layer. Toe protection is provided as an integral part of the foot of the bank to prevent undercutting causes by scour. The protection can be divided as falling apron or launching apron, which can be constructed with different materials, e.g. CC blocks, rip-rap, and geobags. The following figure shows revetments and their different components.

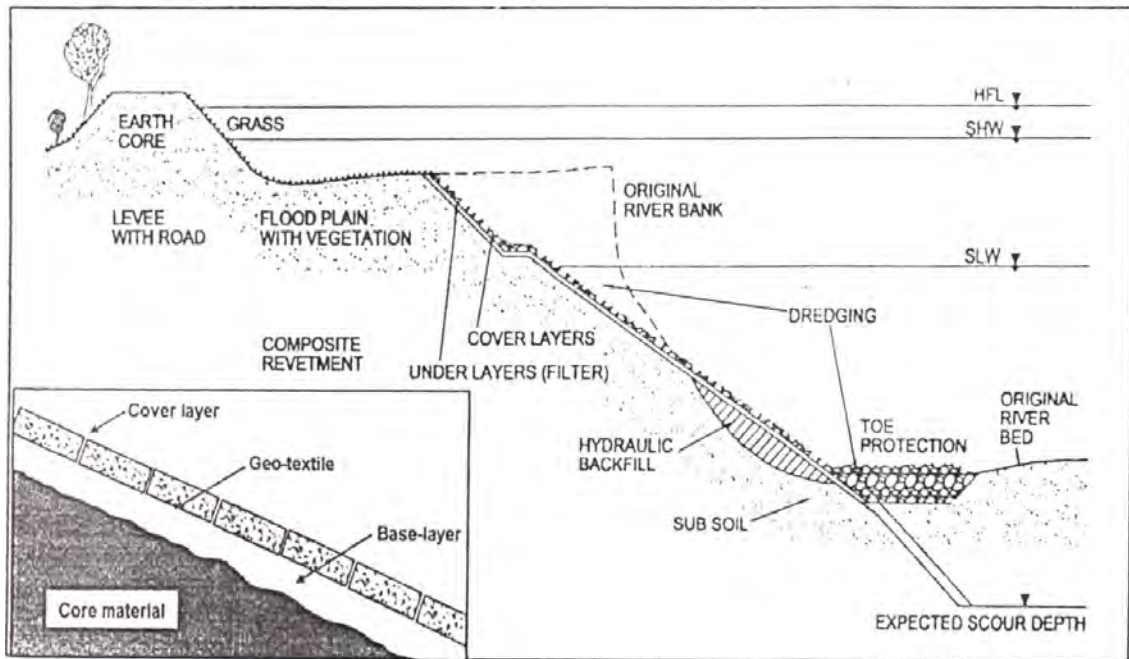


Figure 3.3: Components of a revetment on riverbank

Launching apron consist of interconnected elements that are placed horizontally on the floodplain and normally anchored at the toe of the embankment. The interconnected elements are not allowed to re-change their positions freely during scouring but launch down the slope as a flexible unit. The falling apron, on the other hand, consists of loose elements (e.g., CC blocks, stones, geobags) placed at outer end of the structure. When scour hole approaches the apron, the elements can adjust their position freely and fall down the scouring slope to protect it (Ahmed and Hasan, 2011).

3.4.4 Groynes/Spurs

Groynes are embankment type structures, constructed transverse to the river flow, extending from the bank into the river. That is why, they may also be called as transverse dykes. They are constructed in order to protect the bank from which they are extended by deflecting the current away from the bank. As water is unable to take a sharp embayment, the bank gets protected for certain distance upstream and downstream of the groyne. However, the nose of the groyne is subjected to tremendous action of water and has to be protected by pitching and so on. The action of eddies reduces from the head towards the bank and therefore, the thickness of slope pitching and apron can be reduced accordingly (Garg, 2005).

Classification of groynes based on alignment types are:

- (i) Normal groyne: It is also called ordinary groyne and is aligned perpendicular to the bank line.

- (ii) Repelling groyne: This type of groyne pointing upstream has the property of repelling the flow away from it.
- (iii) Attracting groyne: This type of groyne pointing downstream has the property of attracting the flow towards it.

The mentioned three types of groynes are illustrated in the following figure:

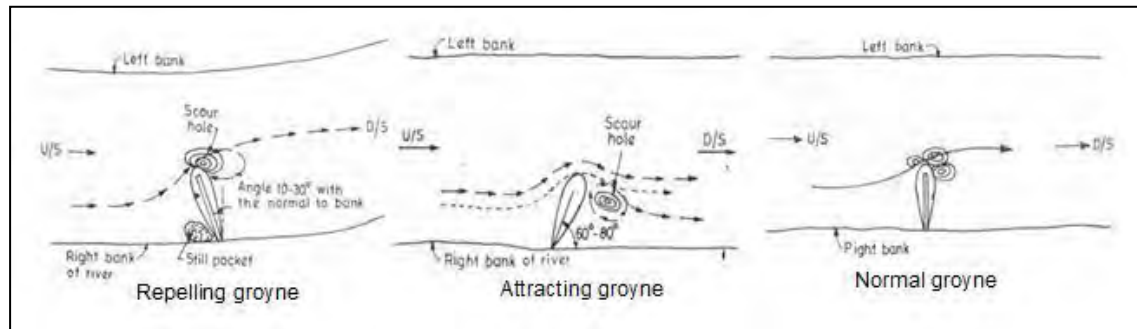


Figure 3.4: Types of groynes based on alignment

Classification of groynes based on material used:

- (i) Impermeable groyne
- (ii) Permeable groyne

3.4.4.1 Length of Groynes/Spurs (L_g)

Groyne length depends on location, purpose, spacing, and economics of construction. The total length of the groyne includes the anchoring length, referring to the part embedded in the bank, and the working length, referring to the part protruding into the flow. The length can be established by determining the channel width and depth desired. The working length is usually around a quarter of the mean width of the free surface; the anchoring length is recommended to be less than a quarter of the working length. The maximum length of groyne is equal to the distance between the bank and the river zone where no groyne encroachment is allowed. Such a zone should be determined in advance, as part of a river training strategy. Groyne intruding this zone may divert the river and trigger bank erosion at other locations over a large distance.

3.4.4.2 Spacing between Groynes/Spurs (S_g)

The spacing between groynes is measured at the riverbank between the groyne roots. It is related to river width, groyne length, flow velocity, angle to the bank, orientation to the flow, bank curvature, and purpose, but it is mostly expressed as a multiple of the groyne length.

(Richardson, E. V., Stevens, M. A., Simons, 1975) recommends a spacing of 1.5 to 6 times the upstream projected groyne length. In order to obtain a well-defined deep navigation channel, a spacing of 1.5 to 2 times the groyne length is recommended, whereas for bank protection the spacing is increased to 2 to 6 times the groyne length. There are, however, successful examples of bank protection with short groynes spaced at 10 to 100 times their length, but there the banks are protected with riprap or vegetation. If the spacing between groynes is too large, a meander loop may form between groynes. If the groynes are spaced too close together, on the other hand, construction costs will be higher and the system would work less efficiently, not making full use of each individual groyne (Alauddin, 2011).

3.5 Structural Intervention in the Jamuna River

Being the most unpredictable river all over the world, the Jamuna experienced lots of structural intervention in its life. For control and train the Jamuna River several types of structures at different places have been executed. A brief discussion about the structural intervention in the Jamuna is given below.

3.5.1 Groynes/Spurs

A permeable spur at Kamarjani during the dry season. The German Development Cooperation supported the Flood Action Plan (FAP) of the Bangladesh Government, initiated in 1989, for riverbank protection and active floodplain management (components 21 and 22). Out of the 26 components FAP 21 & 22 were by far the largest components. The first pilot works were built in the area of Kamarjani near Gaibandha. Permeable spurs, consisting of several rows of steel piles produced by German medium sized businesses and deeply driven into the riverbed along more than 1.5 km of riverbank, were designed to reduce the destructive flow velocities and orient the river flow parallel to the bank (Picture 1). While successful and still performing well after 15 years, the impressive spurs demonstrated also that it is difficult to address the ever shifting river erosion with fixed protection of limited lengths. After some years the river began shifting to the west, leaving the spurs effective only during the flood season.



Figure 3.5: Permeable groune for Jamuna Bank protection At Kamarjani (FAP21/22)

3.5.2 Revetments and Hard points

Different section of the Bahadurabad revetment during the dry season. The initial riverbank protection concept relied on the concept of “hard points” to try and address the unpredictable nature of erosion and deposition. Hard points are designed to locally protect strategically important areas, such as bridges, large settlements, and ferry terminals. The FAP 21/22 project broadly followed this concept during the second implementation, but r with the view to develop an easy to implement solution making maximum use of local materials and technologies. An 800 m long curved riverbank protection structure (revetment) was developed, which consists of eight different sections, testing different materials and construction methodologies (Fig.8). The revetment protects the village of Kulkandi near the important railway ferry terminal of Bahadurabad. The protection work was completed in 1997 and was constantly monitored producing a large quantity r of systematic data which contributed greatly to the understanding of the interaction between river erosion and protective works. Riverbank protection build under an ADB financed Jamuna-Meghna River Erosion Mitigation Project (JMREMP)(© Press Section, German Embassy, Dhaka) After three successful pilot works implemented over a period of 7 years (1994 to 2000) the German development cooperation ended its activities in the area of erosion protection in 2001 and training activities in 2005. In coordination with the Government of Bangladesh, Germany agreed on new priority areas for future development cooperation. The Asian Development

Bank (ADB) took up the development of riverbank protection from 2001 and recently World Bank expressed some interest. GIZ and CIDA (Canada) finance supporting components, focussing on biodiversity and erosion prediction and warning. Specifically the ADB initiative of the Jamuna-Meghna River Erosion Mitigation Project strongly built on the experience gained through the KfW supported FAP 21/22. Continued systematic development of technologies piloted under FAP 21/22 has reduced the per km cost to USD 2.5 million, and as such allows the stabilization of longer reaches for predominantly agricultural areas to be economically viable. As a consequence the limited “Hard Point” approach has been largely abandoned and the protection and stabilization of longer reaches is now envisaged (Matin, 2016).



Figure 3.6: Permeable groune for Jamuna Bank protection At Kamarjani

Different types of structural intervention in the Jamuna River for the last 25 years is shown in Table: 3:1. From the table it is evident that most of the structures inserted into the river for controlling and training of the river have been damaged. These are the unpredictable characteristics of the river Jamuna.

Table 3.1: List of various structural intervention in Brahmaputra/Jumna and the present status

Name of structure	Construction period	Exposed to the flow		Comments
		Minor channel	Major channel	
Kamarjani permeable groyne	1994-95		1995	Major damages
Hasnapara Spur 1	2001-02	2002-03		Performance is not clear as it does not exposed to main channel
Hasnapara Spur 2	2001-02	2002-03		Performance is not clear as it does not exposed to main channel
Titparal Revetment	2005-06		2005-11	Minor damages but effective
Kalitola	1997-98		1997-11	Minor and major damages but effective
Sariakandi	1997-98		1997-11	Effective
Mathurapara	1997-98		1997-07	
Devdanga Revetment	2005-06		2005-08	Minor damages
Chandanbaisa (belmouth)	2001-02		2002-08	Damaged
Baniajan Spur	2001-02	2002-03		
Meghai Spur 1	1999-00	2000-01	2004	Damaged in 2004
Meghai Spur 2	1999-00	2000-01		
Meghai Spur 3	1999-00	2000-01		
Singrabari Spur 1	1998-99		2002-03	Exposed for one year, damaged
Singrabari Spur 2	1998-99		2002-03	Damaged in 2002
Shuvagacha Spur 1	1999-00		2002-03	Damaged in 2002
Shuvagacha Spur 2	1999-00		2002-03	Damaged in 2003
Simla Spur 1	1999-01		2003	Damaged in 2003
Simla Spur 2	1999-01		2005	Exposed for one year
Simla Spur 3	1999-01		2002	Damaged in 2002
Shailabari Groyne	1980-81		1997-04	Damaged in 2004
Sirajganj Revetment	1997-98		1998-11	Minor damages, effective
Bangabandhu Bridge Right Guide Bund	1996-98		1996-11	Effective
Betil Spur	2000-02	2001-04		Damaged in 2004, after repairing damaged again 2007
Enayetpur Spur	2000-02	2001-04		Damaged in 2004, repaired in 2006
PIRDP, Geobag revetment	2004-06		2004-11	Effective

Major channel: Perennial channel, Minor channel: Ephemeral channel

Name of structure	Construction period	Exposed to the flow		Comments
		Minor channel	Major channel	
Bahadurabad Revetment	1996-97		1997-98 2008-11	Effective
Ghutail	1999-00		20003-04 2007-11	Major damage, Effective
Pingna	2005-06	2005-06		Exposed only to the minor channel
Nolin bazaar	2001-02	2002-03		Rate of erosion was small
Bhuapur Revetment	1996-97	1998-99		
Bangabandhu Bridge Left Guide Bund	1997-98		1998-11	Effective

3.6 River Response

Rivers have achieved a state of equilibrium throughout it reaches over a period of time. Change in a river due to any interference is a time depending morphological process in nature (Vries, 1993). Rivers always try to achieve a stable state of equilibrium throughout it reaches over a period of time. Any manmade and natural interference will lead to response of the river. The combined use of dredging, contraction dikes, and disposal of dredged material in the dike fields can induce major changes in the cross-sectional characteristics of a river. This direct physical displacement and the resulting change in channel shape can retard the movement of bed-load sediments through a river system (Lagasse, 1986). Three modes of response can be discerned in the morphological response of rivers to natural changes or human interventions: bed level changes, planform changes and changes in bed sediment composition. Planform changes are produced by bank retreat as a result of erosion and bank advance as a result of accretion (Mosselman, 1998, 2006). Langendoen and Alonso (2008) modeled the incised river for the evolution of flow and stream bed components.

3.6.1 River Responses Type

Any manmade and natural interference will lead to response of the river. This is called River Response. Here the manmade interferences are-

- Discharge regulation
- Water level regulation
- Normalization of X- section
- Canalization
- Withdrawal of sediment
- Withdrawal of water etc

Natural interference involves-

- Exceedence limit state on river channel
- Earthquake induced effect etc.

Response to the river for all these interferences is very complex task as many variables are involved in the process. For any river improvement works, the response of river needs to be evaluated qualitatively or quantitatively to some extent.

3.6.2 Qualitative Response

Lane (1955) expressed the influence of size and input of bed material load on the slope of a stable channel using:

$$Q_s D \propto Q i \quad \dots\dots\dots (3.1)$$

where, Q_s = Sediment discharge and D = amount and size of bed material load, Q = discharge and i = channel slope. This qualitative relation, often represented as ‘Lane’s balance’, indicates how the slope of a channel responds to a change in any of the three independent variables: discharge, sediment load and sediment calibre given that the width and planform of the channel remain constant. The balance shows that, for a given discharge, an increase in the quantity or calibre of sediment load input to the reach cause the increase of slope of channel and vice versa (Figure 3.1) . Lane (1955) presented six classes of change in the river that can cause aggradation or degradation. These are:

- i. increasing the amount and/or size of the input sediment load,
- ii. decreasing the amount and/or size of the input sediment load,
- iii. raising of base level,
- iv. lowering of base level,
- v. moving the base level further away without changing its elevation, and
- vi. moving the base level closer without changing its elevation.

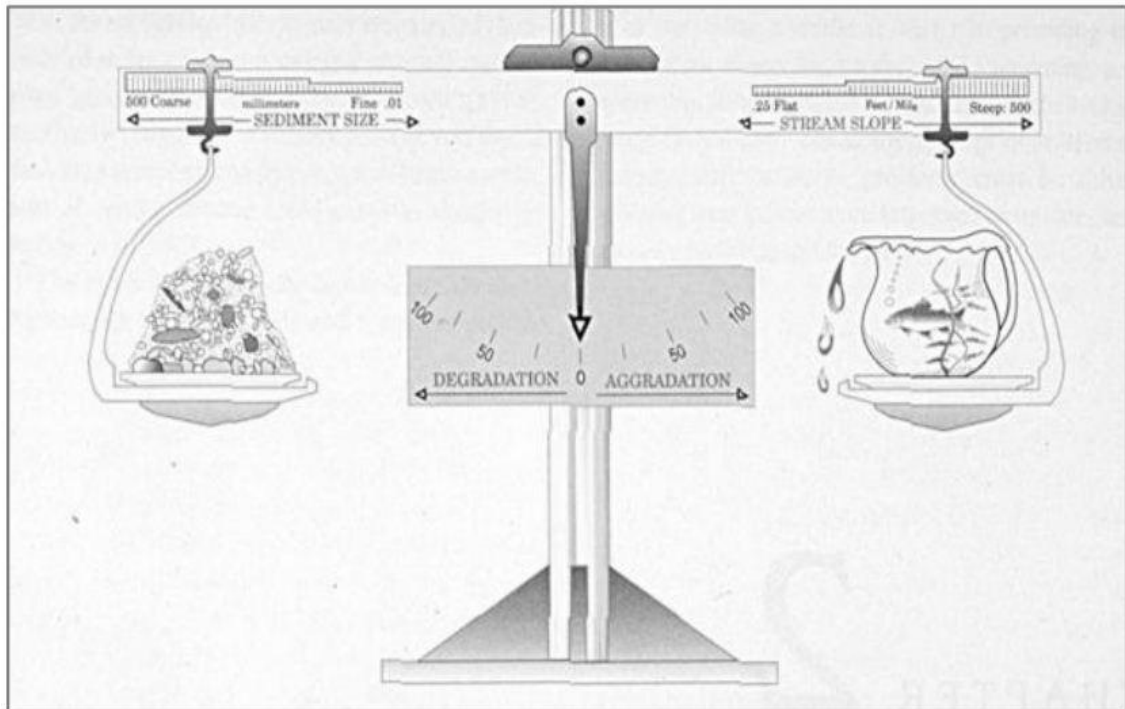


Figure 3.7: Lane's balance (Source: Sarker, 2008)

Instead of the sediment load, (Schumm, 1969) investigated the effect of changes in the characteristic size of the boundary sediment on the geometry of the channel. He used the percentage of silt-clay in the channel perimeter materials as an independent variable controlling channel width, depth, slope and sinuosity. (Schumm, 1985) indicated that as the percentage of silt-clay increases, the width and slope of a stable channel decrease, while depth increases. Schumm neglected the role of the sediment load in forming the channel though he did recognize the role of the sediment load in affecting the slope.

3.7 Mathematical Modeling

Many modelling packages are available which can simulate hydrodynamic as well as morphological characteristics of a river. Moreover, modelling packages are so advanced that it can now simulate intervention phenomenon on river through control structure. There are few softwares available that can simulate the flow through control structures and sediment transport with bed level changes in river systems. There are mainly HEC-RAS, MIKE 11, MIKE 21C, Delft 3D, SMS etc. Different types of analysis are being done with these models in different cases and purposes. Steady flow analysis (Ahmad, Bhat and Ahmad, 2016), flood inundation mapping (Goodell, C, Warren, 2006), flood prediction (Timbadiya, Patel and Porey, 2011) are commonly done by HEC-RAS model. Hydrodynamic analysis of rivers with

SMS model (Ahmed and Hasan, 2011) is also an essential tool now a days. MIKE 21C is a professional software for river and coastal analysis with model studies. Different hydrodynamic as well as morphological analysis of river (Morianou *et al.*, 2015)(Musfequzzaman, 2012)(Noor, 2013) and coastal engineering are carried out with this modeling tool. Delft3D is a multidimensional open source modeling tool for academic purpose as well as professional also. The details about Delft3D is described in the next section.

3.8 Delft3D Model

Delft3D is a software package developed by Deltares (former WL|Delft Hydraulics) for 2D or 3D computations for coastal, river and estuarine areas. The model consists of a number of integrated modules which together allow the simulation of hydrodynamic flow (under the shallow water assumption), computation of the transport of water-borne constituents (e.g., salinity and heat), short wave generation and propagation, sediment transport and morphological changes, and the modelling of ecological processes and water quality parameters (Lesser *et al.*, 2004). The Delft3D package consists of several modules such as for flow, tide, wave, water quality etc. grouped around a common interface. Delft3D-FLOW is one of those modules. The FLOW module is a multidimensional (2D-depth-averaged or 3D) hydrodynamic simulation program that calculates unsteady flow and transport phenomena with a free surface. It aims at modelling flow phenomena of which the horizontal length scales are significantly larger than the vertical length scales (Zijl, 2002). In this section, some information about the governing equations and the assumptions used will be given.

3.8.1 Numerical Aspects of Delft3D-FLOW

Delft3D-FLOW is applied for modelling a wide range of different flow conditions: e.g. turbulent flows in laboratory flumes, tidal flow in estuaries and seas, rapidly varying flows in rivers, density driven flows by thermal discharges, wind driven flows in lakes and ocean dynamics. For all these applications (with complete different length scales) Delft3D-FLOW should give a solution. For the choice of the numerical methods, robustness had high priority.

3.8.1.1 Staggered grid

The numerical method of Delft3D-FLOW is based on finite differences. To discretise the 3D shallow water equations in space, the model area is covered by a curvilinear grid. It is assumed that the grid is orthogonal and well-structured. The grid co-ordinates can be defined either in a Cartesian or in a spherical co-ordinate system. In both cases a curvilinear grid, a file with curvilinear grid co-ordinates in the physical space, has to be provided. Such a file may be generated by a grid generator, see the User Manual of RGFRID. The numerical grid transformation is implicitly known by the mapping of the co-ordinates of the grid vertices from the physical to the computational space (Manual, 2013).

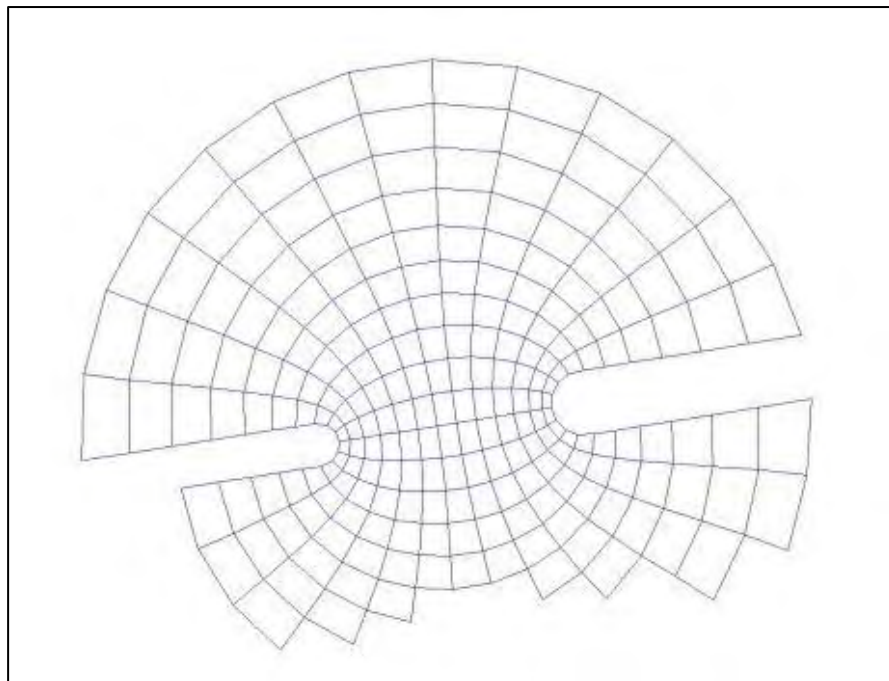


Figure 3.8: Example of a grid in Delft3D-FLOW

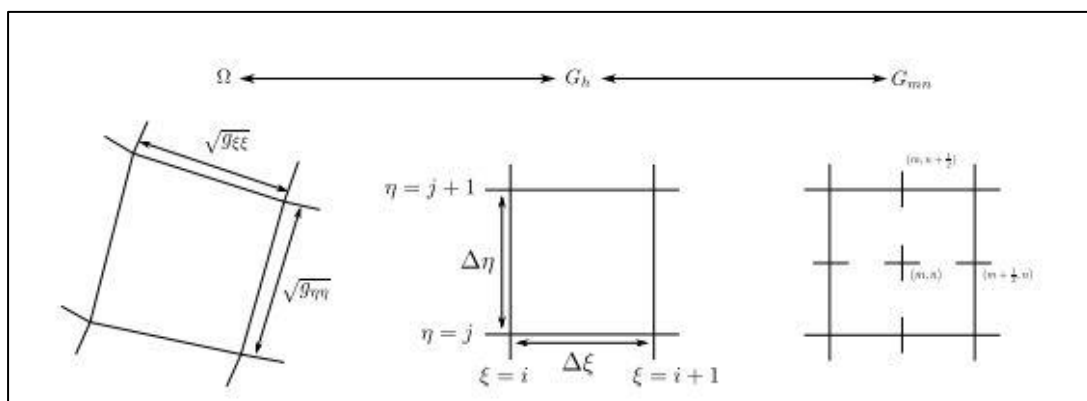


Figure 3.9: Mapping of physical space to computational space

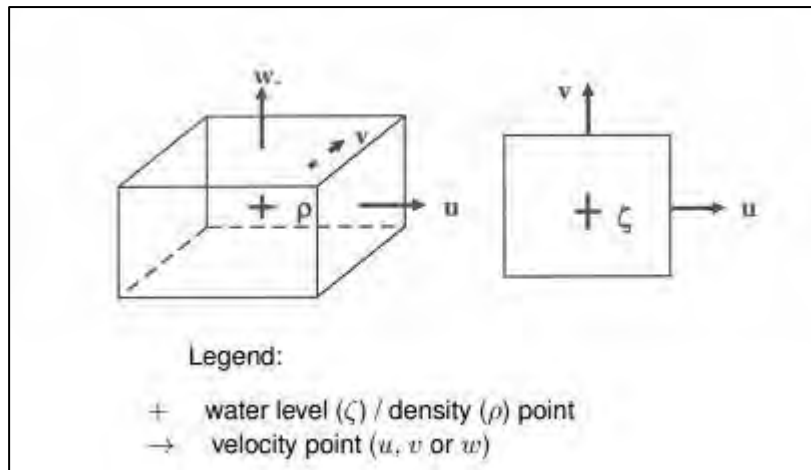


Figure 3.10: Grid staggering, 3D view (left) and top view (right)

3.8.1.2 Definition of model boundaries

The horizontal model area is defined by specifying the so-called computational grid enclosure (automatically generated by RGFGRID). The computational grid enclosure consists of one or more closed polygons that specify the boundaries of the model area. There are two types of boundaries: closed boundaries along “land-water” lines (coastlines, riverbanks) and open boundaries across the flow field. The open boundaries are artificial and chosen to limit the computational area. The polygons consist of line pieces connecting water level points on the numerical grid, with a direction parallel to the grid lines or diagonal (45 degrees) through the grid. The computational cells on the grid enclosure are land points (permanent dry) or open boundary points. An island may be removed from the computational domain by specifying a closed polygon (“land-water line”) as part of the grid enclosure. If a computational grid enclosure is not specified, then a default rectangular computational grid is assumed. A default enclosure is spanned by the lines connecting the water level points (1, 1), (Mmax, 1), (Mmax, Nmax) and (1, max).

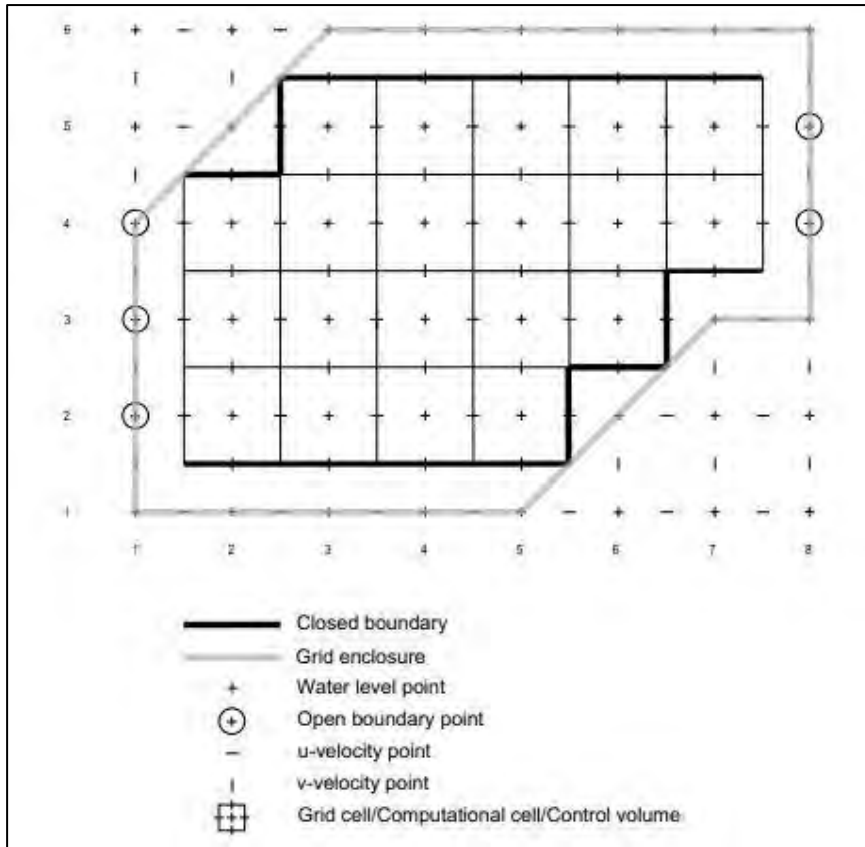


Figure 3.11: Example of Delft3D model area

3.8.2 Hydrodynamic equations

Delft3D-FLOW solves the Navier Stokes equations for an incompressible fluid, under the shallow water and the Boussinesq assumptions. In the vertical momentum equation the vertical accelerations are neglected, which leads to the hydrostatic pressure equation. In 3D models the vertical velocities are computed from the continuity equation. The set of partial differential equations in combination with an appropriate set of initial and boundary conditions is solved on a finite difference grid. In the horizontal direction Delft3D-FLOW uses orthogonal curvilinear co-ordinates. Two co-ordinate systems are supported:

- Cartesian co-ordinates (ξ, η)
- Spherical co-ordinates (λ, ϕ)

The boundaries of a river, an estuary or a coastal sea are in general curved and are not smoothly represented on a rectangular grid. The boundary becomes irregular and may introduce significant discretization errors. To reduce these errors boundary fitted orthogonal curvilinear

co-ordinates are used. Curvilinear co-ordinates also allow local grid refinement in areas with large horizontal gradients.

Spherical co-ordinates are a special case of orthogonal curvilinear co-ordinates with:

$$\begin{aligned} \xi &= \lambda \\ \eta &= \phi \\ \sqrt{G_{\xi\xi}} &= R \cos \phi \\ \sqrt{G_{\eta\eta}} &= R \end{aligned} \quad \dots (3.2)$$

in which λ is the longitude, ϕ is the latitude and R is the radius of the Earth (6 378.137 km).

In Delft3D-FLOW the equations are formulated in orthogonal curvilinear co-ordinates. The velocity scale is in physical space, but the components are perpendicular to the cell faces of the curvilinear grid. The grid transformation introduces curvature terms in the equations of motion.

In the vertical direction Delft3D-FLOW offers two different vertical grid systems: the σ coordinate system (σ -model) and the Cartesian Z co-ordinate system (Z -model). The hydrodynamic equations described in this section are valid for the σ co-ordinate system. The equations for the Z co-ordinate system are similar.

3.8.2.1 The σ co-ordinate system

The σ -grid was introduced by Phillips (1957) for atmospheric models. The vertical grid consists of layers bounded by two σ -planes, which are not strictly horizontal but follow the bottom topography and the free surface. Because the σ -grid is boundary fitted both to the bottom and to the moving free surface, a smooth representation of the topography is obtained. The number of layers over the entire horizontal computational area is constant, irrespective of the local water depth (Figure 3.13). The distribution of the relative layer thickness is usually non-uniform. This allows for more resolution in the zones of interest such as the near surface area (important for e.g. wind-driven flows, heat exchange with the atmosphere) and the near bed area (sediment transport).

The σ co-ordinate system is defined as:

$$\sigma = \frac{z - \zeta}{d + \zeta} = \frac{z - \zeta}{H} \quad \dots (3.3)$$

with

z	the vertical co-ordinate in physical space
ζ	the free surface elevation above the reference plane (at $z = 0$)
d	the depth below the reference plane
H	the total water depth, given by $d + \zeta$.

At the bottom $\sigma = -1$ and at the free surface $\sigma = 0$ (Figure 3.12). The partial derivatives in the original Cartesian co-ordinate system are expressed in σ co-ordinates by the chain rule introducing additional terms. The flow domain of a 3D shallow water model consists in the horizontal plane of a restricted (limited) area composed of open and closed (land) boundaries and in the vertical of a number of layers. In a σ co-ordinate system the number of layers is the same at every location in the horizontal plane, i.e. the layer interfaces are chosen following planes of constant σ , (Figure 3.13). For each layer a set of coupled conservation equations is solved.

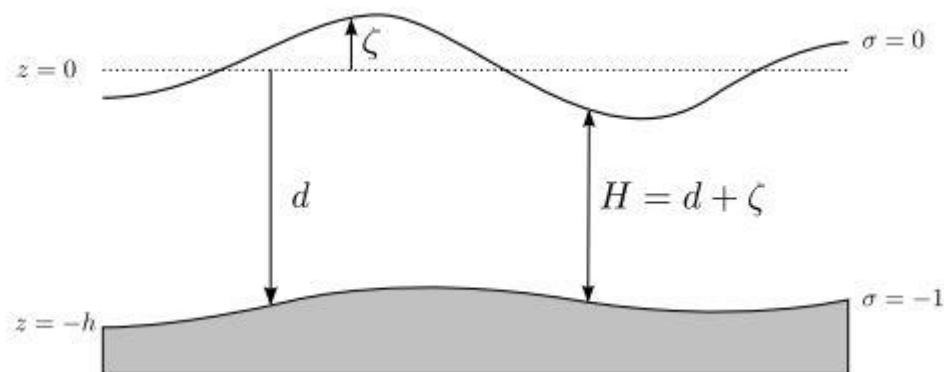


Figure 3.12: Definition of water level (ζ), depth (h) and total depth (H)

3.8.2.2 Cartesian co-ordinate system in the vertical (Z-model)

In coastal seas, estuaries and lakes, stratified flow can occur in combination with steep topography. Although the σ -grid is boundary fitted (in the vertical), it will not always have enough resolution around the pycnocline. The co-ordinate lines intersect the density interfaces that may give significant errors in the approximation of strictly horizontal density gradients. Therefore, recently a second vertical grid coordinate system based on Cartesian co-ordinates (Z-grid) was introduced in Delft3D-FLOW for 3D simulations of weakly forced stratified water systems. The Z-grid model has horizontal co-ordinate lines that are (nearly) parallel with density interfaces (isopycnals) in regions with steep bottom slopes. This is important to reduce

artificial mixing of scalar properties such as salinity and temperature. The Z-grid is not boundary fitted in the vertical. The bottom (and free surface) is usually not a co-ordinate line and is represented as a staircase (zig-zag boundary; Figure 3.13).

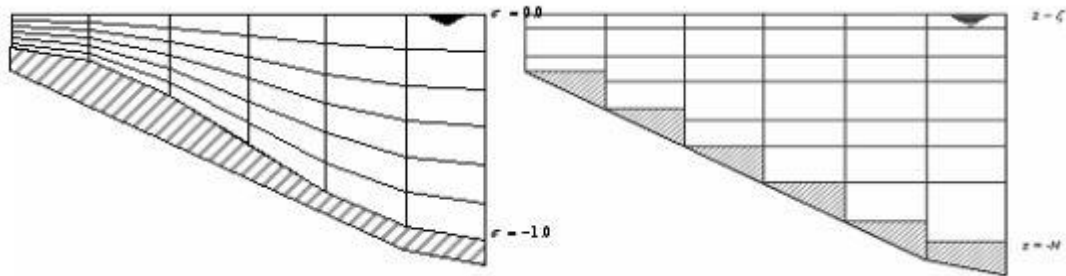


Figure 3.13: Example of σ - and Z-grid

3.8.2.3 Continuity equation

The depth-averaged continuity equation is derived by integration the continuity equation for incompressible fluids over the total depth, taken into account the kinematic boundary conditions at water surface and bed level and is given by:

$$\frac{\partial \zeta}{\partial t} + \frac{1}{\sqrt{G_{\xi\xi}}\sqrt{G_{\eta\eta}}} \frac{\partial((d + \zeta)U\sqrt{G_{\eta\eta}})}{\partial \xi} + \frac{1}{\sqrt{G_{\xi\xi}}\sqrt{G_{\eta\eta}}} \frac{\partial((d + \zeta)V\sqrt{G_{\xi\xi}})}{\partial \eta} = (d + \zeta)Q \quad \dots\dots (3.4)$$

with U and V the depth averaged velocities

$$U = \frac{1}{d + \zeta} \int_d^\zeta u \, dz = \int_{-1}^0 u \, d\sigma \quad \dots\dots\dots (3.5)$$

$$V = \frac{1}{d + \zeta} \int_d^\zeta v \, dz = \int_{-1}^0 v \, d\sigma \quad \dots\dots\dots (3.6)$$

and Q representing the contributions per unit area due to the discharge or withdrawal of water, precipitation and evaporation:

$$Q = \int_{-1}^0 (q_{in} - q_{out}) d\sigma + P - E \quad \dots\dots\dots (3.7)$$

with q_{in} and q_{out} the local sources and sinks of water per unit of volume [1/s], respectively, P the non-local source term of precipitation and E non-local sink term due to evaporation. We remark that the intake of, for example, a power plant is a withdrawal of water and should be modelled as a sink. At the free surface there may be a source due to precipitation or a sink due to evaporation.

3.8.2.4 Momentum equations in horizontal direction

The momentum equations in ξ - and η -direction are given by:

$$\begin{aligned} \frac{\partial u}{\partial t} + \frac{u}{\sqrt{G_{\xi\xi}}} \frac{\partial u}{\partial \xi} + \frac{v}{\sqrt{G_{\eta\eta}}} \frac{\partial u}{\partial \eta} + \frac{\omega}{d + \zeta} \frac{\partial u}{\partial \sigma} - \frac{v^2}{\sqrt{G_{\zeta\zeta}}\sqrt{G_{\eta\eta}}} \frac{\partial \sqrt{G_{\eta\eta}}}{\partial \xi} + \frac{uv}{\sqrt{G_{\zeta\zeta}}\sqrt{G_{\eta\eta}}} \frac{\partial \sqrt{G_{\xi\xi}}}{\partial \eta} - f_v \\ = - \frac{1}{\rho_0 \sqrt{G_{\xi\xi}}} P_\xi + F_\xi + \frac{1}{(d + \zeta)^2} \frac{\partial}{\partial \sigma} \left(\nu_V \frac{\partial u}{\partial \sigma} \right) + M_\xi \quad \dots\dots (3.8) \end{aligned}$$

$$\begin{aligned} \frac{\partial v}{\partial t} + \frac{u}{\sqrt{G_{\xi\xi}}} \frac{\partial v}{\partial \xi} + \frac{v}{\sqrt{G_{\eta\eta}}} \frac{\partial v}{\partial \eta} + \frac{\omega}{d + \zeta} \frac{\partial v}{\partial \sigma} + \frac{uv}{\sqrt{G_{\zeta\zeta}}\sqrt{G_{\eta\eta}}} \frac{\partial \sqrt{G_{\eta\eta}}}{\partial \xi} - \frac{u^2}{\sqrt{G_{\zeta\zeta}}\sqrt{G_{\eta\eta}}} \frac{\partial \sqrt{G_{\xi\xi}}}{\partial \eta} + f_u \\ = - \frac{1}{\rho_0 \sqrt{G_{\eta\eta}}} P_\eta + F_\eta + \frac{1}{(d + \zeta)^2} \frac{\partial}{\partial \sigma} \left(\nu_V \frac{\partial v}{\partial \sigma} \right) + M_\eta \quad \dots\dots (3.9) \end{aligned}$$

The vertical eddy viscosity coefficient ν_V is defined in Equation 3.10. Density variations are neglected, except in the baroclinic pressure terms, P_ξ and P_η represent the pressure gradients. The forces F_ξ and F_η in the momentum equations represent the unbalance of horizontal Reynold's stresses. M_ξ and M_η represent the contributions due to external sources or sinks of momentum (external forces by hydraulic structures, discharge or withdrawal of water, wave stresses, etc.).

$$\nu_V = \nu_{mol} + \max(\nu_{3D}, \nu_V^{back}) \quad \dots\dots\dots (3.10)$$

with ν_{mol} the kinematic viscosity of water. The 3D part ν_{3D} is computed by a 3D-turbulence closure model.

3.8.2.5 Vertical velocities

The vertical velocity ω in the adapting σ -co-ordinate system is computed from the continuity equation:

$$\frac{\partial \zeta}{\partial t} + \frac{1}{\sqrt{G_{\xi\xi}}\sqrt{G_{\eta\eta}}} \frac{\partial((d + \zeta)u\sqrt{G_{\eta\eta}})}{\partial \xi} + \frac{1}{\sqrt{G_{\xi\xi}}\sqrt{G_{\eta\eta}}} \frac{\partial((d + \zeta)v\sqrt{G_{\xi\xi}})}{\partial \eta} + \frac{\partial \omega}{\partial \sigma} = (d + \zeta)(q_{in} - q_{out}) \quad \dots (3.11)$$

Without these, the equations for hydrostatic pressure assumption, floating structures, Coriolis force etc. are also considered here (Manual, 2013).

3.8.3 Transport equations

The flows in rivers, estuaries, and coastal seas often transport dissolved substances, salinity and/or heat. In Delft3D-FLOW, the transport of matter and heat is modelled by an advection-diffusion equation in three co-ordinate directions. Source and sink terms are included to simulate discharges and withdrawals. Also first-order decay processes may be taken into account. A first-order decay process corresponds to a numerical solution which is exponentially decreasing. For more complex processes e.g. eutrophication, biological and/or chemical processes the water quality module D-Water Quality should be used.

The transport equation here is formulated in a conservative form in orthogonal curvilinear co-ordinates in the horizontal direction and σ co-ordinates in the vertical direction:

$$\begin{aligned} \frac{\partial(d + \zeta)c}{\partial t} + \frac{1}{\sqrt{G_{\xi\xi}}\sqrt{G_{\eta\eta}}} \left\{ \frac{\partial[\sqrt{G_{\eta\eta}}(d + \zeta)uc]}{\partial \xi} + \frac{\partial[\sqrt{G_{\xi\xi}}(d + \zeta)vc]}{\partial \eta} \right\} + \frac{\partial \omega c}{\partial \sigma} \\ = \frac{d + \zeta}{\sqrt{G_{\xi\xi}}\sqrt{G_{\eta\eta}}} \left\{ \frac{\partial}{\partial \xi} \left(D_H \frac{\sqrt{G_{\eta\eta}}}{\sqrt{G_{\xi\xi}}} \frac{\partial c}{\partial \xi} \right) + \frac{\partial}{\partial \eta} \left(D_H \frac{\sqrt{G_{\xi\xi}}}{\sqrt{G_{\eta\eta}}} \frac{\partial c}{\partial \eta} \right) \right\} + \frac{1}{d + \zeta} \frac{\partial}{\partial \sigma} \left(D_V \frac{\partial c}{\partial \sigma} \right) \\ - \lambda_d(d + \zeta)c + S \quad \dots (3.12) \end{aligned}$$

with D_H the horizontal diffusion coefficient, D_V the vertical diffusion coefficient, λ_d representing the first order decay process and S the source and sink terms per unit area due to the discharge q_{in} or withdrawal q_{out} of water and/or the exchange of heat through the free surface Q_{tot} :

$$S = (d + \zeta)(q_{in}c_{in} - q_{out}c) = Q_{tot} \quad \dots (3.13)$$

The total horizontal diffusion coefficient D_H is defined by

$$D_H = D_{SGS} + D_V + D_H^{back} \quad \dots\dots\dots (3.14)$$

with D_{SGS} the diffusion due to the sub-grid scale turbulence model and a user defined diffusion coefficient for the horizontal is used D_H^{back} . The horizontal diffusion coefficient may be used for calibration is independent of the horizontal eddy viscosity. This eddy diffusivity depends on the constituent.

The vertical diffusion coefficient D_V is defined by

$$D_V = \frac{v_{mol}}{\sigma_{mol}} + \max(D_{3D}, D_V^{back}) \quad \dots\dots\dots (3.15)$$

with D_{3D} the diffusion due to turbulence model in vertical direction and with v_{mol} the kinematic viscosity of water and σ_{mol} is either the (molecular) Prandtl number for heat diffusion or the Schmidt number for diffusion of dissolved matter.

For vertical mixing, the eddy viscosity ν_V is defined at input via the GUI (e.g. in case of a constant vertical eddy viscosity) or computed by a 3D-turbulence model. Delft3D-FLOW will also compute the vertical diffusion coefficients by taking into account the turbulence Prandtl-Schmidt number.

For shallow-water flow, the diffusion tensor is an-isotropic. Typically, the horizontal eddy diffusivity D_H exceeds the vertical eddy diffusivity D_V . The horizontal diffusion coefficient is assumed to be a superposition of three parts:

1. The 2D part D_{SGS} (*sub-grid scale turbulence*), due to motions and mixing that are not resolved by the horizontal grid.
2. The contribution due to 3D turbulence, D_{3D} , which is related to the turbulent eddy viscosity and is computed by a 3D turbulence closure model.
3. D_H^{back} representing the Reynolds-averaged equations and/or accounting for other unresolved horizontal mixing.

For depth-averaged simulations, the horizontal eddy diffusivity should also include dispersion by the vertical variation of the horizontal flow (so-called Taylor-shear dispersion). Delft3DFLOW has an option (so-called HLES approach) solving explicitly the larger scale horizontal turbulent motions. Then the 2D part $DSGS$ is associated with mixing by horizontal motions and forcing that cannot be resolved on the grid. The horizontal background diffusion

coefficient is represented by D_H^{back} and it is specified at input and it should account for all other forms of unresolved mixing (in most cases it is calibration parameter).

In addition to the vertical eddy diffusivity estimated by a 3D turbulence model may specify a background or “ambient” vertical mixing coefficient accounting for all other forms of unresolved mixing. In strongly stratified flows, breaking internal waves may be generated which are not modelled by the available 3D turbulence models of Delft3D-FLOW. Instead, can be specified the so-called Ozmidov length scale L_{oz} . Then, the 3D-turbulence part D_{3D} is defined as the maximum of the vertical eddy diffusivity computed by the turbulence model and the Ozmidov length scale:

$$D_{3D} = \max \left(D_{3D} 0.2 L_{oz}^2 \sqrt{-\frac{g}{\rho} \frac{\partial \rho}{\partial z}} \right) \dots\dots\dots (3.16)$$

For all turbulence closure models in Delft3D-FLOW a vertical background mixing coefficient D_H^{back} has to be specified by you via the GUI, Equation 3.15.

For two-dimensional depth-averaged simulations, the horizontal eddy diffusivity D_H^{back} should also contain a contribution due to the vertical variation of the horizontal flow (Taylor shear dispersion). This part is discarded by depth averaging the 3D advection diffusion equation. For the application of a depth-averaged transport model, the water column should be well mixed and the Taylor shear dispersion should be of secondary importance, otherwise a 3D model should be used for the simulation of the transport of matter.

Several turbulence closure models are implemented in Delft3D-FLOW. All models are based on the so-called “eddy viscosity” concept (Kolmogorov, 1942)(Prandtl, 1945). The eddy viscosity in the models has the following form:

$$v_v = c'_\mu L \sqrt{k} \dots\dots\dots (3.17)$$

Boundary conditions consist of (i) Bed and free surface boundary conditions and (ii) Lateral boundary conditions. Without these, hydrodynamic and morphodynamic equations with bed load and suspended load transport are considered here.

CHAPTER 4

DATA COLLECTION AND METHODOLOGY

4.1 General

In order to develop the mathematical model (hydrodynamic/morphological), various kinds of data of recent and previous years have been collected and compiled. These data also form the basis for further analysis and interpretation of the model results leading to accurate assessment of hydro-morphological condition of the study area. The following steps have been adopted to accomplish the activities mentioned in the objectives. The entire methodology has represented by a flow chart shown in Figure 4.1.

4.2 Work Analysis and Preparing Work Plan

For research work, pre-planning and homework is very much essential. In this study, it has tried to prepare a well understandable work plan. The total work plan has been prepared in such a way that it can fulfill the mentioned objectives of the study. All through it has been tried to follow the plan with some occasional violation for change of strategy. The well-defined flow chart has been prepared at the very beginning of the work plan according to the work analysis. In this flow chart various steps of the work have been defined. Different sub-works are also pre-defined in the work plan. The data collection procedure, its analysis and relevant software would help to reach the goal of objectives were defined. In the work plan it has also been defined about the output of the thesis and its goal. Some trial and error methods have been applied at model simulation and applications on different options.

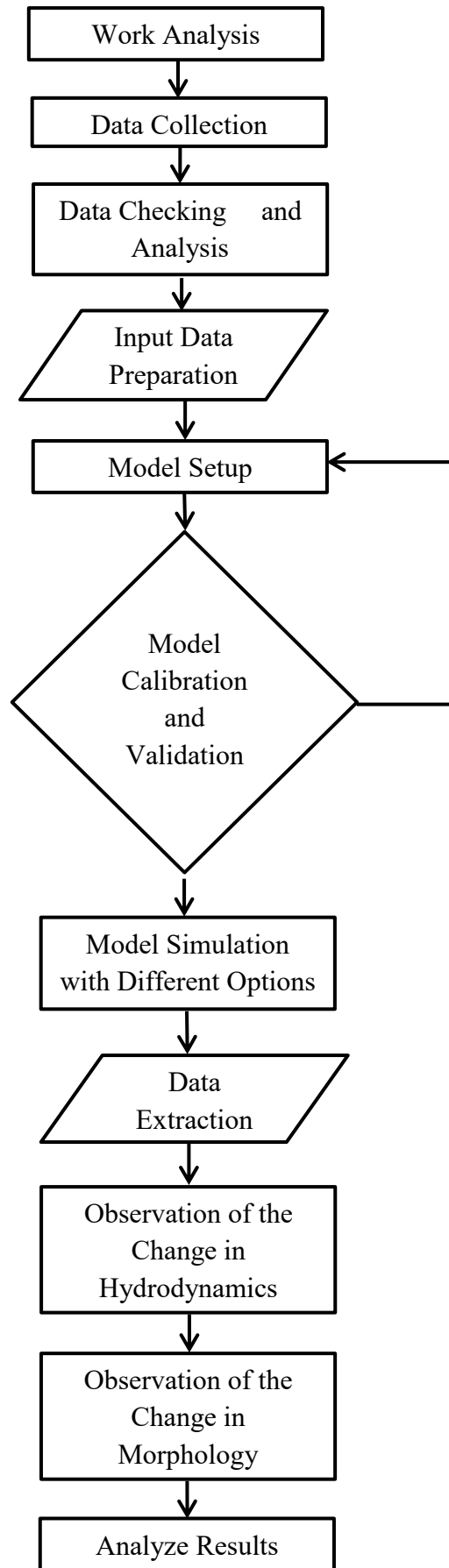


Figure 4.1: Flow chart showing the entire methodology

4.3 Data Collection

First of all it has been determined what sort of data would be needed. After that it has been identified where it would be found. This thesis work requires following data:

- Hydrometric data
- Bathymetric data
- Satellite Image data; and
- Sediment data

Hydrometric data includes water level and discharge. Historical water level and discharge data of Jamuna River has been collected from IWM and BWDB. Data on river cross section, sediment transport within the study area and satellite image data have been collected from Institute of Water Modelling (IWM) and Center for Environmental and Geographic Information Services (CEGIS).

4.3.1 Hydrometric Data

The hydrometric data includes water level and discharge data. Hydrometric data are necessary to define model boundary and to compare the model generated results with the observed data.

Table 4.1 shows the station name and the period of collecting data within the study area.

Table 4.1: Available Water Level & Discharge Data

Name of station	Data type	Duration
Bahadurabad	Discharge & WL	1995-2013
Sirajganj	Water level	1988-2013

Water Level

Historical water level data of the Jamuna River at Bahadurabad, Sirajganj and Aricha have been collected and analyzed to get an idea about the flow pattern and the amount of water is flowing at this location. Figure 4.2 shows the water level hydrographs of Jamuna River at Sirajganj for different periods.

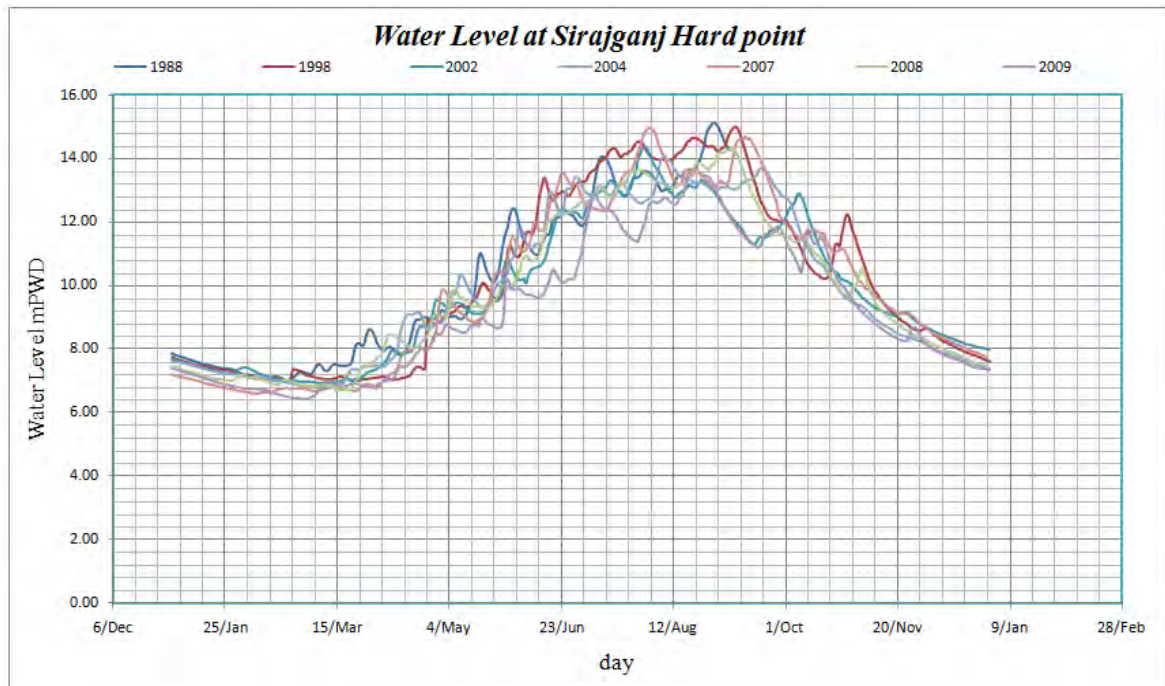


Figure 4.2: Historical water level data at Sirajganj hard point

Discharge

Generally, the peak discharge occurs between July and September and the lowest discharge in February-March of the year. The discharge of the Jamuna River shows significant seasonal variation with snowmelt in the Himalayas and rainfall occurred in Assam and Bangladesh have significant contribution. Figure 4.3 shows the rated discharge hydrographs of the Jamuna River at Bahadurabad for different years.

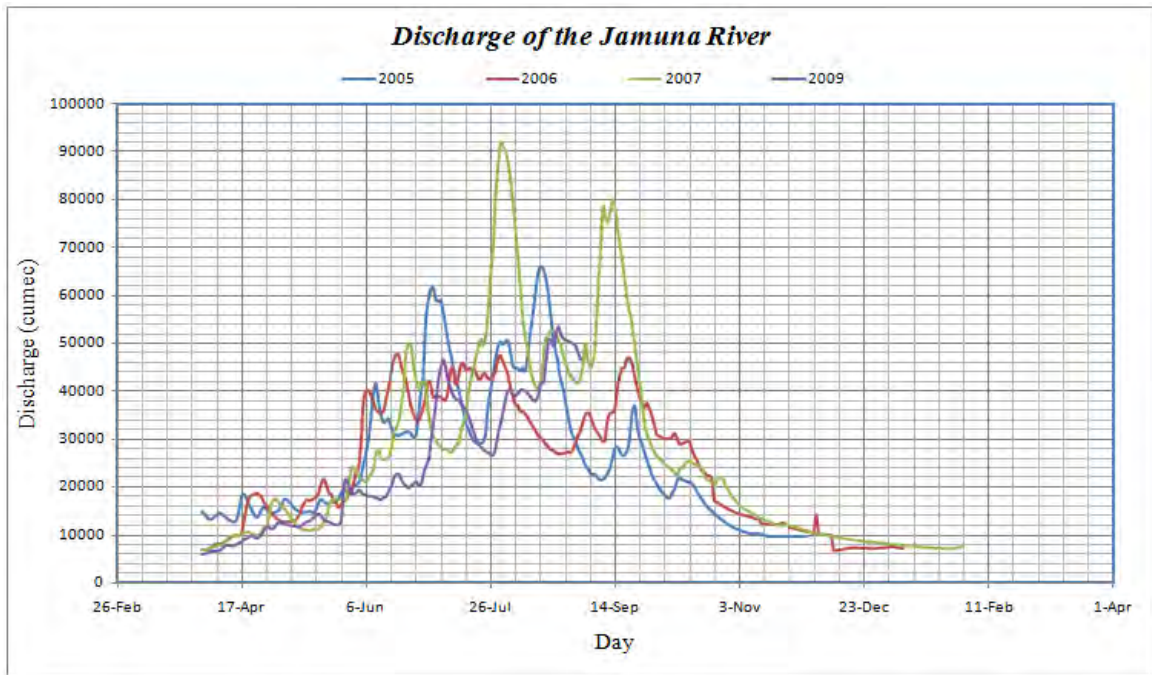


Figure 4.3: Historical discharge hydrographs at Bahadurabad station

4.3.2 Bathymetric Data

The pre-monsoon 2010 bathymetry data of Jamuna River has been collected from IWM. This surveyed bathymetry data covers the reach from 30 km upstream of Bangabandhu Bridge to 20 km downstream of that bridge. Figure 4.4 shows the transect lines of bathymetry data within this reach.

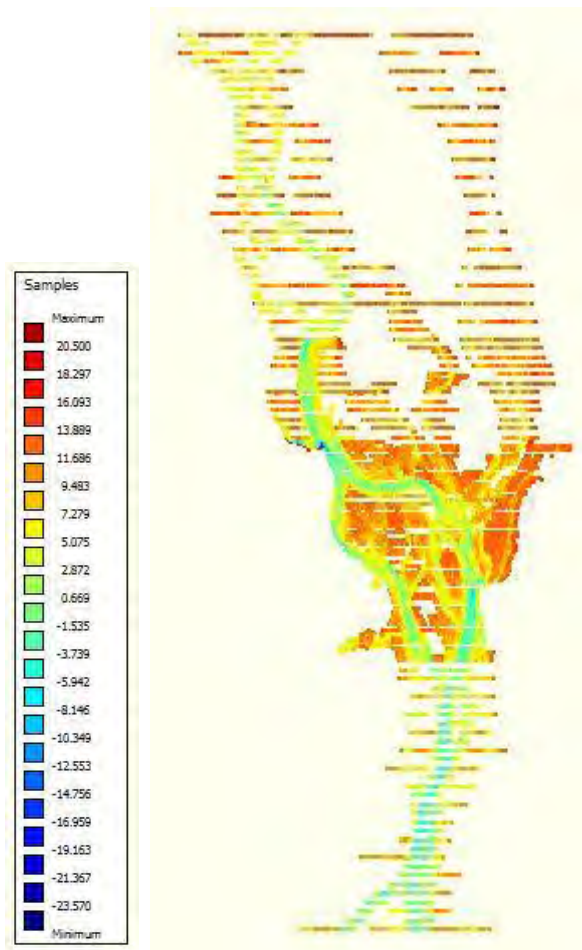


Figure 4.4: Bathymetric data of 50 km reach of the Jamuna River

4.3.3 Satellite Image

The satellite images of Jamuna River for 2010 to 2012 have been collected from CEGIS and used to show the study area and observe the bankline shifting.

4.3.4 Sediment Data

The collected sediment data of the Jamuna River includes suspended sediment and bed sample data. The status of the collected sediment data is shown in Table 4.2.

Table 4.2: Status of collected sediment data of the Jamuna River

Sediment data				
River name	Station name	Station ID	Data period	Source
Jamuna	Bahadurabad	SW46.9L	2000-2012	BWDB

4.3.5 Field Visit and Bed Sample Collection

A reconnaissance field visit was done to observe the actual field conditions, to collect some bed sample data and to interact with the officials of Bangladesh Water Development Board (BWDB) office of Sirajganj. Two samples of the bed material of the Jamuna River were collected from the study area. Necessary information was collected from the officials of Sirajganj BWDB. The bed samples were analyzed to determine the mean diameter of the bed materials. The results of the bed sample analysis are given below:

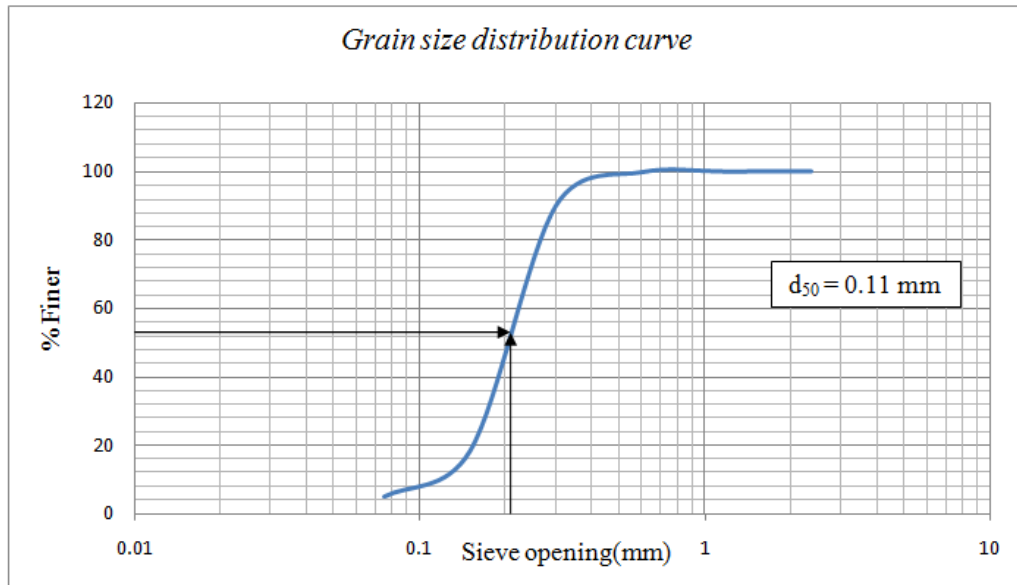


Figure 4.5: Grain size distribution of sample 1

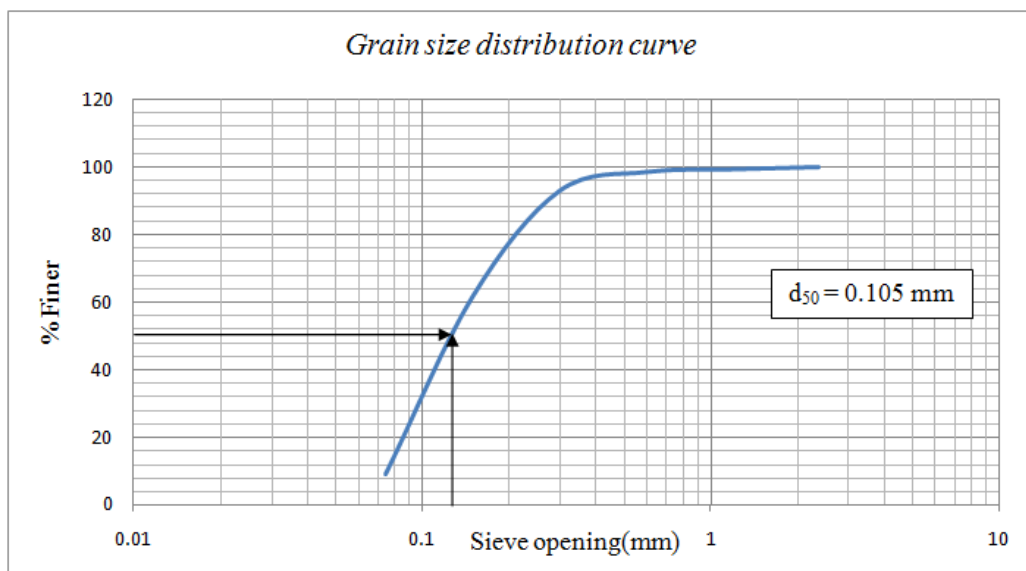


Figure 4.6: Grain size distribution of sample 2

From soil sample 1 the value of d_{50} is 0.11 mm and from sample 2 it is 0.101 mm. The two values are approximately equal. Average of the above two value is 0.11 mm. Using the value of d_{50} critical bed shear stress can be determined by Fischenich formula.

Fischenich, (2001) lists the following equations presented by Julien to approximate the critical shear stress for particles of various sizes.

$$\tau_{cr} = 0.25 d_*^{-0.6} \times g (\rho_s - \rho_w)d \tan\phi ; \text{ for silts and sands} \dots\dots\dots (4.1)$$

Where

$$d_* = d \left[\frac{(G-1)g}{\nu^2} \right]^{1/3} \dots\dots\dots (4.2)$$

ϕ = angle of repose of the particle, G = specific gravity of sediment, g = acceleration due to gravity, ρ_s = density of sediment, ρ_w = density of water, ν = kinematic velocity and d = size of the particle of interest.

For the soil of Jamuna River, $\phi = 30^0$, $G = 2.65$, $g = 9.81 \text{ m/s}^2$, $\rho_s = 2650 \text{ kg/m}^3$, $\rho_w = 1000 \text{ kg/m}^3$, $\nu = 10^{-6} \text{ m}^2/\text{s}$, $d_{50} = 0.11 \text{ mm}$. $d_* = 2.783$.

The value of critical shear stress $\tau_{cr} = 0.14 \text{ N/m}^2$

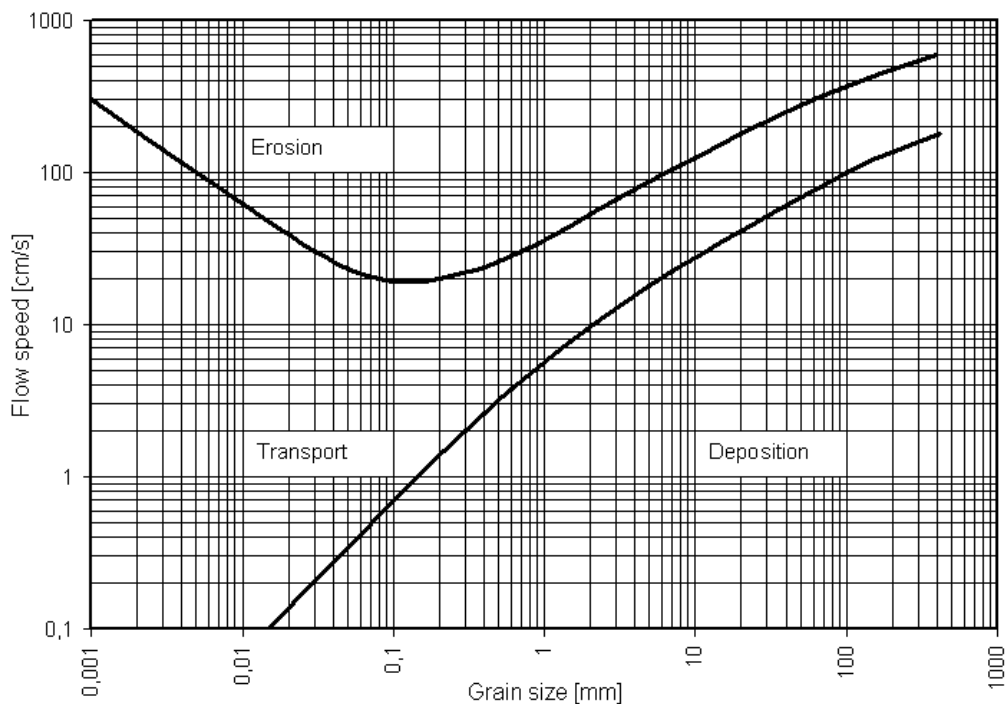


Figure 4.7: Hjulströms diagram (Hjulström, 1935)

Figure 4.7, which is known as Hjulströms diagram, shows the relationship between the flow velocity and grain size associated with the sediment transport. There are three zones as erosion, deposition and transport. Depending upon the value of flow velocity and grain size, the morphological feature can be assessed whether it will cause erosion, deposition or transportation. In this specific case of the Jamuna River, the average grain size is 0.11 mm and the critical velocity is 20 cm/s (0.2 m/s). From the figure, if the velocity is more than 20 cm/s, erosion will take place. For deposition, the velocity should be less than 0.7 cm/s. The transport zone lies in between the above two values for this grain size.

4.4 Methodology

To fulfill the objectives of this study, river morphodynamics have been analyzed with modeling software. Here, the change in hydrodynamic parameters as well as morphology has been assessed simulating the 50 km reach of the Jamuna River with Delft3D modeling software. Now in the next section, the typical model setup in Delft3D software has been discussed and in the next chapter the model setup for the selected reach of the Jamuna River has been shown.

4.5 Model Setup

Deltares has developed a unique, fully integrated computer software suite for a multi-disciplinary approach and 3D computations for coastal, river and estuarine areas. It can carry out simulations of flows, sediment transports, waves, water quality, morphological developments and ecology. It has been designed for experts and non-experts alike. The Delft3D suite is composed of several modules, grouped around a mutual interface, while being capable to interact with one another. Delft3D-FLOW, which this manual is about, is one of these modules. Delft3D-FLOW is a multi-dimensional (2D or 3D) hydrodynamic (and transport) simulation program which calculates non-steady flow and transport phenomena that result from tidal and meteorological forcing on a rectilinear or a curvilinear, boundary fitted grid.

In order to set up a hydrodynamic model at first an input file must be prepared. All parameters to be used originate from the physical phenomena being modelled. Also from the numerical techniques being used to solve the equations that describe these phenomena, and finally, from decisions being made to control the simulation and to store its results. Within the range of realistic values, it is likely that the solution is sensitive to the selected parameter values, so a concise description of all parameters is required. The input data defined is stored into an input

file which is called the Master Definition Flow file or MDF-file. To do this, one should use the FLOW Graphic User Interface (GUI). In the GUI (Fig. 4.8), the process of the model setup consists some sub-sections that are described below.

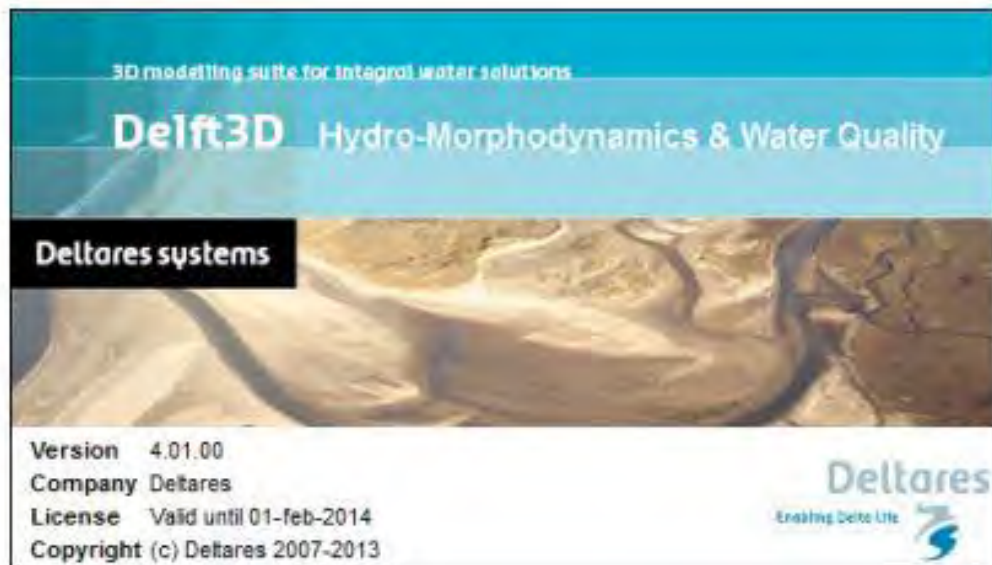


Figure 4.8: Title window of Delft3D

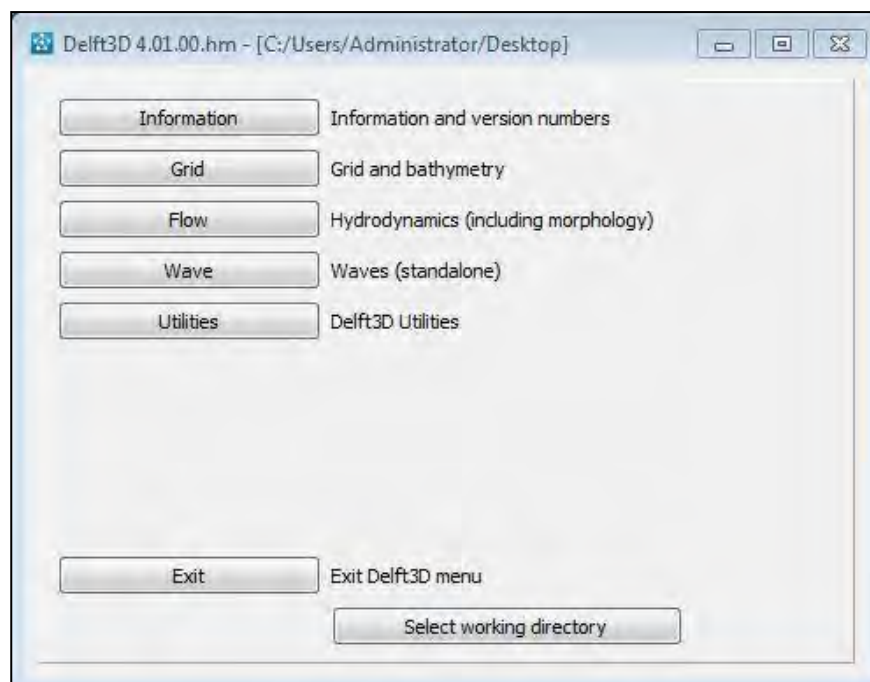


Figure 4.9: Graphic User Interface (GUI) of Delft3D

4.5.1 RGFRID

RGFRID is a graphical program for generation and manipulation of grids, allowing the generation of orthogonal, curvilinear grids of variable grid size for the computations. The variable grid sizes allow for a high resolution in the area of interest and a lower resolution far away at the model boundaries, thus saving computational effort. Furthermore, the grid lines may be curved to follow land boundaries and channels smoothly, avoiding the so-called staircase boundaries that may induce artificial diffusion. The grid-generator RGFRID is designed so that grids can be created and modified with minimum effort, fulfilling the requirements of smoothness and orthogonality. Various grid manipulation options are provided in order to fine tune the grid. All operations are incorporated in a graphical interface, providing easy control of the grid generation process.

4.5.2 QUICKIN

QUICKIN is a graphical program for interpolation and modification of bathymetric data to the form accepted by the Delft3D modules. Often the depth samples (raw data) are originated from various sources, each of different date, quality and resolution. In order not to contaminate high quality samples with low quality samples, QUICKIN allows for subsequent loading of data sets. The FLOW and WAVE modules use equations that in fact are averaged over the grid dimensions. Therefore, the best results are obtained if the model bathymetry approximates the real bathymetry in an averaged sense rather than in a local sense. Thus, if the sample resolution is higher than the grid resolution, an averaging method is required. On the other hand, if there are less sample points than grid points, a triangulation interpolation method is preferred. The various interpolation methods and step-by-step approach of generating an optimal model bathymetry are operated from a graphical user interface. Fig. 4.9 shows the window for RGFRID and QUICKIN.

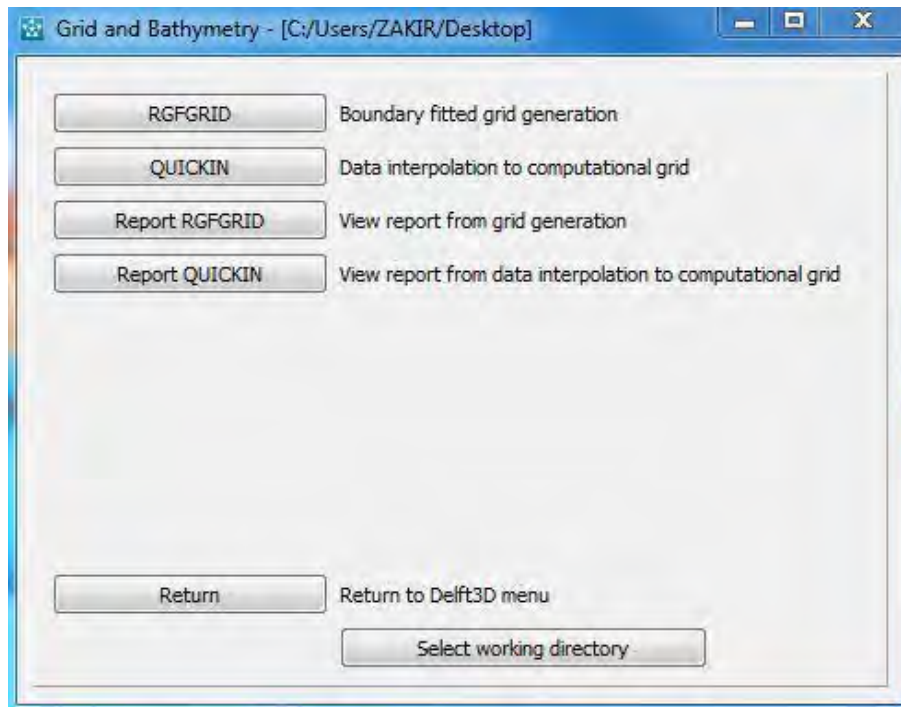


Figure 4.10: RGFGRID and QUICKIN window

4.5.3 QUICKPLOT

QUICKPLOT is a post-processing program used to visualize the outcome of different simulation processes, with the possibility of a graphical and/or numerical representation of the results. QUICKPLOT allows uniform access to all types of data files produced by the Delft3D modules, to select and visualize computational results and measured data.

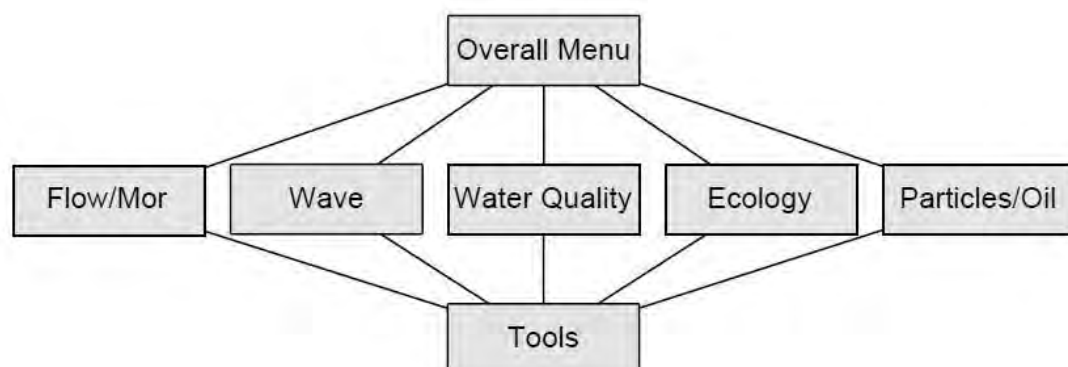


Figure 4.11: Structure of Delft3D

4.5.4 Dry Points

Dry points are grid cells centred around a water level point that are permanently dry during a computation, irrespective of the local water depth and without changing the water depth as seen from the wet points. Dry points are specified as a line of dry points; a single dry point is specified as a line of unit length.



Figure 4.12: Sub-data group Dry points

4.5.5 Thin Dams

Thin dams are infinitely thin objects defined at the velocity points which prohibit flow exchange between the two adjacent computational cells without reducing the total wet surface and the volume of the model. The purpose of a thin dam is to represent small obstacles (e.g. break-waters, dams) in the model which have sub-grid dimensions, but large enough to influence the local flow pattern. Thin dams are specified as a line of thin dams; a single thin dam is specified as a line of unit length. The line of thin dams is defined by its indices of begin and end point, $(m1;n1)$ and $(m2;n2)$, respectively, and the direction of thin dam (u- or v-direction). Thin dams can be specified either manually or via an imported file with mask `<thd>`.

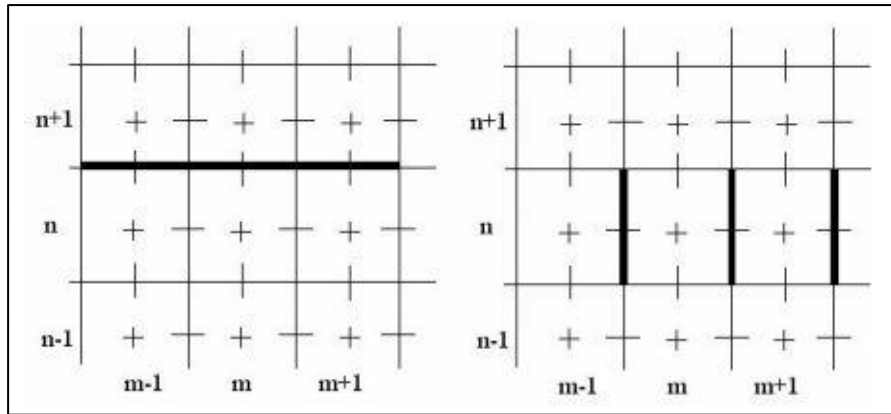


Figure 4.13: Equivalence of v-type thin dams (left) and u-type thin dams (right) with the same grid indices, ($M-1$ to $M+1$, N)

4.5.6 Modeling Framework

For the objectives of this research, only the FLOW modules and MOR modules have been used. In fact, in this case the MOR module is not working as an independent unit, but as a morphology extension integrated to the FLOW module. Thus, the sediment transport option in FLOW allows the use of several of the existing functionalities in the MOR module has been used. During the simulation, the FLOW module calculates non-steady flow and transport phenomena that result from tidal and meteorological forcing on a rectilinear or a curvilinear, boundary fitted grid (previously generated using RGFGRID). The hydrodynamic conditions (velocities, water elevations, density, salinity, vertical eddy viscosity and vertical eddy diffusivity) calculated in the FLOW module is used as input to the MOR modules. The MOR module integrates the effects of waves, currents and sediment transport on morphological developments, which are used for the next simulation of the FLOW modules. This is a cyclical routine that can be modeled as a hierarchical tree structure of processes, the process tree, in which time intervals for the elementary processes are defined. Processes may be executed a fixed number of times, for a given time span or until some condition is met. The link between the involved process modules (FLOW and MOR) occurs via a dynamic coupling. This allows a feedback between the processes which can affect water flow and sediment movement.

4.5.7 Space and Time Variation

Physical phenomena vary on space and time, therefore a dimensional description of the natural processes is required for an accurate representation of the reality. The numerical hydrodynamic modeling system FLOW solves the unsteady shallow water equations in two (depth-averaged) or in three dimensions. The system of equations consists of the horizontal equations of motion, the continuity equation, and the transport equations for conservative constituents. In this case, to model the morphological conditions in Jamuna River, it has been decided to use a time dependent, two-dimensional approach, because the sediment transport, which is the process of interest for this study, can efficiently and accurately be modeled in 2D. Besides, 2D modeling requires less computational time, therefore allowing more test-runs for the calibration as well as for the representation of multiple scenarios. Furthermore, the variation of time scales for the diverse natural processes (ranging from the order of hours or days in the hydrodynamic simulations, to the order of months and years in the morphological simulations) represents a difficulty for the integrated modeling of such processes. Long morphological simulations are achieved by using the morphological time scale factor that scales up the speed of the changes in the morphology to a rate that it begins to have a significant impact on the hydrodynamic flows. The implementation of the morphological time scale factor is achieved by simply multiplying the erosion and deposition fluxes from the bed to the flow and vice-versa by this scale factor, at each computational time-step. This allows accelerated bed-level changes to be incorporated dynamically into the hydrodynamic flow calculations.

4.5.8 Model Stability Check, Calibration and Validation

In case of a model study, stability of the model is checked first. If the model is unstable, then it will not run. When the model run with the given parameters successfully, then it can be said as stable model. After simulation, calibration is must for a model. If not calibrated, the model is valueless. When the model is calibrated with the real data and shows satisfactory results then the model is validated against other similar types of data. The calibration for existing situation has been done to check the accuracy of the developed model with real physical process of the river using the boundary data (discharge and water level). The base model has been calibrated for the 2012 hydrological year and validated against the year of 2013. Moreover sediment transport has also been calibrated with the historical sediment discharge available. To do this sediment rating curve has been prepared and model

simulated sediment discharge and corresponding flow discharge was extracted. Then the relation between sediment discharge and flow discharge of the simulated results have been tried to keep close to the sediment rating curve. Here several sediment transport formulas were used in different simulation to get the appropriate relationship.

4.5.9 Different Option Simulation

After calibration the model is ready to run various sceneries for various analyses. Here the different options are structural intervention in the river. Groynes/spurs of varying number and spacing have been inserted to observe the hydro-morphological change of the selected reach of the river Jamuna. The following Table 4.3 shows the simulations for different options.

Table 4.3: Simulation of the model with different options

Run no.	Condition	Spacing and Length (S/L) ratio of groyne	Observation parameters
Base	Without any structure	--	Hydrodynamic and morphologic
Option 1	With number of groyne 1	--	Hydrodynamic and morphologic
Option 2	With number of groyne 2	1.0	Hydrodynamic and morphologic
Option 3	With number of groyne 2	1.5	Hydrodynamic and morphologic
Option 4	With number of groyne 2	2.0	Hydrodynamic and morphologic
Option 5	With number of groyne 3	1.0	Hydrodynamic and morphologic
Option 6	With number of groyne 3	1.5	Hydrodynamic and morphologic
Option 7	With number of groyne 3	2.0	Hydrodynamic and morphologic

4.5.10 Data Extraction

Finally data have been extracted using QUICPLOT according to the requirement. Here in this thesis work for development of relationship between the number and/or spacing of the groyne and sedimentation, it has been required to extract the following data-

- Water level and water depth
- Depth Averaged velocity
- Total transport
- Bed shear stress
- Plan view
- Cross-section
- Erosion/sedimentation
- Velocity vector

CHAPTER 5

MODEL SETUP FOR SELECTED REACH OF THE JAMUNA RIVER

5.1 General

Mathematical modeling in engineering practice has made the analysis and prediction of different parameters easier with compared to the previous hand calculation. To evaluate such parameters involved in the river response due to structural intervention, a two-dimensional hydro-morphological model, Delft3D has been used. Using this modeling software a model of the Jamuna River in a selected reach has been set. The various key steps of the model setup are described below.

5.2 Model Setup for Selected Reach of the Jamuna River

Two-Dimensional model (Hydrodynamic and Morphological) has been developed using Delft3D Modelling Software (Deltares, open source software, Netherlands), which is an advanced mathematical modelling software for simulation of hydrodynamics for unsteady flow, sediment transport, morphology and water quality for fluvial, estuarine and coastal environments. Setting up of a 2-D hydro-morphological model comprises firstly, computational grid generation and secondly, preparation of the bathymetry on these grid cells. In this regard, bathymetry of Jamuna River of 50 km reach for the year 2010 has been used for the model. The upstream boundary and downstream boundary have been set up according to the model area then calibration and validation have been done. Finally some transverse structures like groynes have been inserted at the erosion prone area with different numbers and spacing for observing the change in hydrodynamic and morphologic parameters due to the structures. Actually this is an experimental study with mathematical simulation to find out the relationships among the hydrodynamic parameters and morphologic process with the varying number and spacing of the structures in a braided river like the Jamuna.

5.2.1 Grid Generation

The curvilinear grid has been generated based on the bathymetric survey in 2010. The minimum grid size is $50\text{ m} \times 50\text{ m}$ and number of grids in M-direction are 152 that are across the river and in N-direction 752 which are along the river, i.e. 114304 grid points in total. The grid has land boundaries as well. The model simulates the hydrodynamic and morphological parameters in every computational grid point. The computational grid is shown in Figure 5.1.

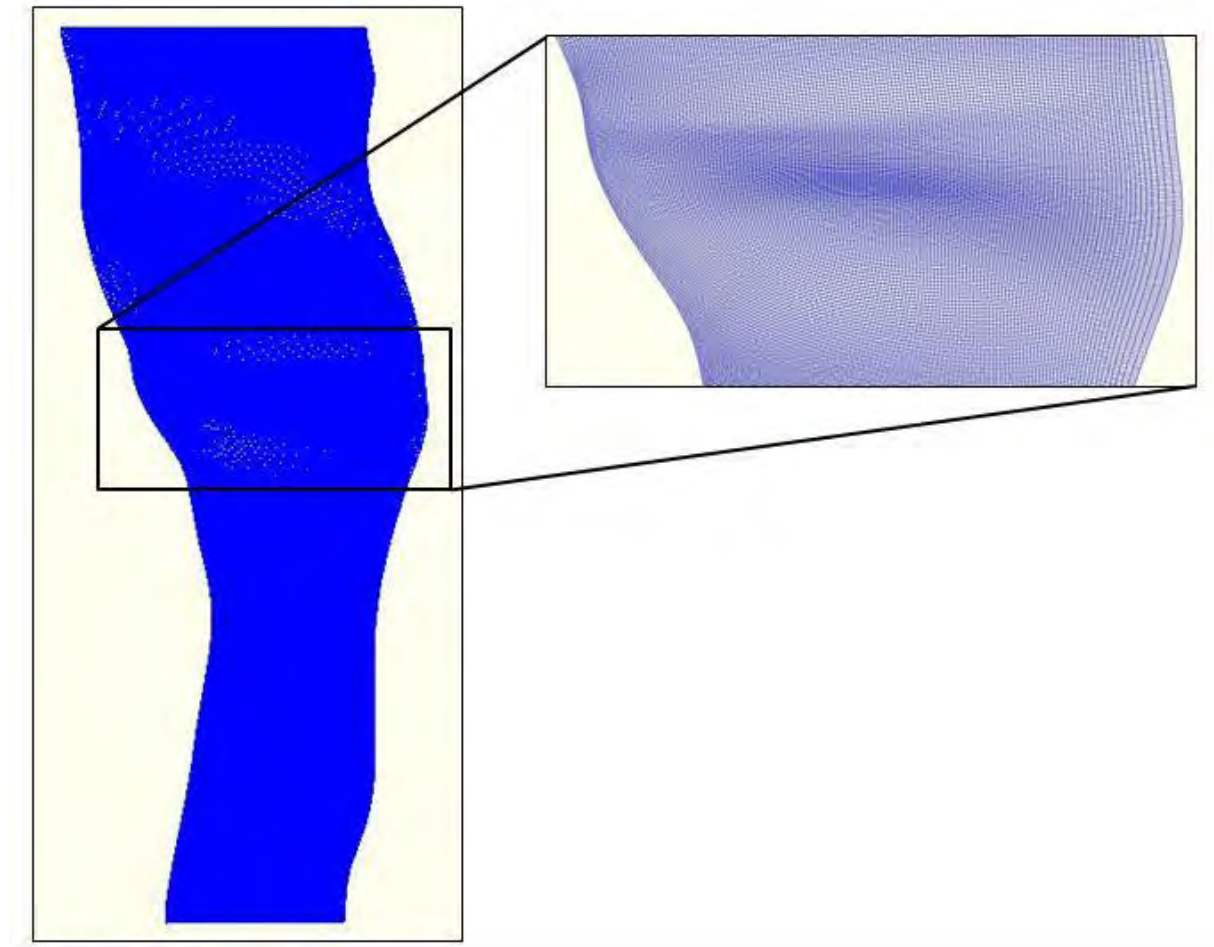


Figure 5.1: Computational Grid cell of Jamuna River in the study area

5.2.2 Bathymetry

The bathymetry of the model has been prepared based on data from the IWM bathymetric survey carried out during Pre-monsoon 2010. A part of the initial bathymetry of the model appears in Figure 5.2. To simulate the morphological model with different hydrological flood events, the bathymetry data has been superimposed on the curvilinear grid (Figure

5.1). It means every grid cell contains river cross-section data and after model simulation every grid cell produces hydrological and hydraulic parameters like, water level, discharge, water depth, velocity, bed scour and others.

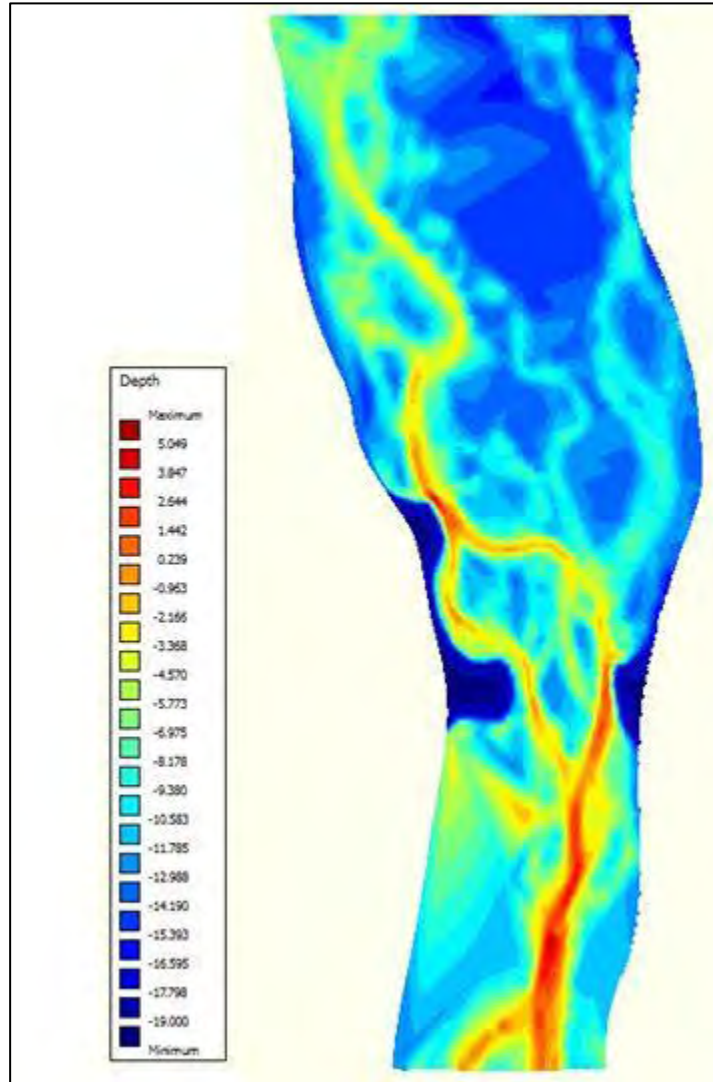


Figure 5.2: Model bathymetry of Jamuna River in the study area

5.2.3 Boundary Conditions

Developed morphological model has been simulated for flow conditions all through the year. Upstream boundary of the model is located at about 21 km upstream of Sirajganj Hard point (29 km upstream of the Jamuna Bridge) which is far enough for inaccuracy in upstream conditions would have negligible impacts to analysis results. For upstream boundary of the model, discharge time series data was used for both short term and long term simulations. The time series discharge data measured at Bahadurabad. Figure 5.3 represents

the upstream boundary location. Downstream boundary of the model is 19 km far from the hard point.

For the downstream boundary water level time series data was used. At the downstream boundary of the model (20 km downstream of the bridge) there was no observed water level data. Water level data for that location has been generated based on the water surface slope of the Jamuna comparing the observed water level data at Sirajganj hard point. Figure 5.3 also represents the downstream boundary location.



Figure 5.3: Upstream and downstream boundaries of the model

The time series discharge data for upstream and time series water level data for downstream are shown in Figure 5.4 and 5.5 respectively.

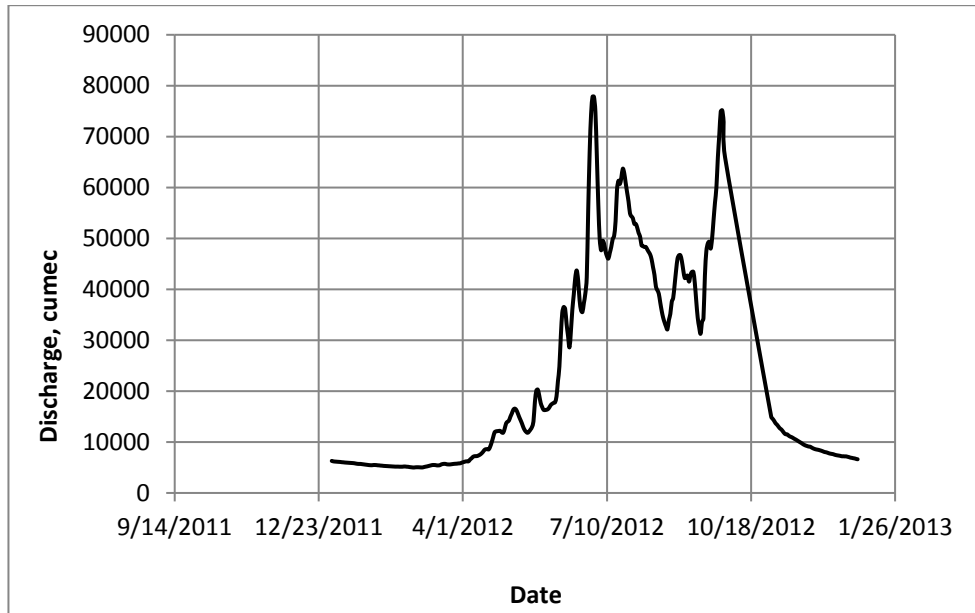


Figure 5.4: Flow conditions applied at upstream boundary of the model

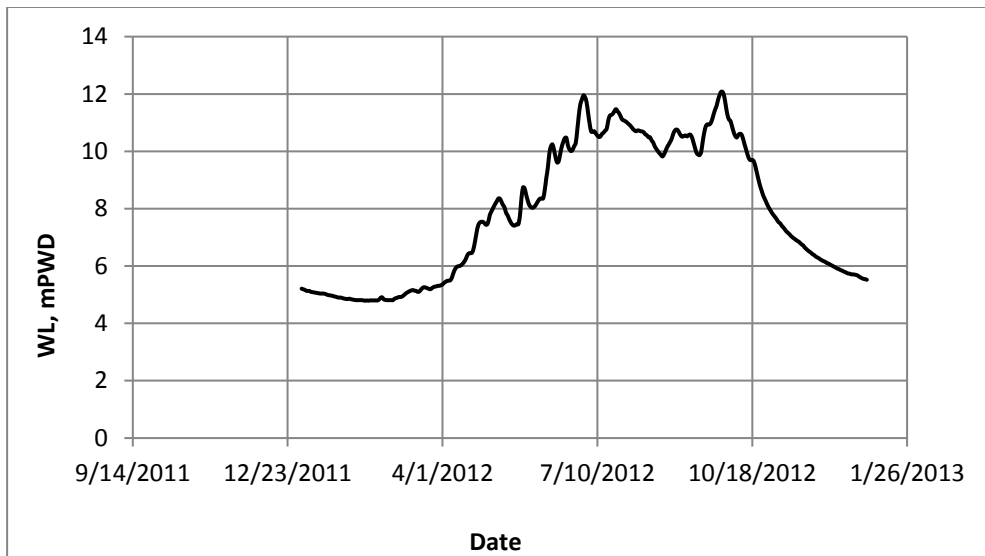


Figure 5.5: Downstream water level boundary for the model

5.2.4 Additional Parameters

The following parameters have been used for simulation of the 2-D morphological model of Jamuna River.

Table 5.1: Summary of the parameters used for the model of Jamuna River

Time step (min)	Sediment transport equation	Manning's n	Eddy viscosity (m ² /s)	Morphological scale factor
1	Van Rijn	0.018	1	1.0

5.2.5 Model Calibration

The base model has been calibrated for the 2012 hydrological year. Total four simulations have been made to achieve the goal. The calibration plot is shown in Figure 5.6. Here the Manning's roughness coefficient 'n' is the tuning parameter for calibration. For the calibration of the model, the monsoon period of 2012 hydrologic year has been simulated with the necessary data and boundary conditions. For comparison, the measured water level data of Sirajganj hard point station (SW 49) was available. Different simulations have been done for one month (July 2012) with the tuning parameter Manning's n to match the simulated water level data with the observed. Here the trial n values are 0.018, 0.020, 0.025 and 0.030 respectively. The maximum percentage of error for n value 0.018, 0.020, 0.025 and 0.030 are 1.39%, 3.39%, 7.76% and 11.81% respectively. So, n = 0.018 is the best match for the calibration as shown in Figure 5.6 also. Then the calibration has been done for the total monsoon (June to September) of the year 2012 which is shown in Figure 5.7. The maximum percentage of error in this case is 7.39% which is quite acceptable.

After the mentioned calibration, another one has been done comparing the simulated water level with the water level data at Bangabandhu Bridge site. Though the actual measured data of Bangabandhu Bridge site was not available but from the water surface slope of the Jamuna (7 cm/km) the data at Bridge site has been generated with respect to the Sirajganj station. The second calibration also shows satisfactory results. Fig. 5.8 shows the water level calibration figure at Bangabandhu Bridge site. Both the calibrations shows satisfactory results and the percentage of errors are quite acceptable (Moriasi *et al.*, 2007).

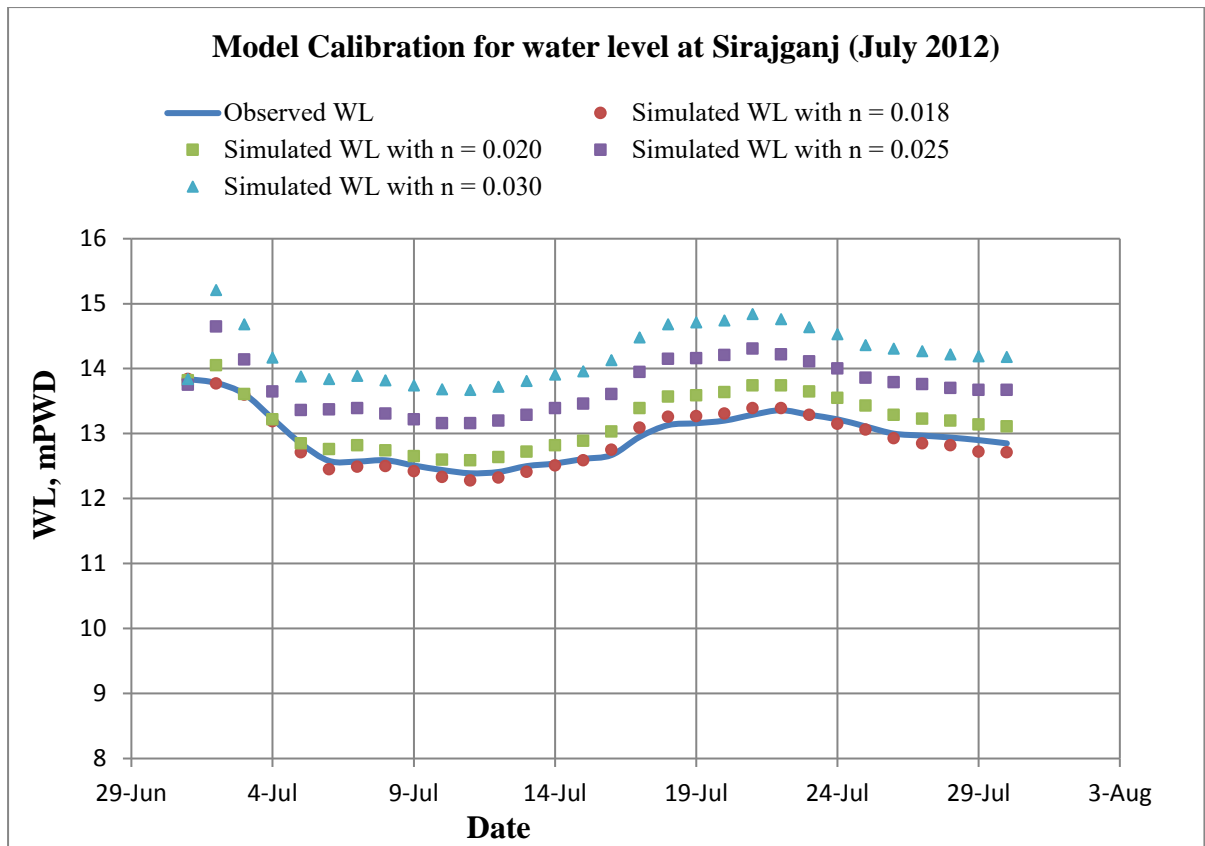


Figure 5.6: Comparison of model simulated and observed water levels of Jamuna River at Sirajganj for different 'n'.

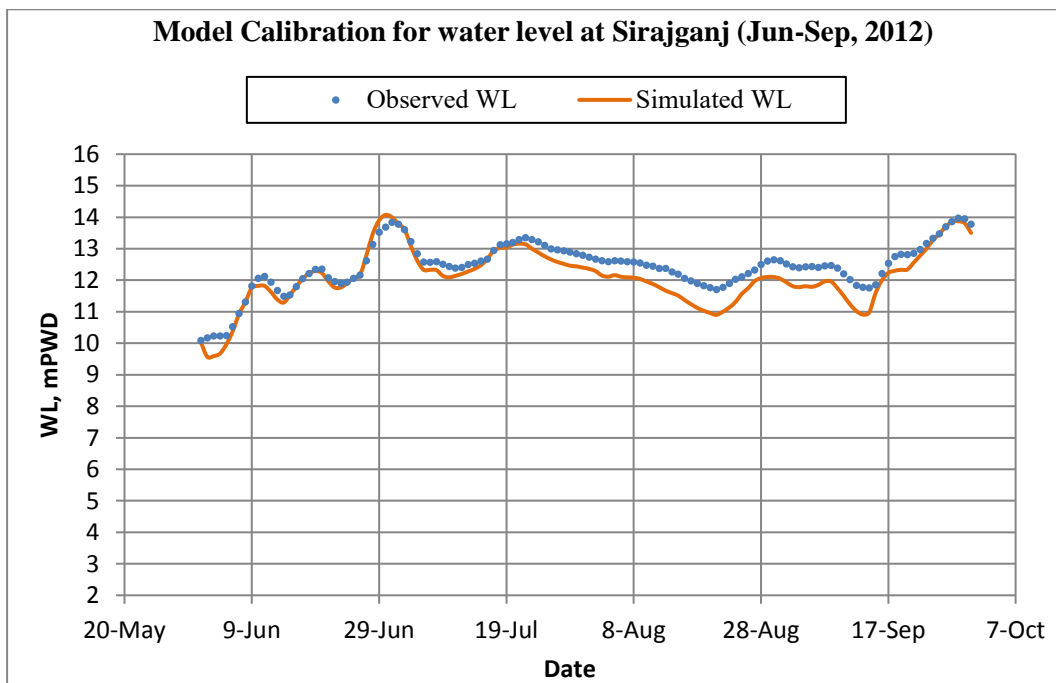


Figure 5.7: Comparison of model simulated and observed water levels of Jamuna River at Sirajganj for the monsoon of 2012

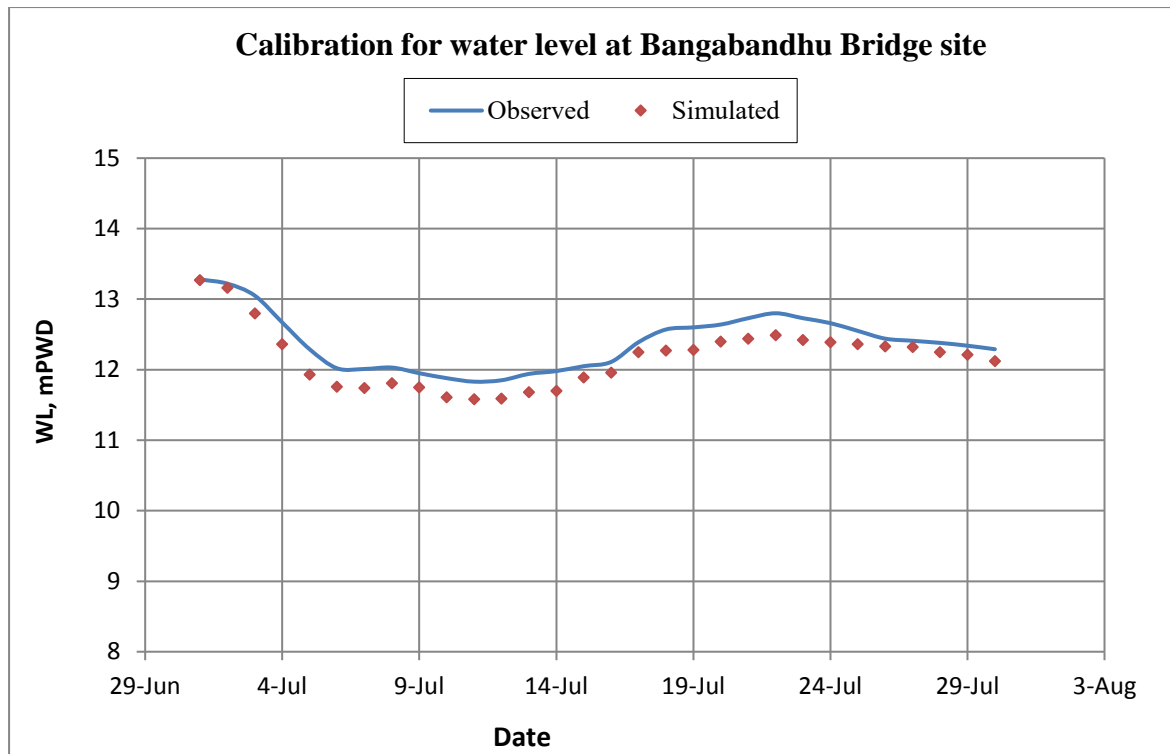


Figure 5.8: Calibration of the model at Bangabandhu Bridge site for water level

5.2.6 Model Validation

Here the simulated results have also been checked for validation with the water level data of 2013 shown in Figure 5.9. In front of Sirajganj hard point it matched quite well and the percentage of error is 4.17% that is quite acceptable.

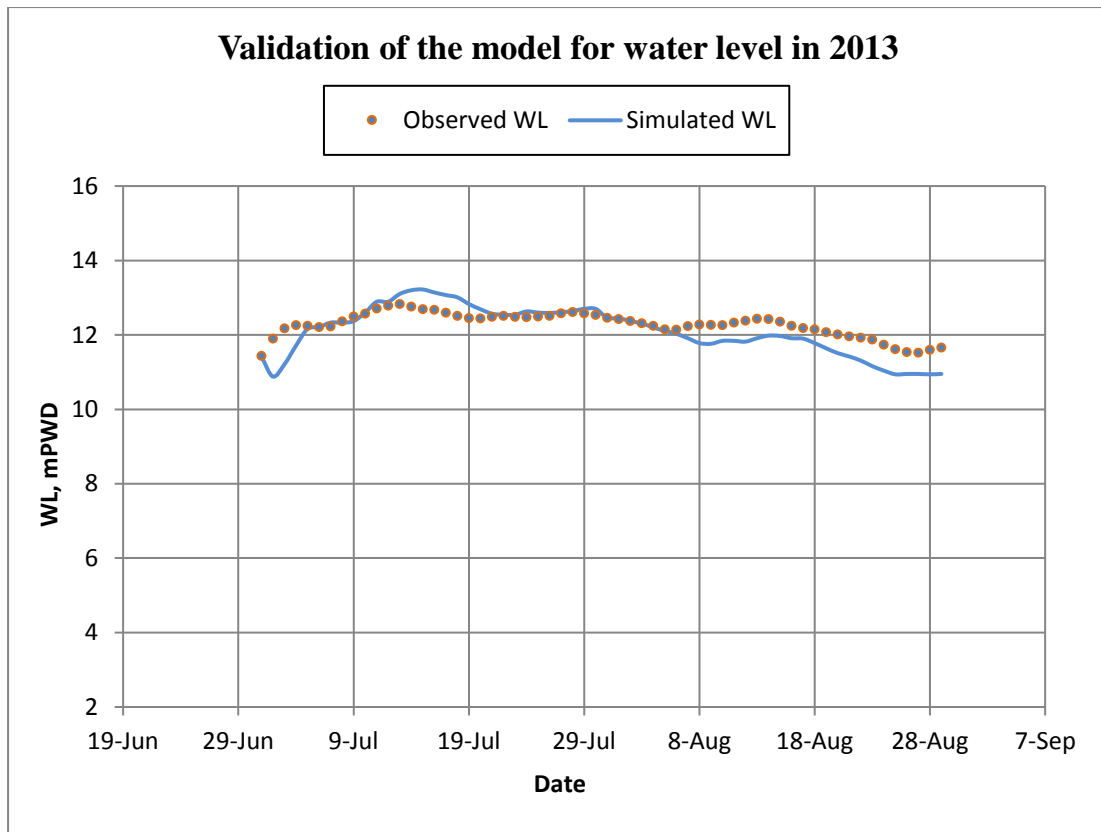


Figure 5.9: Validation of the model simulated and observed water level data at Sirajganj for the year 2013

5.2.7 Morphological Calibration of the Model

Morphological calibration is a difficult task for the river like Jamuna. Here in the model the simulation was done with the equilibrium sediment at inflow boundaries. And from the output of the model, the sediment discharge has been compared with the observed sediment data collected previously in comparison with the respective water discharge. The sediment data of any river in Bangladesh is rare and not available like water level and discharge data and the data is discrete also. So the calibration of the sediment is not quite well as the water level calibration. Here for the morphologic calibration the trend line analysis has been done of the observed data and the simulated data also. There are some differences in the slope of the trend line but in case of sediment calibration, the acceptable limit of percentage error is large and the maximum data observation date is not similar, so the result can be accepted. In case of morphological calibration, the tuning parameter is eddy diffusivity as explained in (Manual, 2013). That's why, the morphological calibration has been done with trial and error method assuming some values of eddy diffusivity.

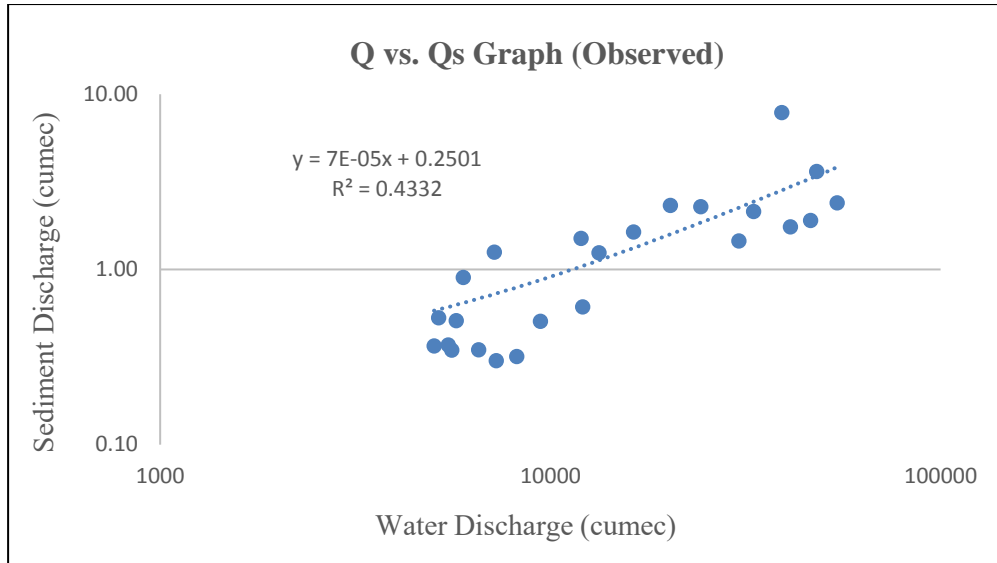


Figure 5.10: Flow discharge vs. observed sediment discharge graph at Bahadurabad

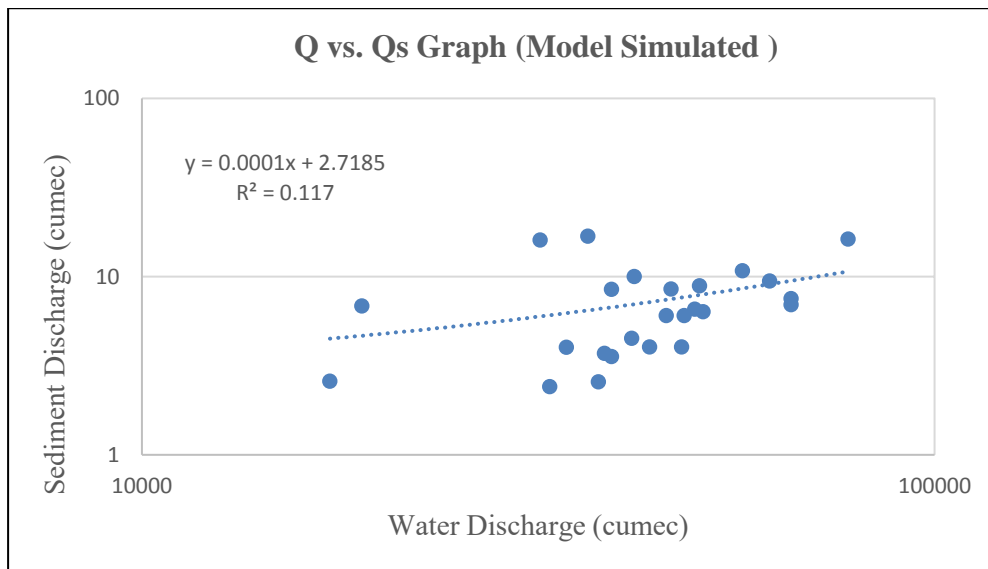


Figure 5.11: Flow discharge vs. simulated sediment discharge graph at Sirajganj

As the actual sediment data is rare and discrete, the morphological calibration has been done comparing the cross-sections with previously surveyed data for pre-monsoon 2011 at Sirajganj Hard point. The value of eddy diffusivity has been assumed as 1, 5 and 10 respectively and the value 10 gives more satisfactory calibration result where the maximum percentage of error (25%) is within the limit. Hence the rest of the simulations have been done using the eddy diffusivity value 10. Thus it can be said that the model has been calibrated hydro-dynamically as well as morphologically also. The following figures show the morphological calibration comparing the cross-sections.

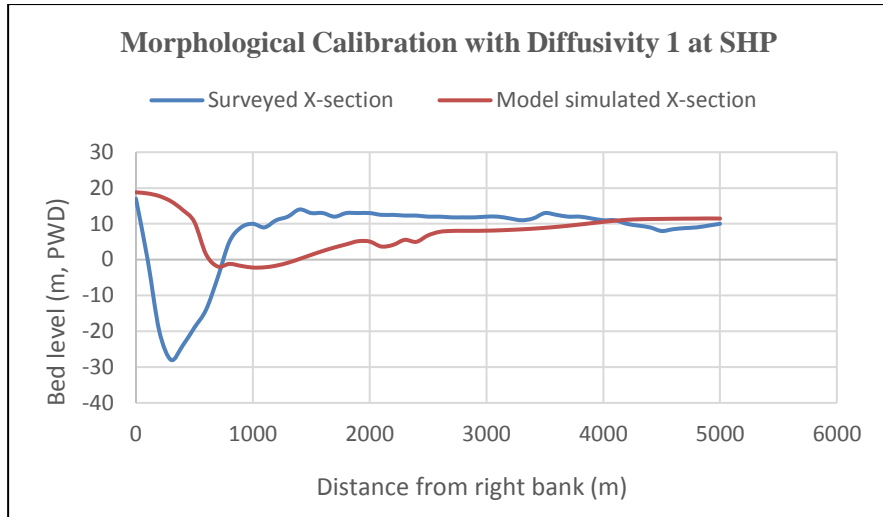


Figure 5.12: Comparison of cross-sections at SHP for pre-monsoon 2011 with diffusivity 1

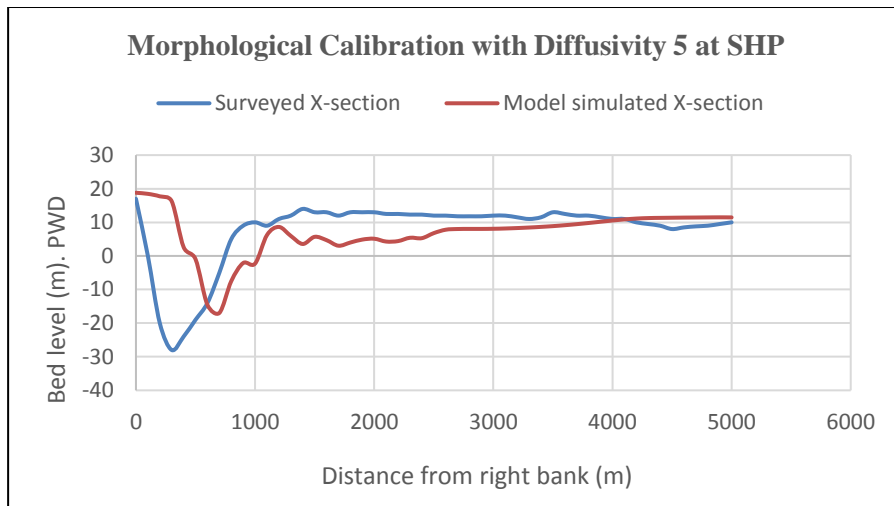


Figure 5.13: Comparison of cross-sections at SHP for pre-monsoon 2011 with diffusivity 5

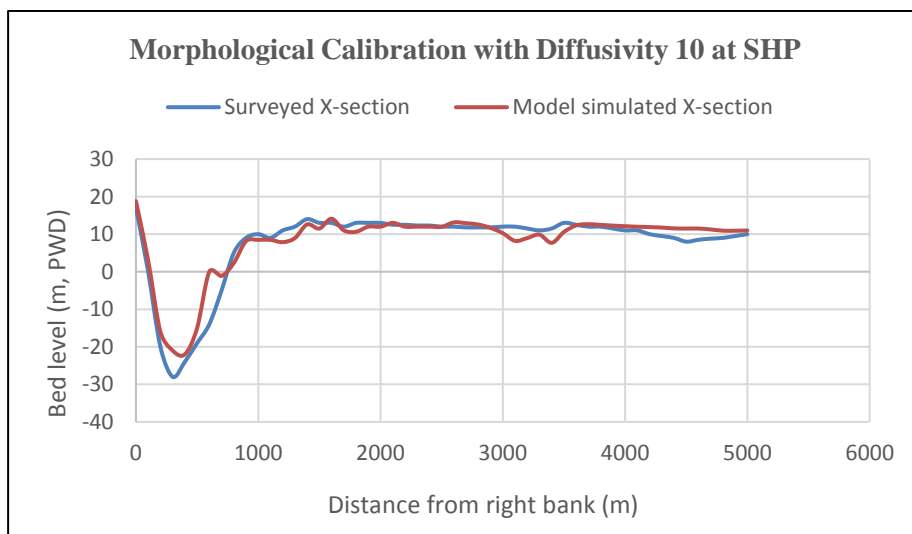


Figure 5.14: Comparison of cross-sections at SHP for pre-monsoon 2011 with diffusivity 10

5.2.8 Comparison of Simulated Water Level between MIKE21C and Delft3D

This comparison is also a validation of the model output. Because MIKE21C is a professional software which is established and many analysis in professional and commercial cases have done using the software. Whereas the model used in this study is Delft3D open source software used in academic purposes mostly. If the model output of the same parameter at the same time period of this two software matches then it will be a strong validation of the Delft3D software used in this study.

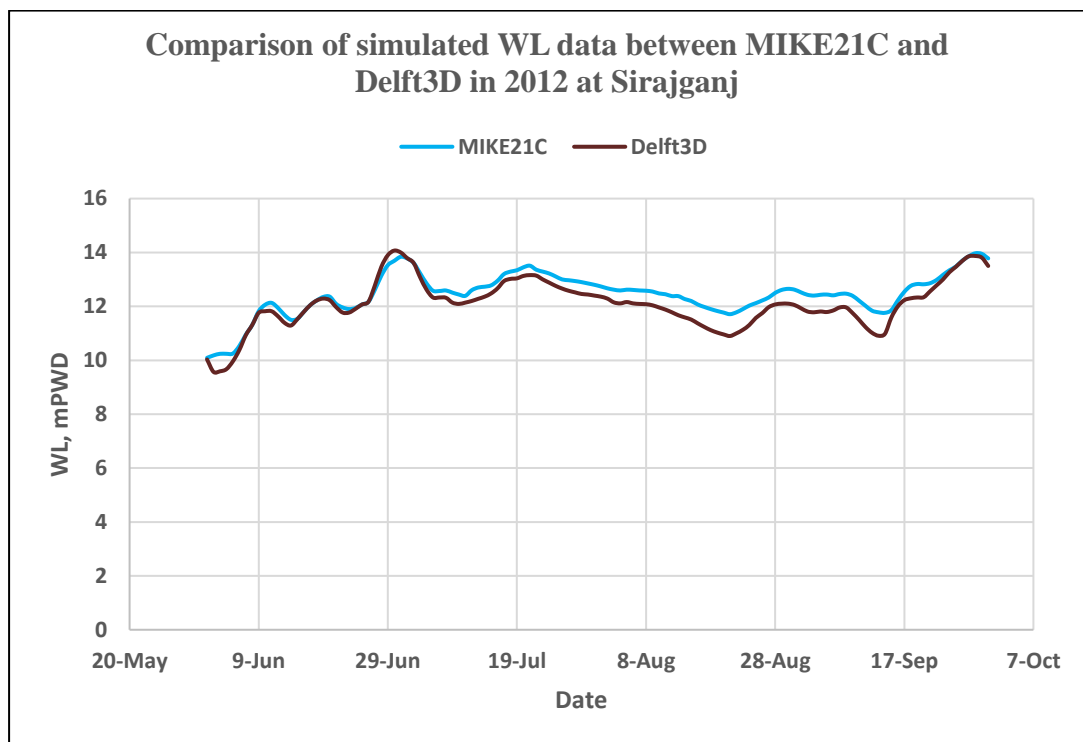


Figure 5.15: Comparison of simulated WL data between MIKE21C and Delft3D in 2012 at Sirajganj

Figure 6.29 shows the comparison between simulated water level as obtained using MIKE21C (Haque, 2018) simulated results. The maximum variation from MIKE21C in this case is 7.41% which is quite acceptable. So, the validation of the Delft3D is done again comparing the result with the established professional software MIKE21C.

5.2.9 Model Stability Analysis

Stability analysis of a model is a prerequisite now a days when working with such type of tools. In this case the fine grid has been taken as $m = 152$ and $n = 752$ and the total number of grid is 114304. Then for stability analysis, a coarser grid has been taken where the number of grid in m and n directions are half of the previous. Here $m = 77$, $n = 377$ and the total number of grid is 29029 which is almost one-fourth of the previous total grid. After simulation with the coarser grid with different time steps the results are as follows in Table 5.2.

Table 5.2: Stability analysis results of the model

Grid type	Grid size (m×n)	No. of grid points	Stability					
			Hydrodynamic			Morphologic		
			Time step			Time step		
			1 min	5 min	10 min	1 min	5 min	10 min
Coarser	77×377	29029	Stable	Stable	Unstable	Stable	Unstable	Unstable
Finer	152×752	114304	Stable	Unstable	Unstable	Stable	Unstable	Unstable

From the stability analysis results, it has been found that in this range of the grid size the model is stable but time step dependent. In case of time step variation the model becomes unstable sometimes. In case of stability analysis, the calibration curves at different points show closer result with the observed data. And the non-stable time steps show almost same results in the model output. The Figure 5.10 shows the calibration curve for stability analysis for coarse grid.

5.3 Model Simulation with Different Options

This study mainly deals with the structural intervention as like groyne or spurs in the erosion prone areas of the right bank of the Jamuna River. So, different number of groynes with different spacing will be inserted into the river to observe the hydro-morphological changes over the year and for future prediction. The length of the groyne normally is about (25-30)% of the average width of the river (Dani *et al.*, 2013). However in this study, groyne length has been assumed as one-fourth of the corresponding channel. Considering the average width of the channel, the length of the groynes ranges from 800 m to 1000 m. The erosion prone areas of the reach is shown in Figure 5.8 which has been collected from BWDB.

Erosion Prone Area of the Jamuna River in Sirajganj District



Figure 5.16: Erosion prone areas at the right bank of the Jamuna River

(Source: BWDB)

Different types of structures have already been constructed in the Jamuna River and among them a number of groynes were also but in most of the cases they were washed out or damaged. In the recent years BWDB has again constructed some cross bars at the right bank of the Jamuna. So, the study interest is here that the number and spacing of groynes might have some influences not to be reached in such vulnerable situation. Because the previously constructed

groynes were single or somewhere multiple but the series of groynes with different spacing has not been experimented more in the BRE. So in this study the comparison among the base situation, single groynes and series of groynes with different spacing has been done. Material concern of the groynes has not been considered only impermeable perpendicular type structures have been inserted to conduct this study. Because the objective of this study was to observe the change in the hydrodynamic and morphologic parameter due to the groynes insertion at BRE at different numbers with different spacing.

The groynes have been inserted at the upstream of the Sirajganj hard point. The locations of the structures are between Simla and Subhagacha. The chainage range is almost BRE km 150 to 158. The shape of the groynes are normal/perpendicular. From the study of (Dani *et al.*, 2013) it was found that groynes with a perpendicular orientation to the oncoming flow were optimal. So the shape of the structures were at right angled to the BRE.

Now the different options of the structural intervention are described as follows in Table 5.3.

Table 5.3: Description of the simulation options

Name of the options	Description of the options
Base	Without any structure
Option 1	With single groyne
Option 2	With 2 groynes with S/L ration 1.0
Option 3	With 2 groynes with S/L ration 1.5
Option 4	With 2 groynes with S/L ration 2.0
Option 5	With 3 groynes with S/L ration 1.0
Option 6	With 3 groynes with S/L ration 1.5
Option 7	With 3 groynes with S/L ration 2.0

Now the options for the structural intervention are shown in figures.

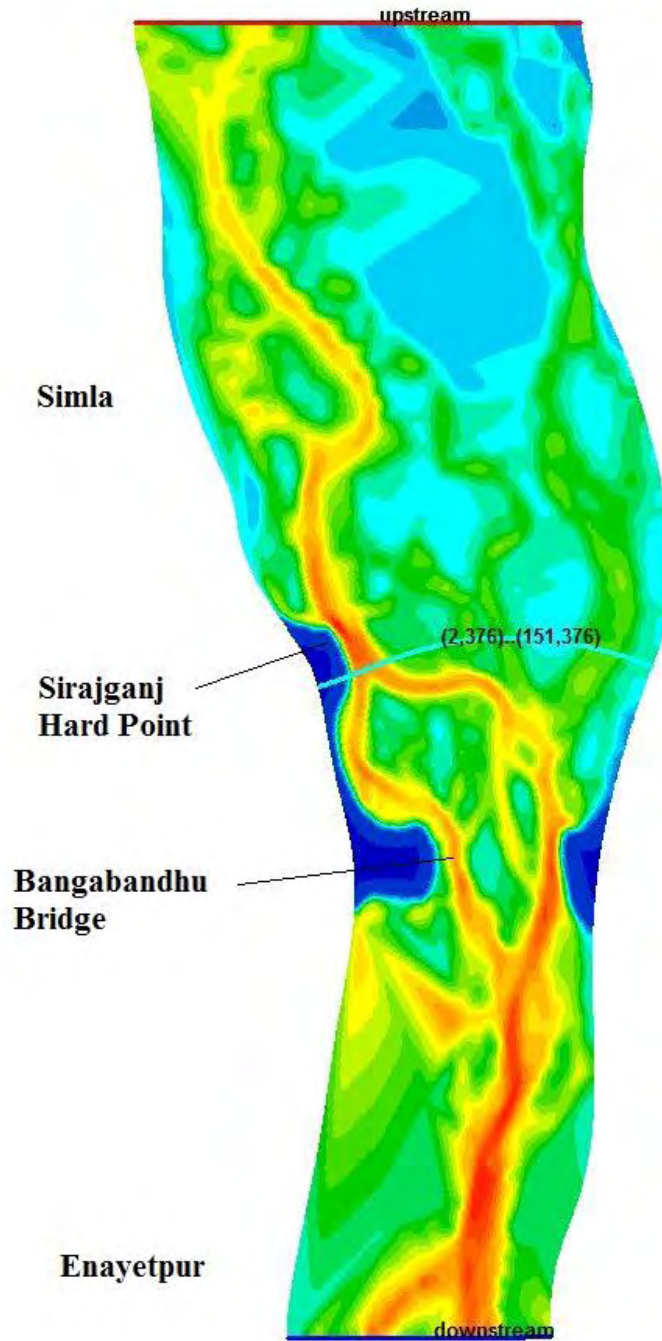


Figure 5.17: Base (without any structure)

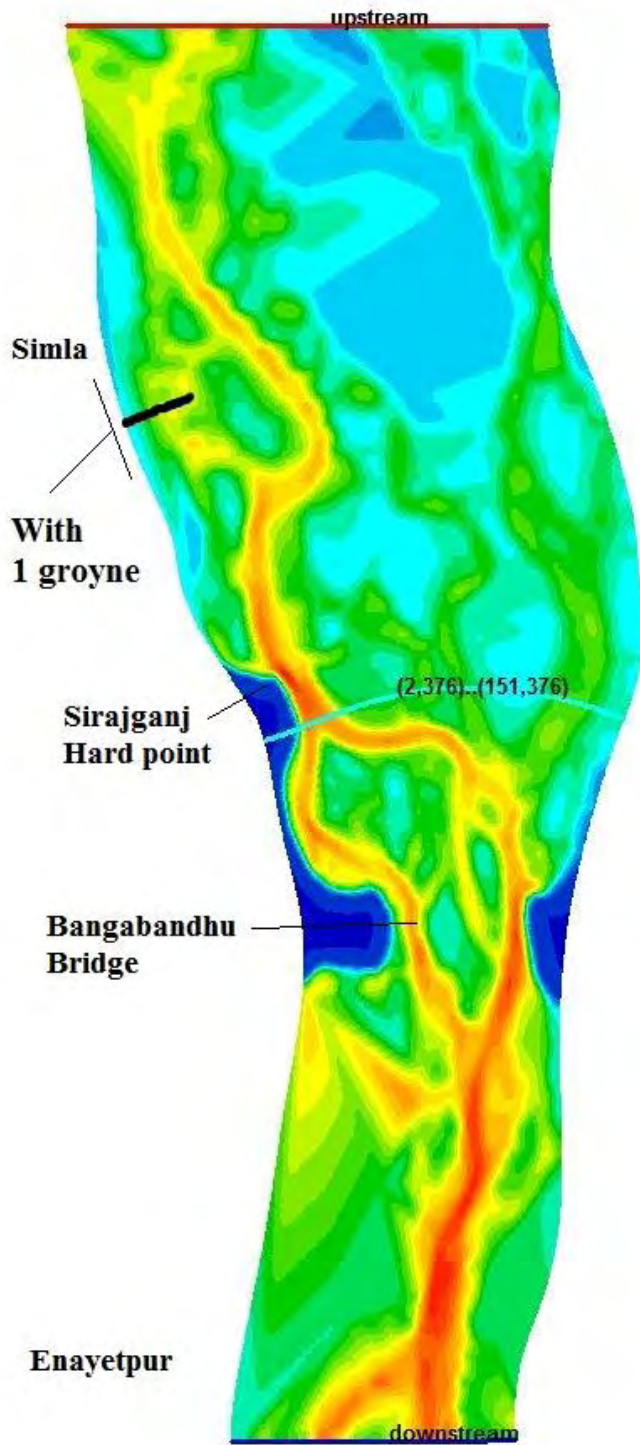


Figure 5.18: Option 1 (Single groyne)

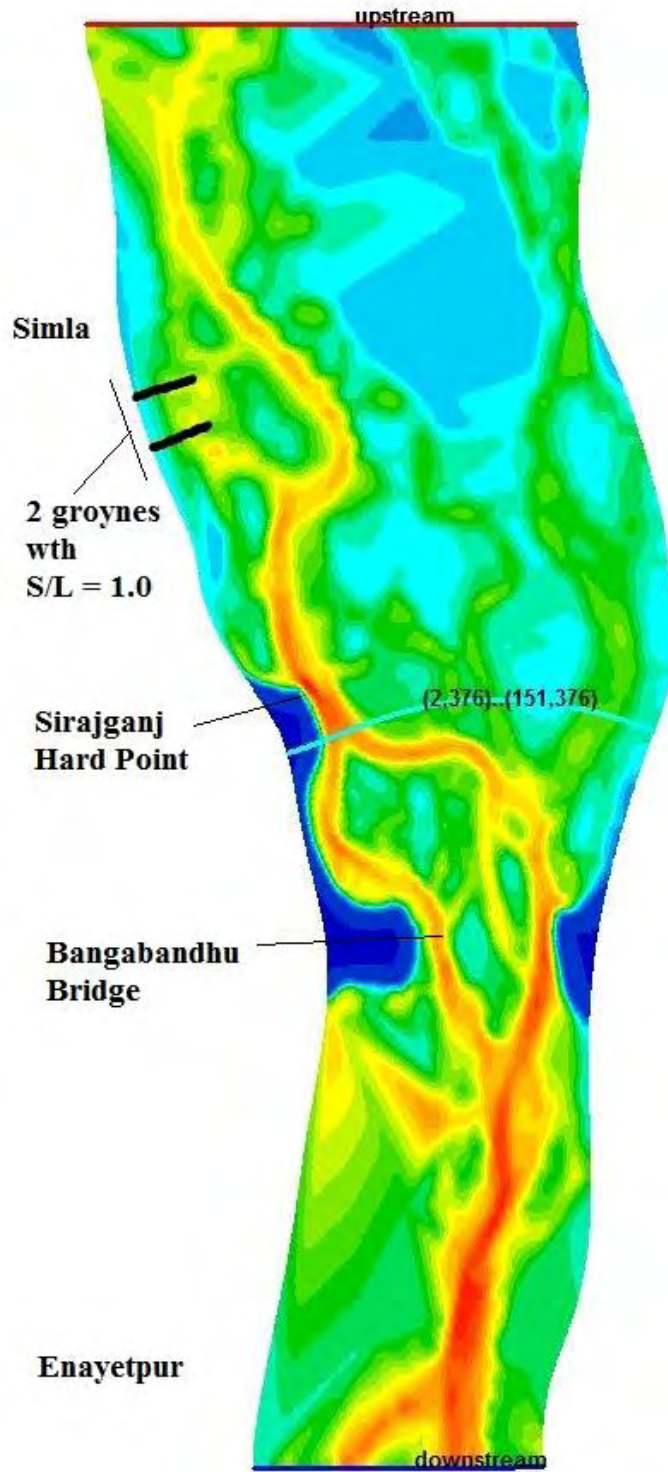


Figure 5.19: Option 2 (2 groynes with S/L ratio 1.0)

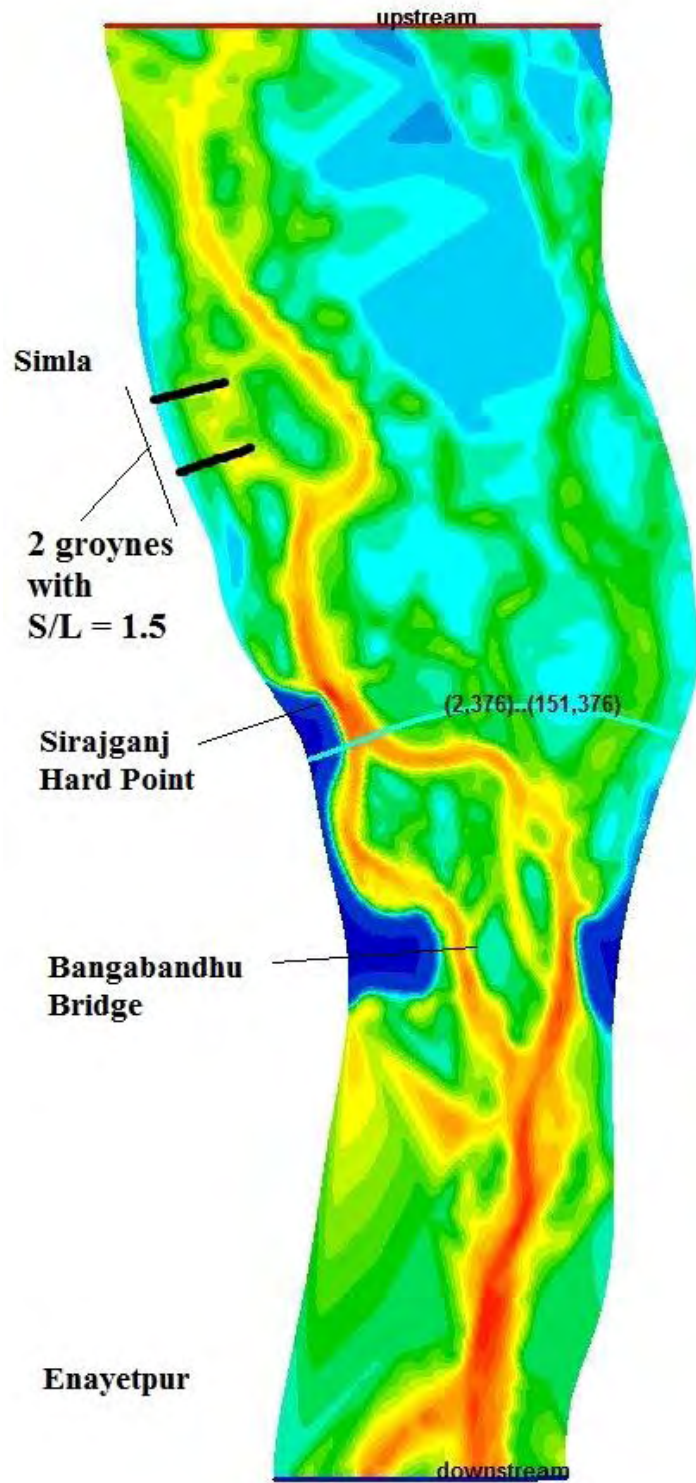


Figure 5.20: Option 3 (2 groynes with S/L ratio 1.5)

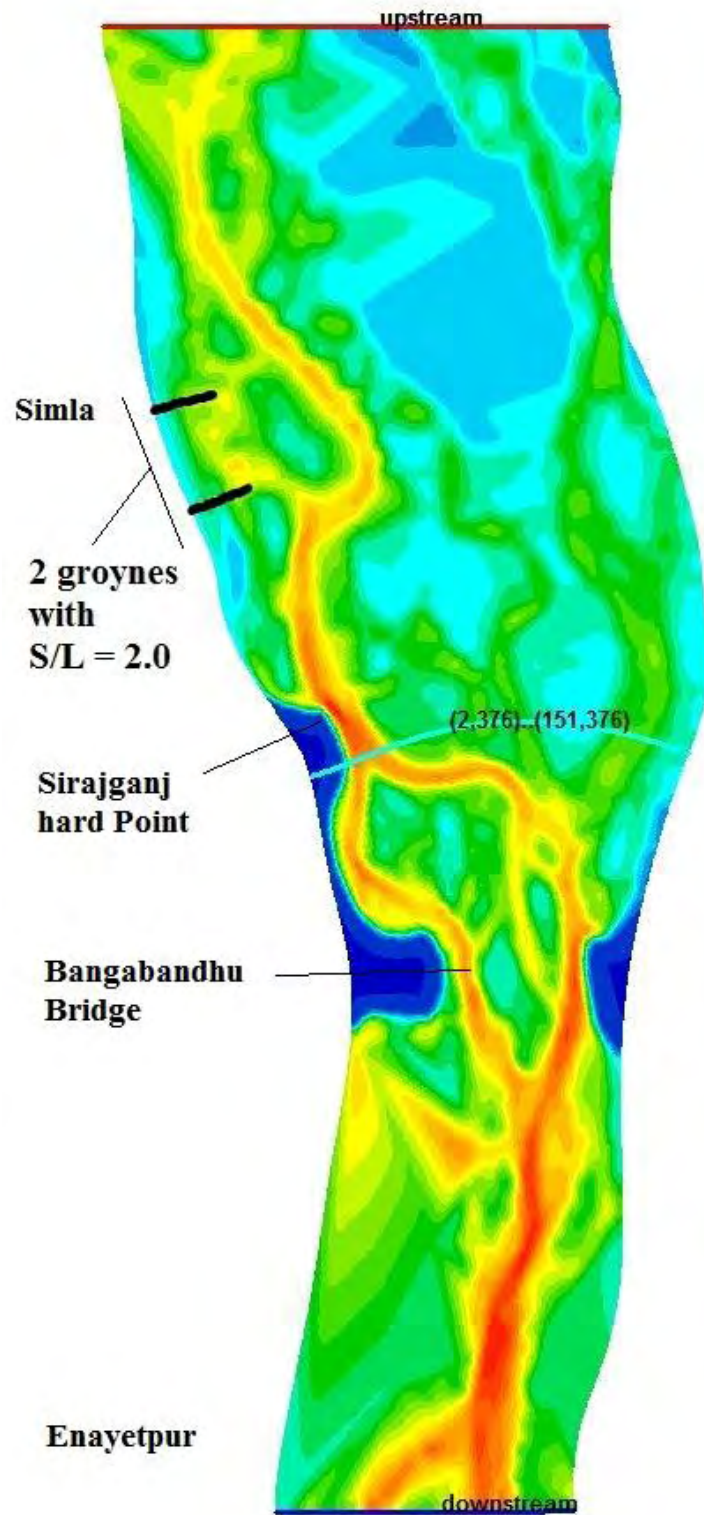


Figure 5.21: Option 4 (2 groyne with S/L ratio 2.0)

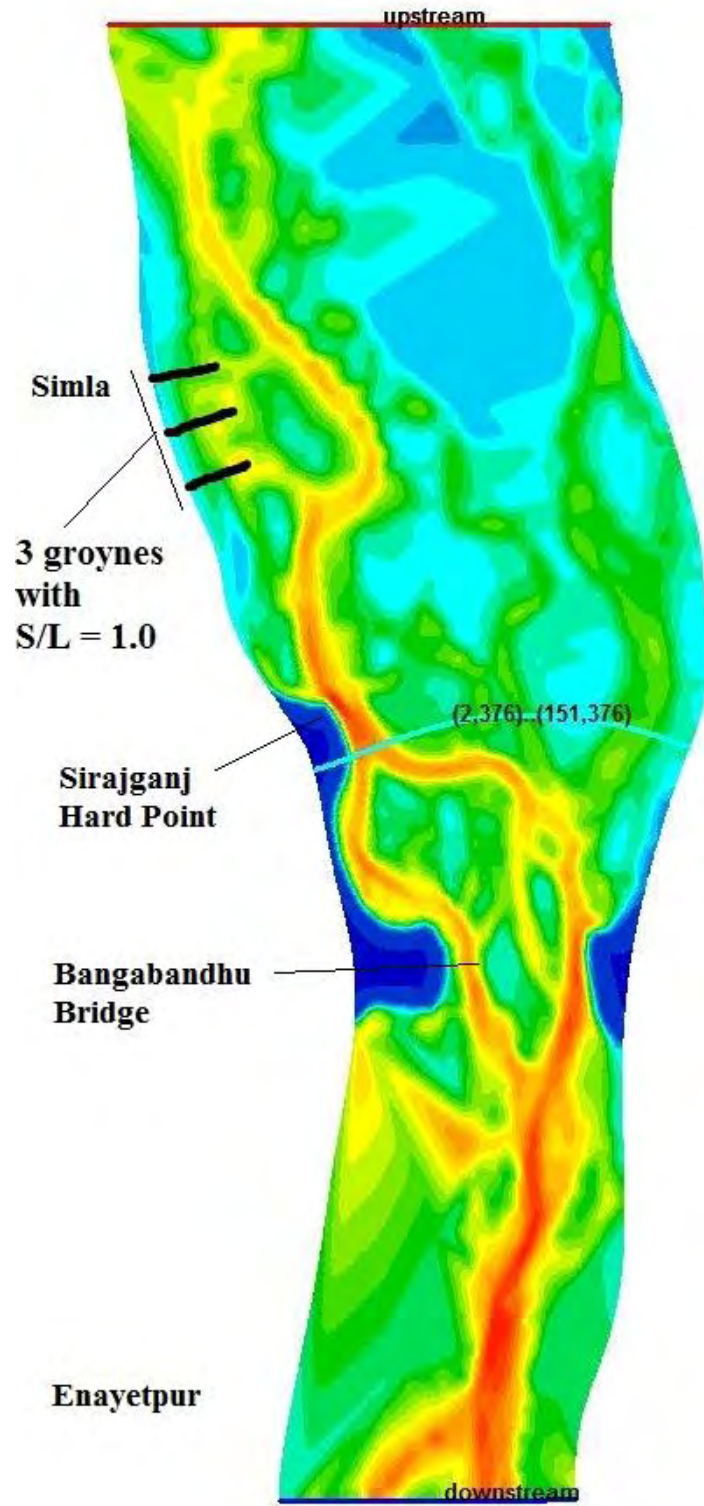


Figure 5.22: Option 5 (3 groyne with S/L ratio 1.0)

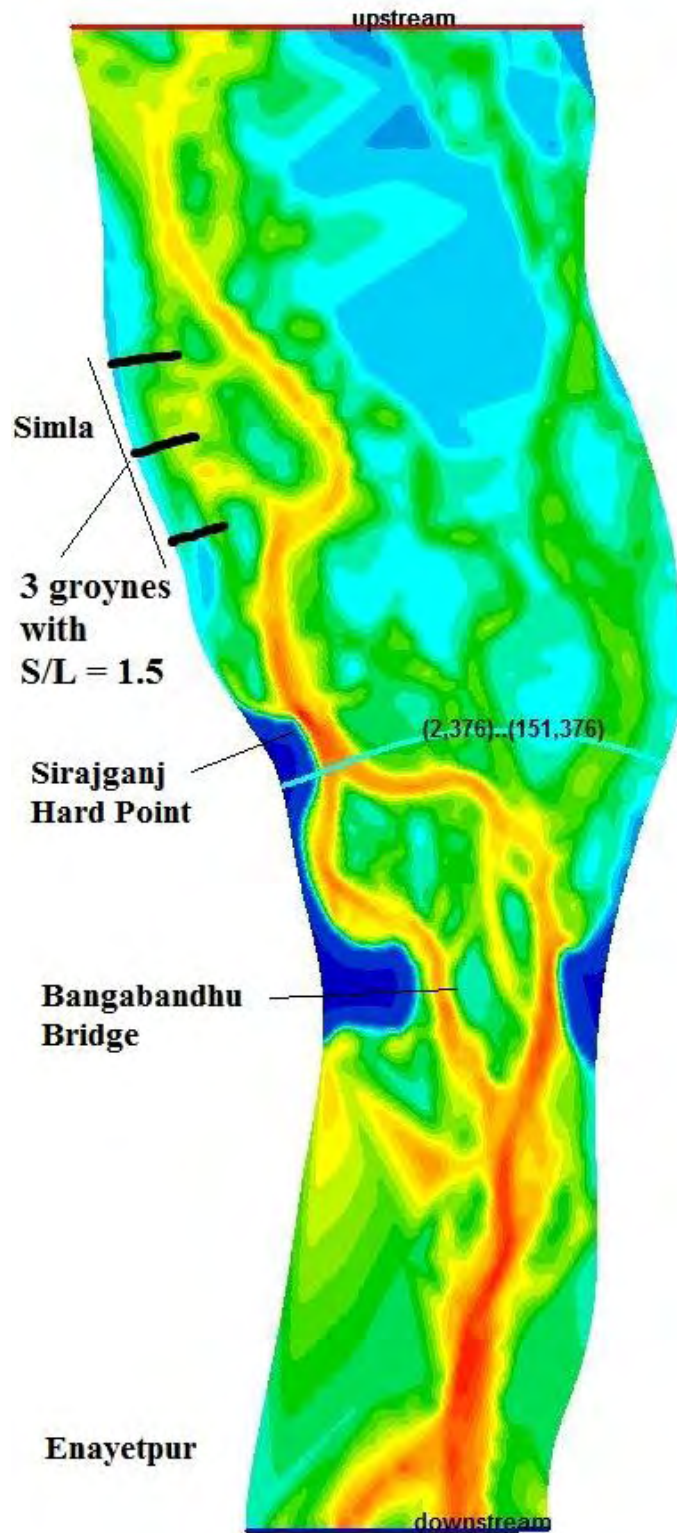


Figure 5.23: Option 6 (3 groyne with S/L ratio 1.5)

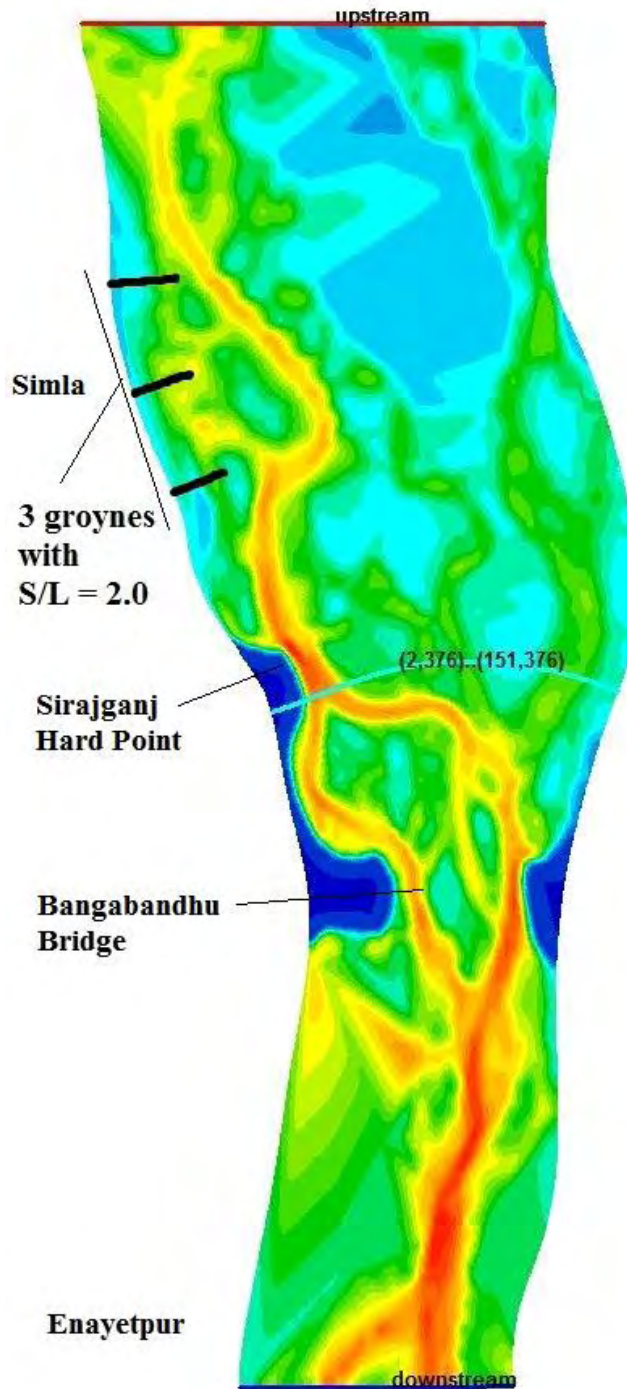


Figure 5.24: Option 7 (3 groyne with S/L ratio 2.0)

All the mentioned cases have been simulated and the response of the corresponding river has been observed. Water level, depth averaged velocity, bed shear stress, erosion/deposition, suspended sediment transportation etc. has been observed and change in the morphology has also been detected.

CHAPTER 6

RESULTS AND DISCUSSIONS

6.1 General

To understand the river response due to structural intervention, the option simulations has been compared with the base condition and also be compared with each other. The hydrodynamic and morphologic parameters are compared and then the relationship between/among them is established. Different cases of the results are shown with figures in the next sections with necessary discussions.

6.2 Observation of Hydrodynamic Parameters

Some sample figures showing the hydrodynamic parameters like, water level, depth averaged velocity, bed shear stress etc. are displayed sequentially to observe the scenarios.

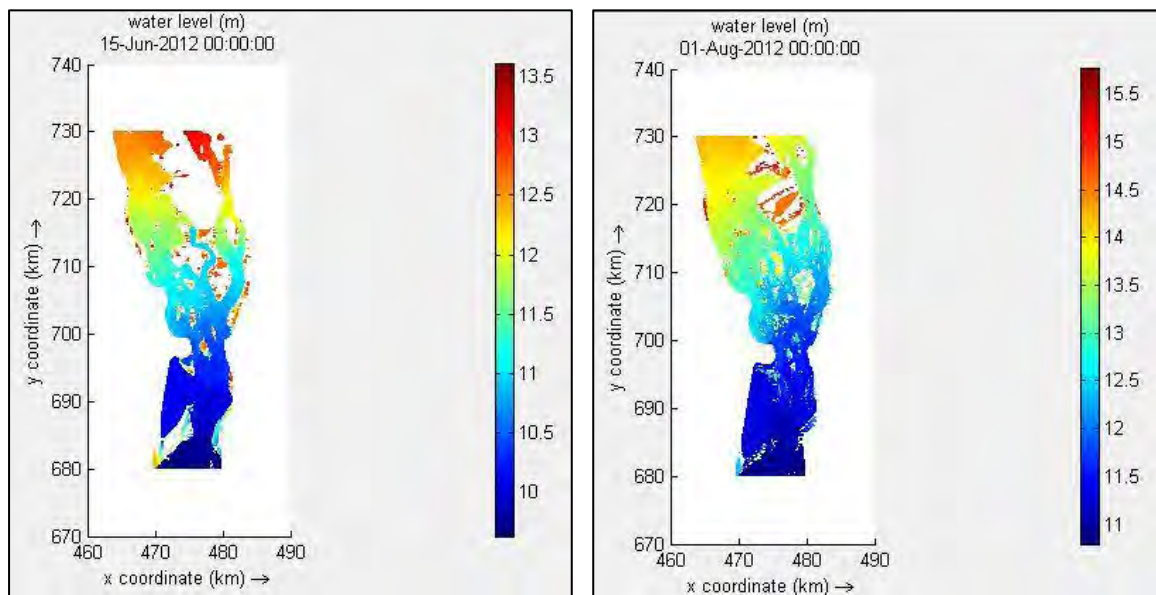


Figure 6.1: Water level at different dates for 2 groynes with $S/L = 1.5$

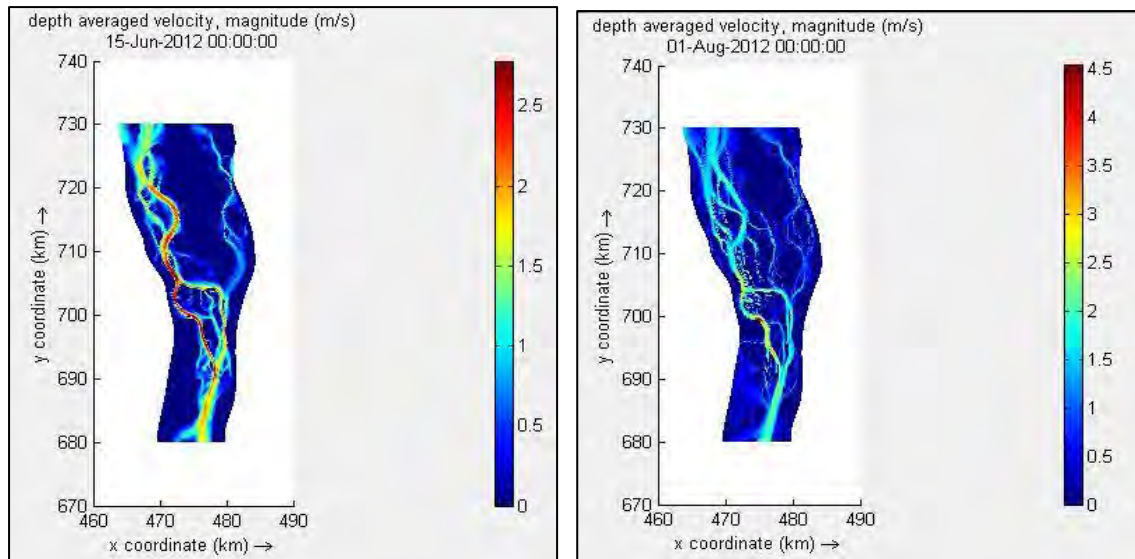


Figure 6.2: Depth averaged velocities at different dates for 2 groynes with $S/L = 1.5$

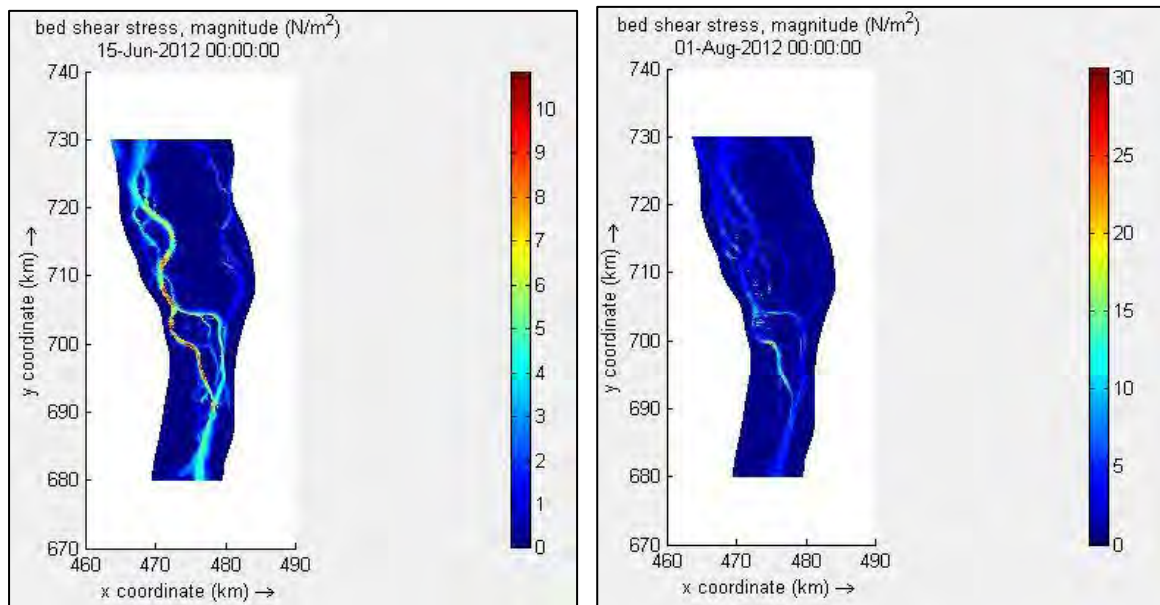


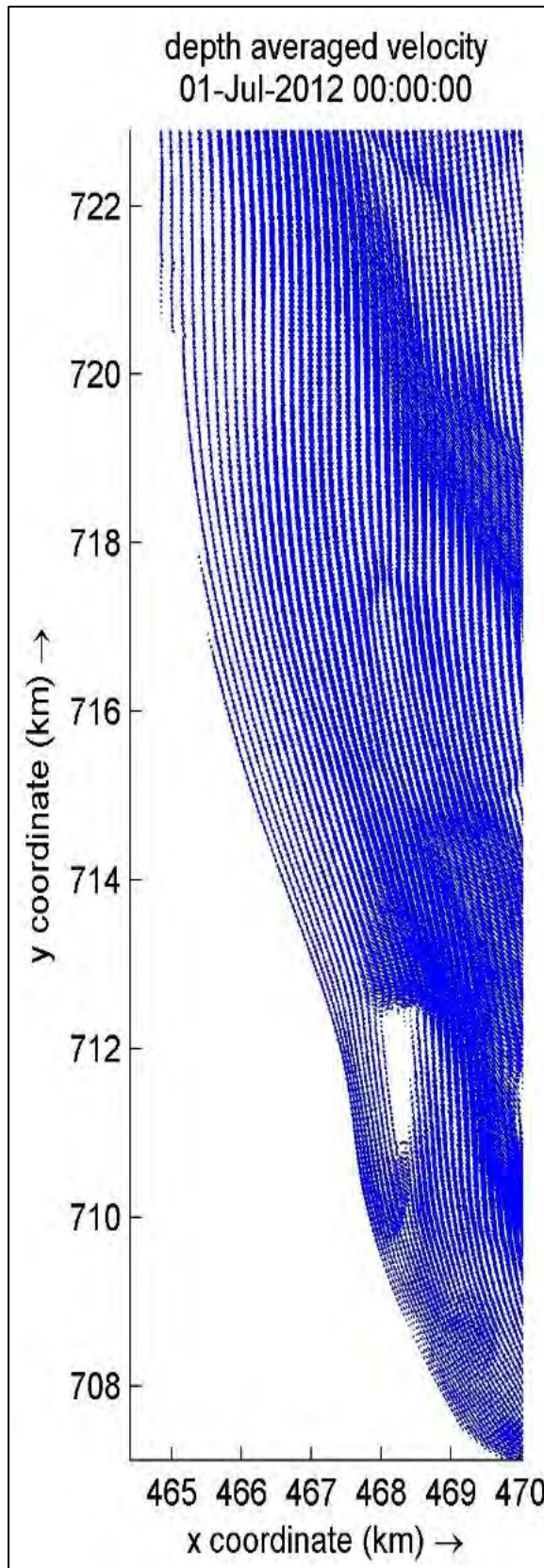
Figure 6.3: Bed shear stress at different dates for 2 groynes with $S/L = 1.5$

The figures mentioned above are the map files of the model output. Now the change in the hydrodynamic parameters with their numerical values has been observed. To do this 4 observation points have been chosen. The points are:

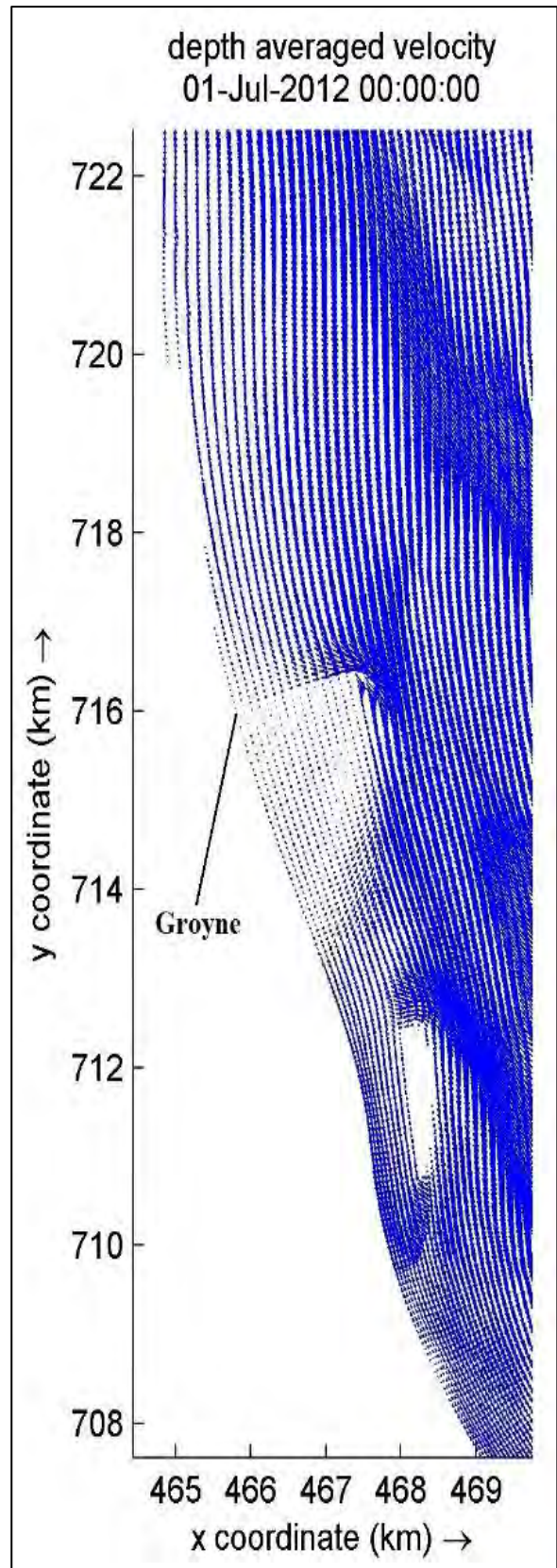
- Upstream of the structure: noted as U/S
- Downstream of the structure: noted as D/S
- Sirajganj Hard Point: noted as SHP
- Bangabandhu Bridge Site: noted as BBS

6.2.1 Velocity Vectors

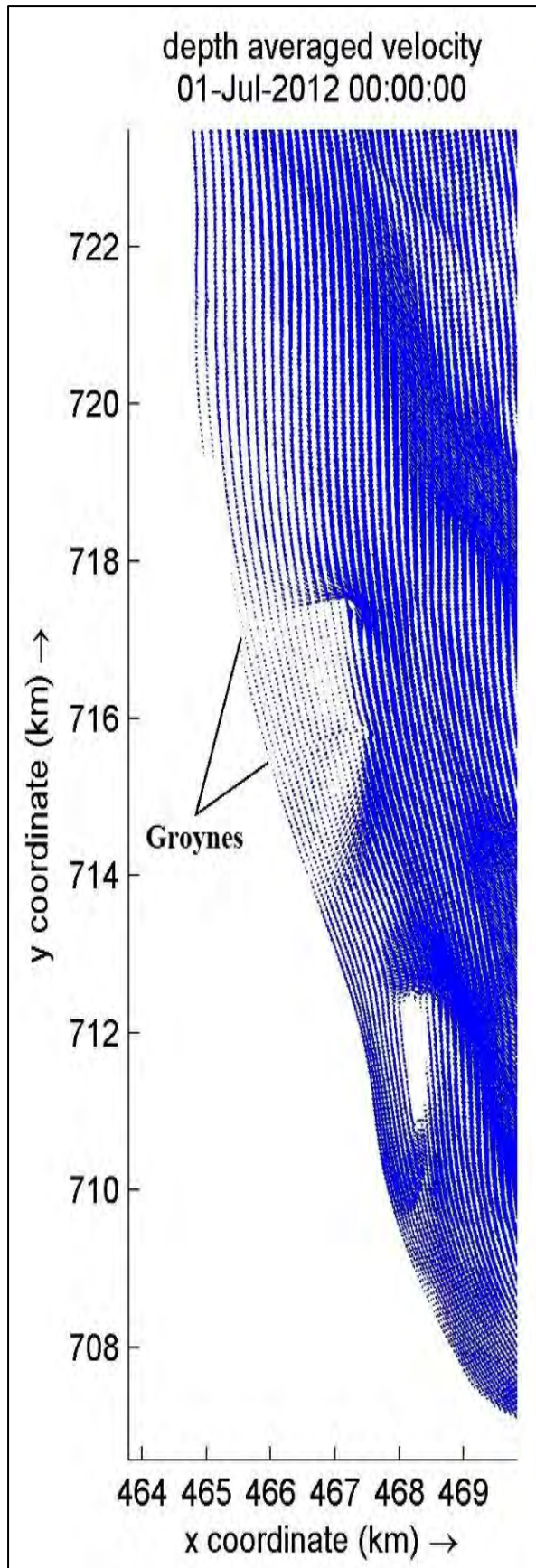
After simulation all the models, the output are taken from the QUICKPLOT option. Here the direction of the velocities are shown for all the cases. As the whole area is large and the vectors are not visible finding the large area, the vectors are shown at the selected small area. The following figures shows the velocity vectors for all the options with the base. From the Figure 6.4, it is observed that due to the insertion of groynes, the direction of flow is diverted away from the bank thus makes the bank free from danger. From the analysis of velocity vectors, it is found that with the increasing number of groyne, the direction of the flow velocity moves away from the river bank. If the spacing is large, the intermediate vectors form curvilinear concave shapes. Another scenario is if the spacing of the groynes is increased, the flow slightly enters into the space between two groynes. Analyzing all the figures in this case, it can be supposed that if the S/L ratio is further increased ($S/L > 2.0$) then the flow reaches the bank making it vulnerable for erosion.



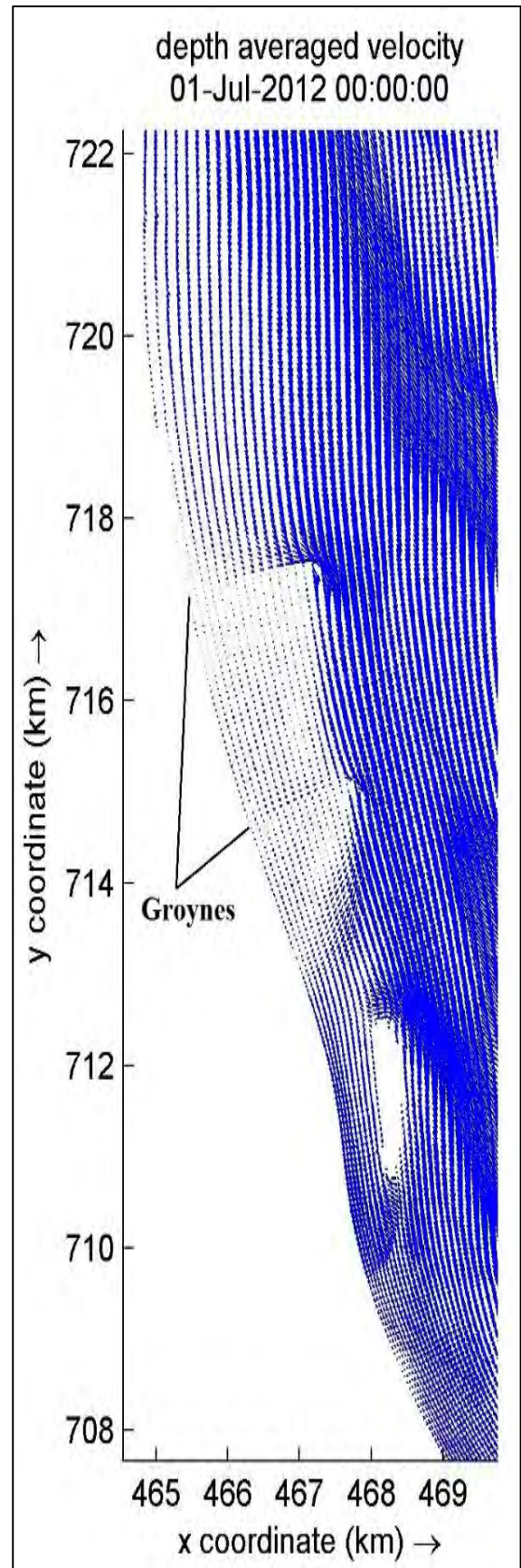
(a)



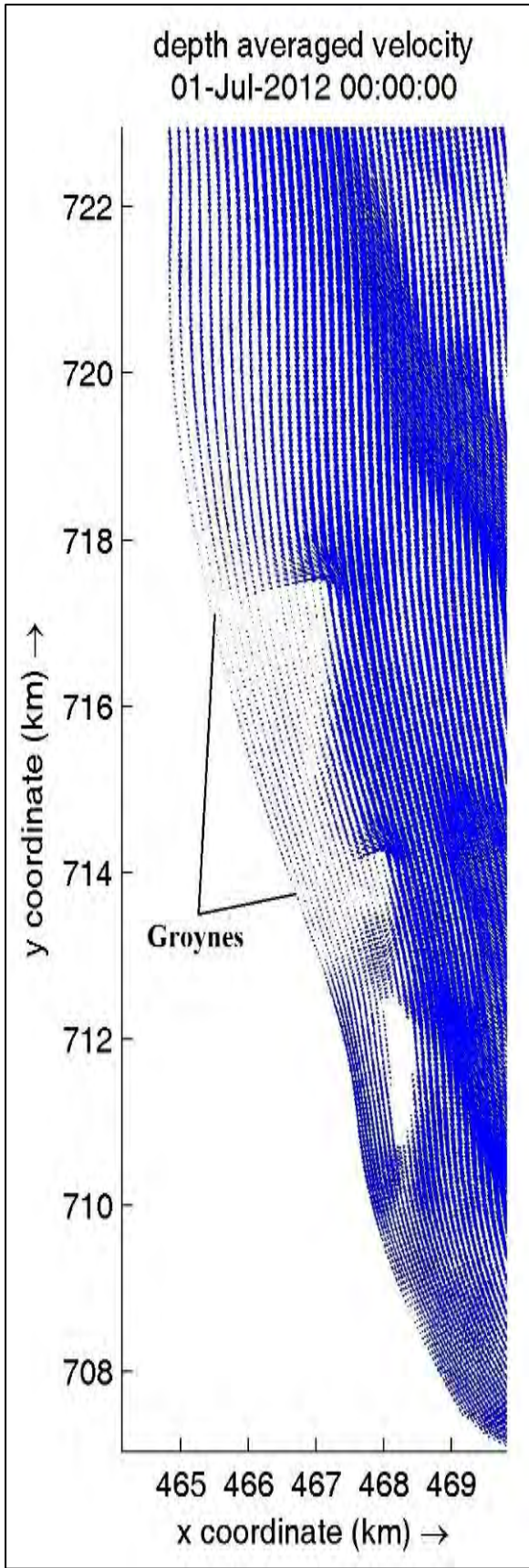
(b)



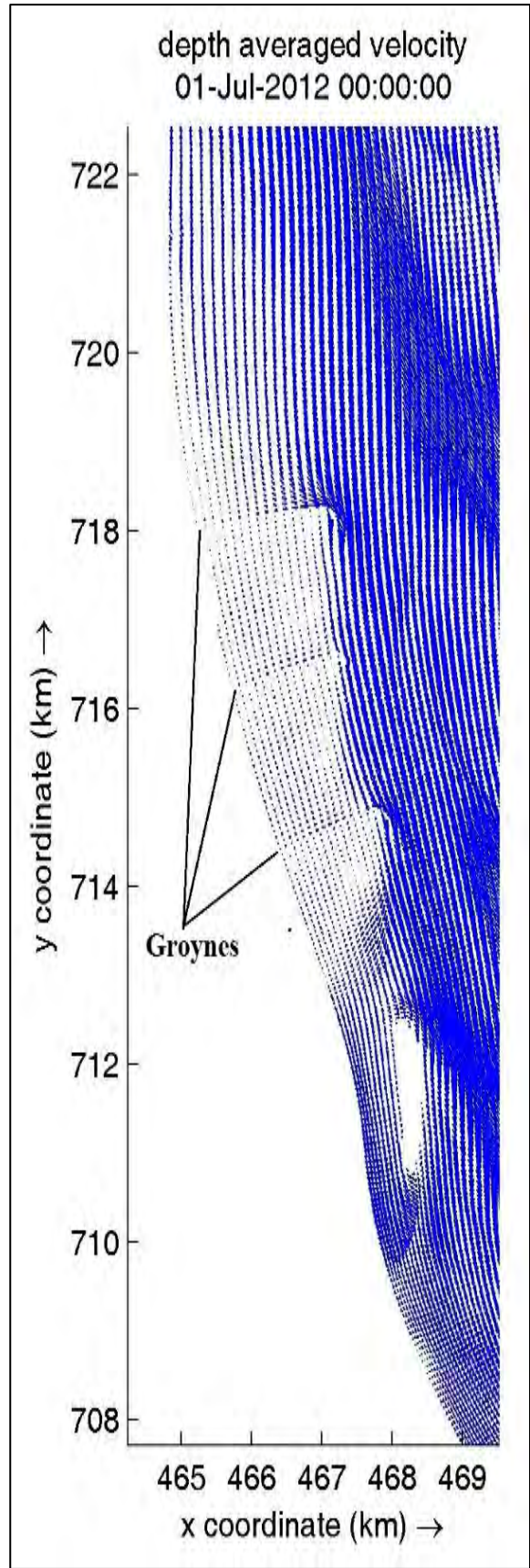
(c)



(d)



(e)



(f)

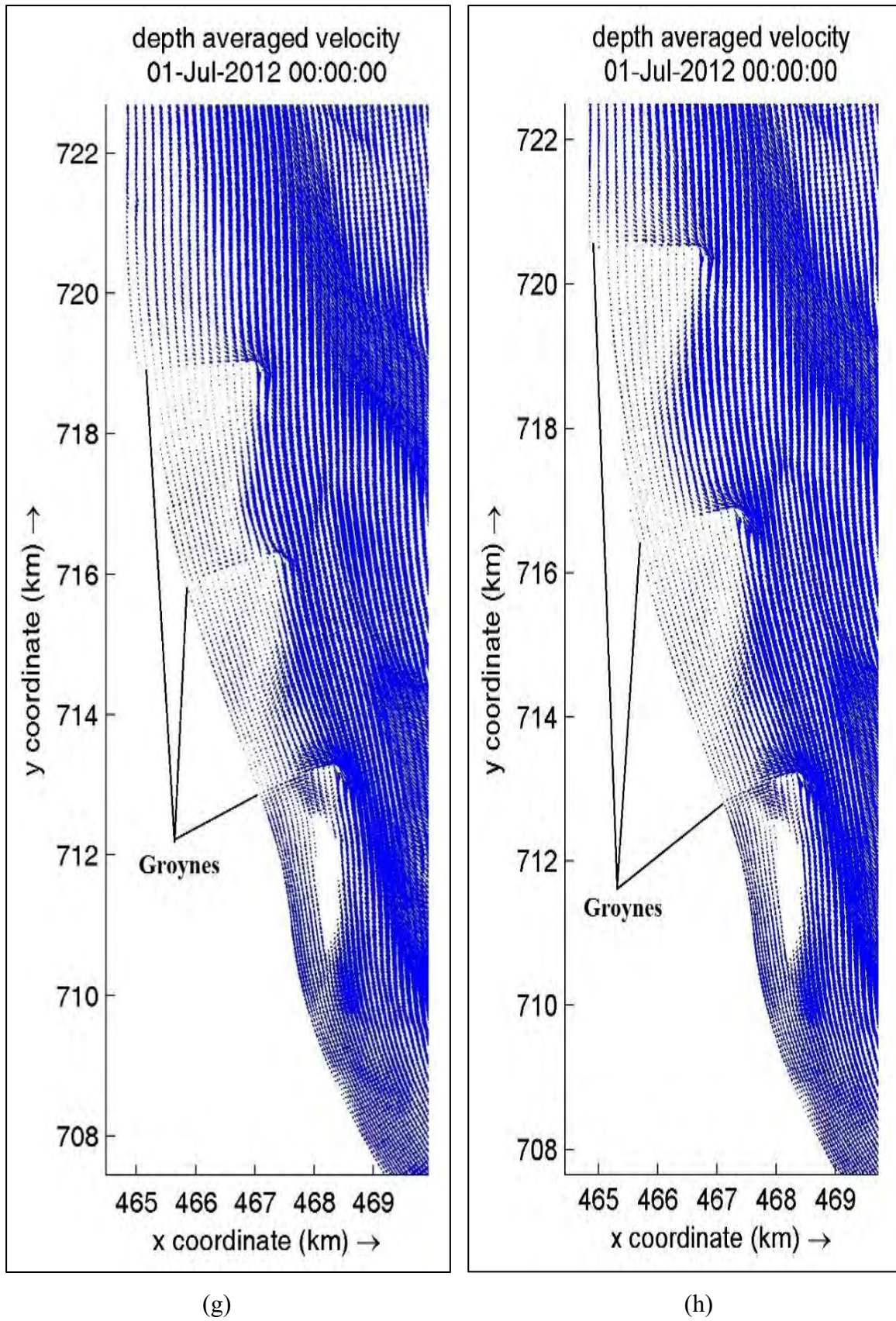


Figure 6.4: Velocity vectors from model output for (a) Base, (b) Option 1, (c) Option 2, (d) Option 3, (e) option 4, (f) Option 5, (g) Option 6 and (h) Option 7

6.2.2 Depth Averaged Velocity

The depth averaged velocity at the upstream and downstream locations reduces as the number of groynes increase. It is obvious that any obstacle reduces the velocity of any fluid. As the groynes are permanent obstacles so at the upstream the velocity reduces. The velocity vectors change their moving directions from the nose of the groynes thus at the downstream point less water can enter with low velocity. So the curves for upstream and downstream show reasonable results. But at SHP and at the BBS the values don't show much fluctuations. This may be due to the long distance between the locations or may be due to the effect of Bangabandhu Bridge or any other reasons because Braided River like the Jamuna is the most unpredictable in behavior. From the velocity map file, it is also observed that the near bank velocity decreases when more structures are inserted into the river. The direction of velocity is described in the velocity vector section (6.2.1). From that section, it is seen that the direction of velocity has been changed after introducing the structures. That's why the magnitude of the velocity near the bank reaches to almost zero sometimes.

Now, the variation of depth averaged velocity with different option at a specific location will be shown. Here, the velocities have been compared option wise with the base condition. The Figure 6.5 and Figure 6.6 express that the due to the insertion of groyne(s), the velocity decreases significantly at the upstream and downstream locations of the structure(s). Consequently at SHP and BBS, there are no significant effect(s) of the structure(s) on velocity with compared to the previous locations (Figure 6.7 and Figure 6.8).

Thus, it can be accomplished that the number of groynes affects the direction and magnitude of the depth averaged velocity basically at the surrounding portions of the structures. Here from the results at the upstream, the changing trend is always decreasing and the maximum depletion of velocity from base is 0.5 m/s for the option 7. In case of downstream, the trend shows some fluctuating behavior up to option 4 but after that for the options 5, 6 and 7 the velocity decreases significantly and the maximum reduction in velocity is 0.9 m/s for the option 7 compared to the base condition. The difference is more for the last three options may be due to the backwater effect of the small sand bar situated immediately downstream of the 3rd groyne. So, it can be supposed that the more the number of groynes, the less the magnitude in velocity. It is obvious that with the increasing number of obstacles in the way of any fluid flow, the speed might reduce. So, in this particular case for velocity the analysis shows reasonable output indicating that the river bank is safer when the number of groynes is more.

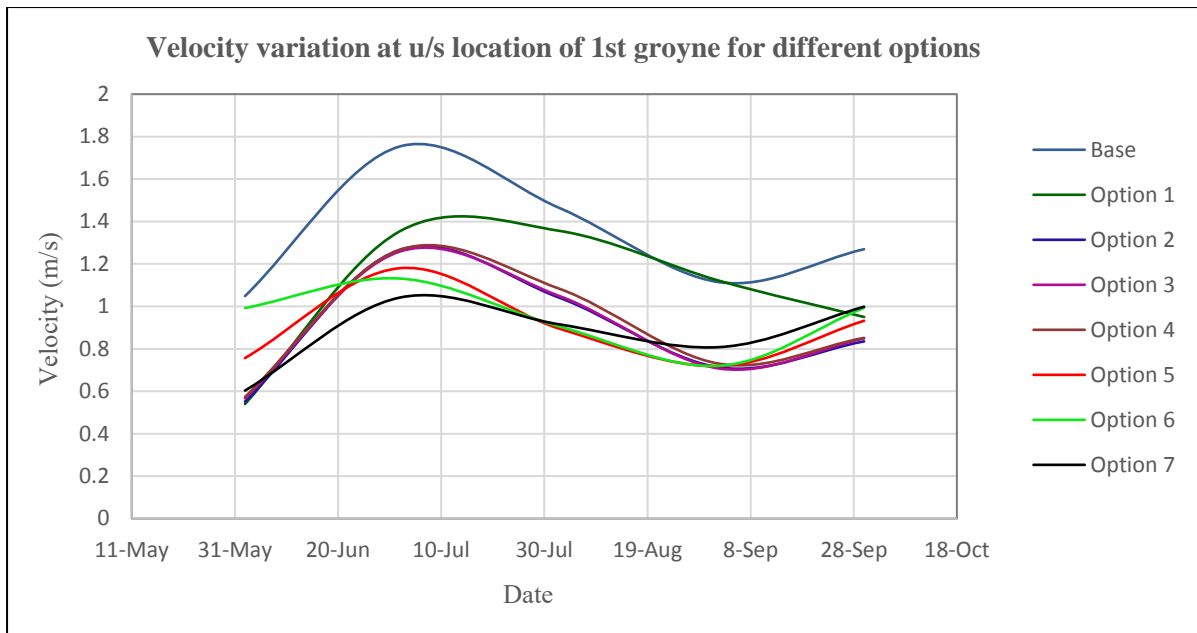


Figure 6.5: Relative comparison of velocity variation at groyne u/s for different options

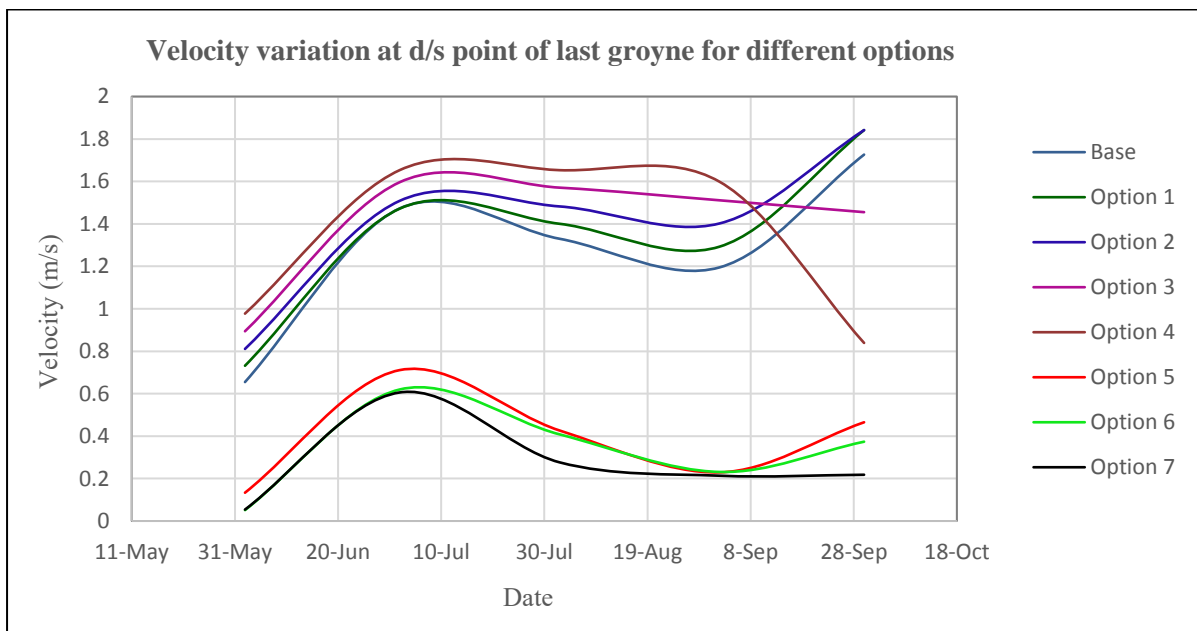


Figure 6.6: Relative comparison of velocity variation at groyne d/s for different options

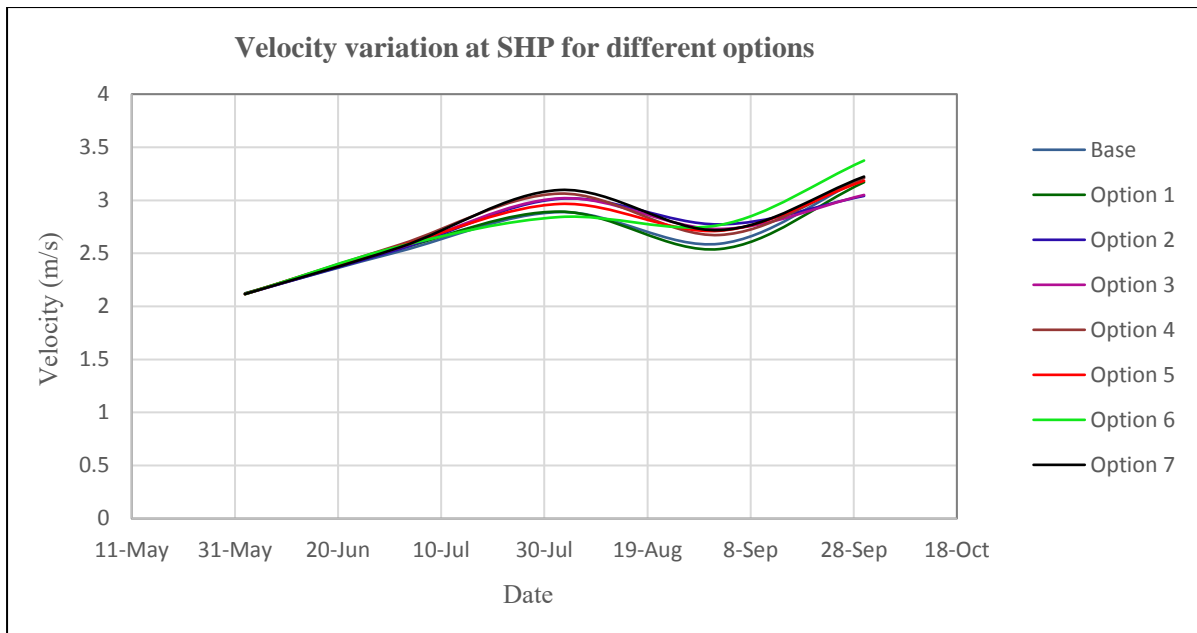


Figure 6.7: Relative comparison of velocity variation at groyne SHP for different options

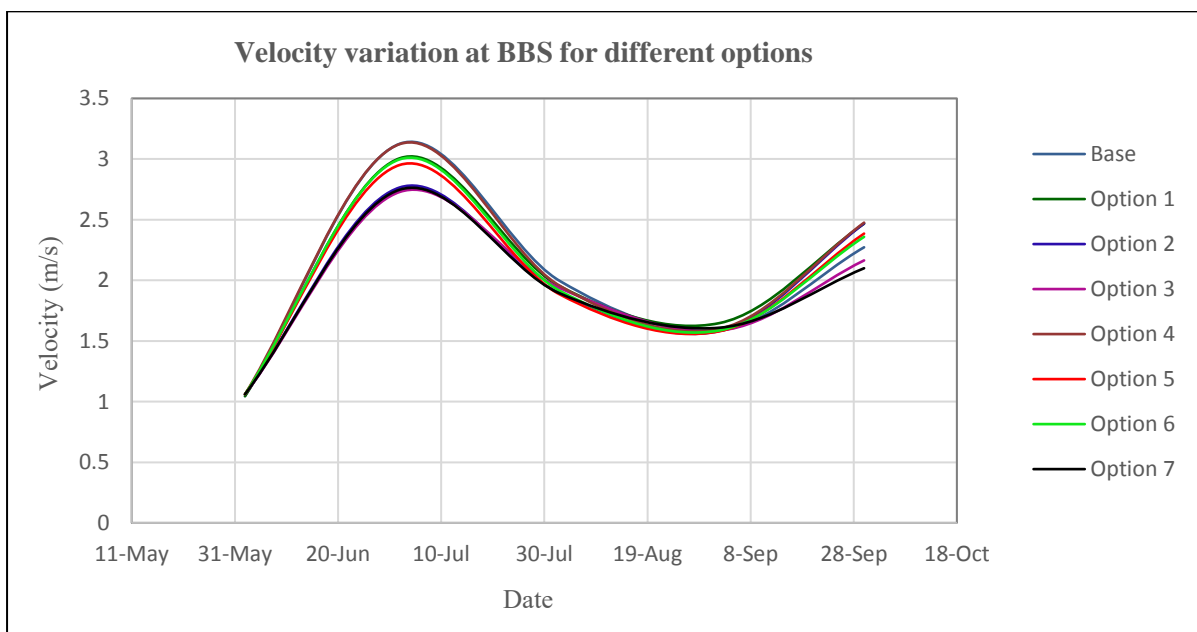


Figure 6.8: Relative comparison of velocity variation at groyne BBS for different options

Some other figures are shown below expressing the specific comparison of the velocity at the upstream and downstream locations of each groyne. At first the Figure 6.9 shows the variation of line velocity immediately upstream of the 1st groyne with respect to base condition. Here, up to the groyne length the velocity decreases significantly and the maximum reduction in velocity is 75%. After crossing the nose of the groyne, a little bit increment of velocity has been noticed (maximum 25%). The effect of groyne extends up to 1 km from the nose.

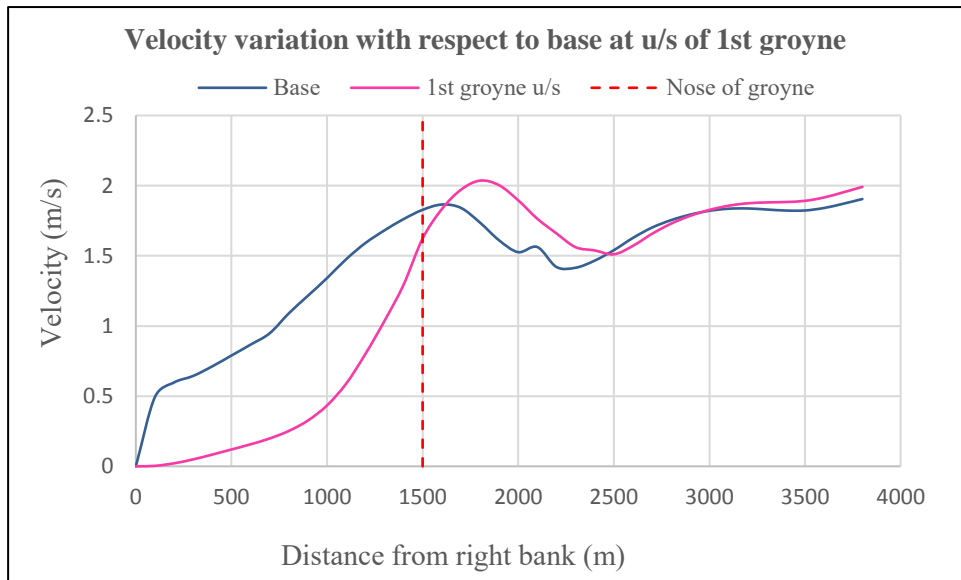


Figure 6.9: Comparison of velocity with base at the u/s of 1st groyne for option 2

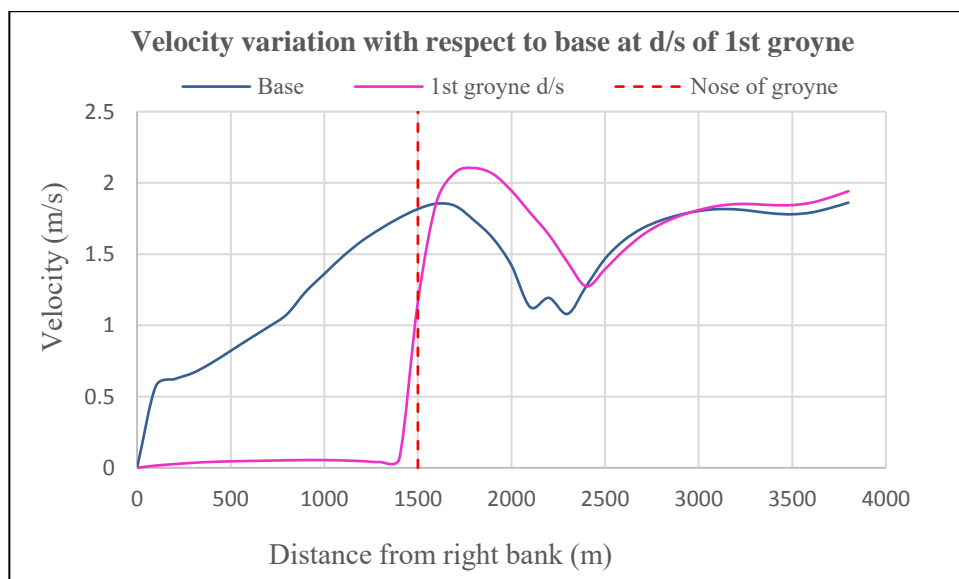


Figure 6.10: Comparison of velocity with base at the d/s of 1st groyne for option 2

Figure 6.10 shows the variation of line velocity immediately downstream of the 1st groyne with respect to base condition. Here, up to the groyne length the velocity decreases considerably and the maximum reduction in velocity is more than 90%. After crossing the nose of the groyne, a little bit increment of velocity has been noticed (maximum 25%). The effect of groyne extends up to 1 km from the nose which is similar to the previous case.

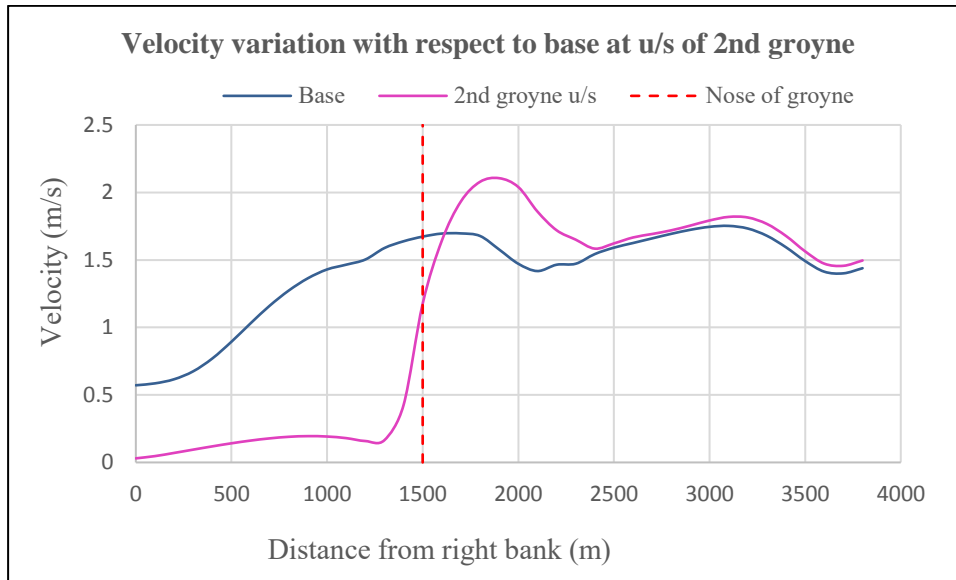


Figure 6.11: Comparison of velocity with base at the u/s of 2nd groyne for option 2

Figure 6.11 and 6.12 show the variation of line velocity immediately upstream and downstream of the 2nd groyne with respect to base condition respectively. For these two cases, variation pattern is almost similar to the Figure 6.10 without some increasing values of velocities up to the groyne length from the bank. The effect of groyne in to the river for all cases show more or less same value which is 1 km from the nose of the groyne.



Figure 6.12: Comparison of velocity with base at the d/s of 2nd groyne for option 2

6.2.2.1 Bank Line Velocity

In this section, comparison of bank line velocities among different groyne spacing are presented. This velocities have been observed along the line near the bank between two consecutive groynes (Figure 6.13). From the observation, it is found that at the base condition the velocities range 0.54 m/s to 0.62 m/s which is considerable higher than the critical value. Because the average grain size of the river is 0.11 mm and for this grain size, the critical velocity is 0.20 m/s (20 cm/sec) according to Hjulströms diagram (Figure 4.7). So, the river bank is susceptible to erosion at normal condition. Also the BWDB has identified this bank as erosion prone area (Figure 5.16). Now for the spacing ratio of the groyne, $S/L = 1.0$, the velocity decreases significantly and belongs to less than or equal to 0.1 m/s. With the increasing option, the magnitude of velocities increase and up to $S/L = 2.0$, the velocity is far from the critical value. But after that the value reaches and crosses the critical velocity line for $S/L = 3.0$ and if this pattern continues, the more spacing option will increase the velocity as well and reach up to the base condition. So, it is risky in this case, to provide spacing ration more than 2.0. Although the spacing ratio 2.5 may remain below the critical line.

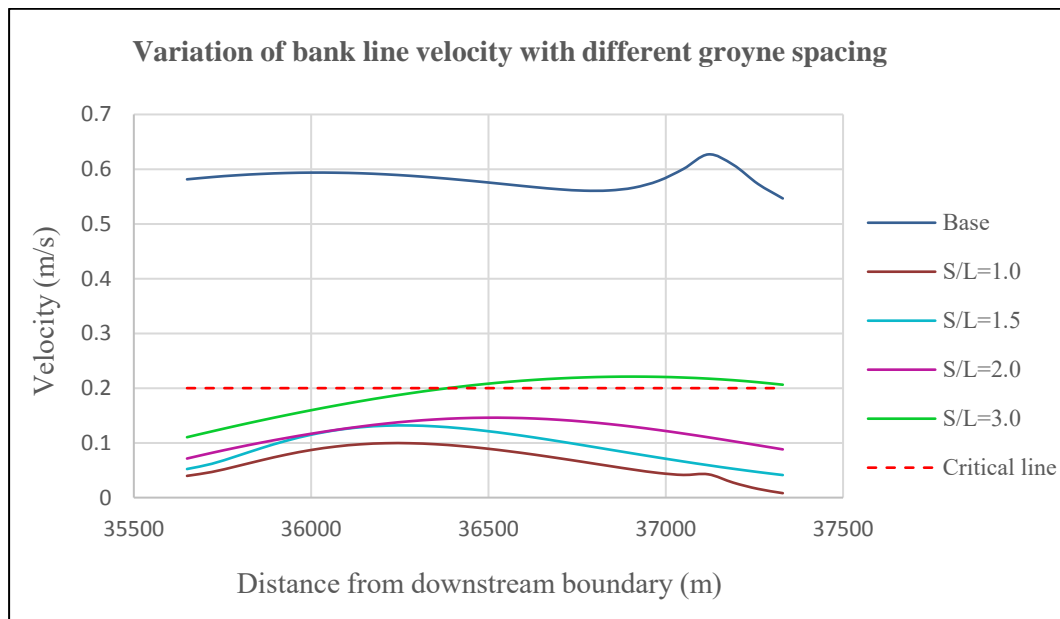


Figure 6.13: Comparison of bank line velocities for different spacing of groynes

6.2.3 Bed Shear Stress

Bed shear stress is the result of drag force. If the velocity of water decreases, simultaneously the magnitude of the drag force will be reduced. That's why the variation of bed shear stress basically follows the velocity variation. From the model output it is observed that at the upstream and downstream locations, the value of bed shear stress decrease significantly with increasing the options (Figure 6.15 and Figure 6.16) and no such effects at SHP and BBS locations (Figure 6.17 and Figure 6.18)

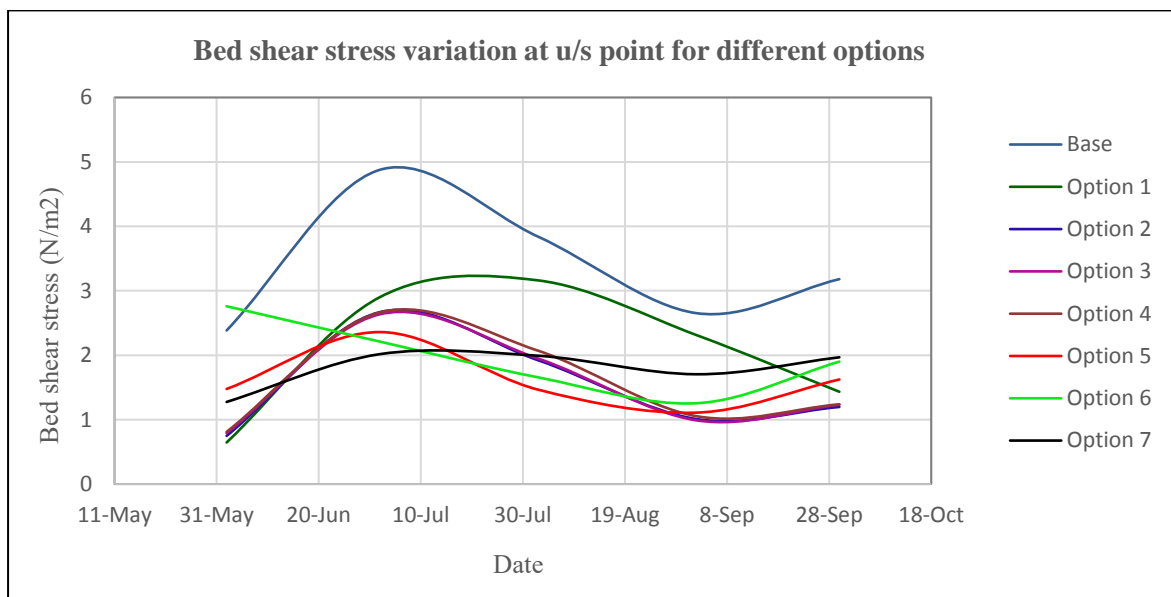


Figure 6.14: Relative comparison of bed shear stress at groyne u/s for different options

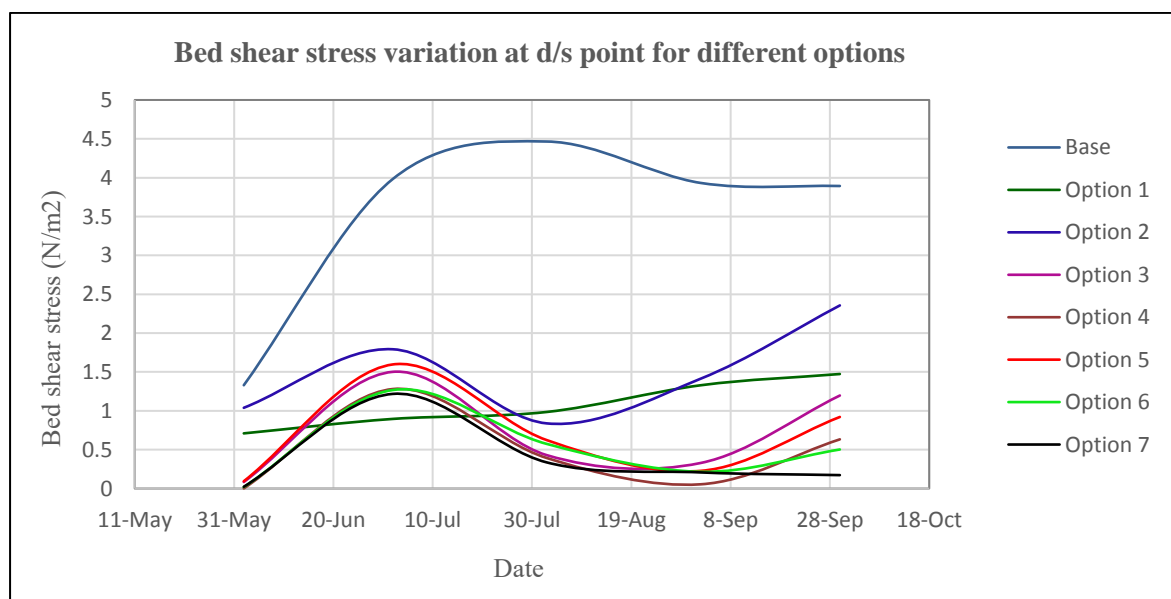


Figure 6.15: Relative comparison of bed shear stress at groyne d/s for different options

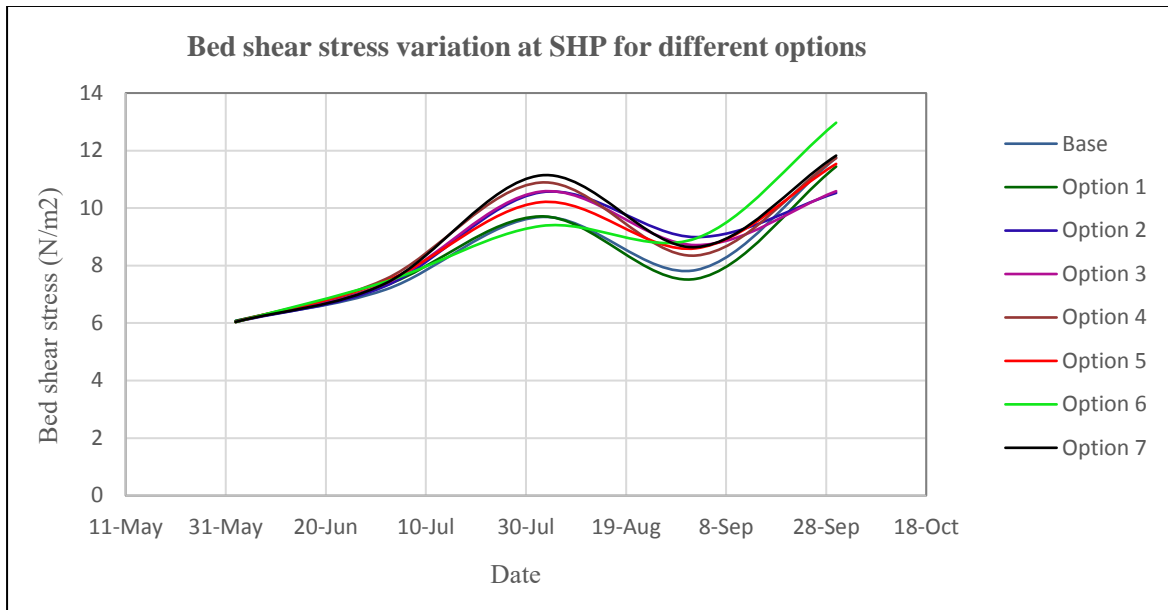


Figure 6.16: Relative comparison of bed shear stress at groyne SHP for different options

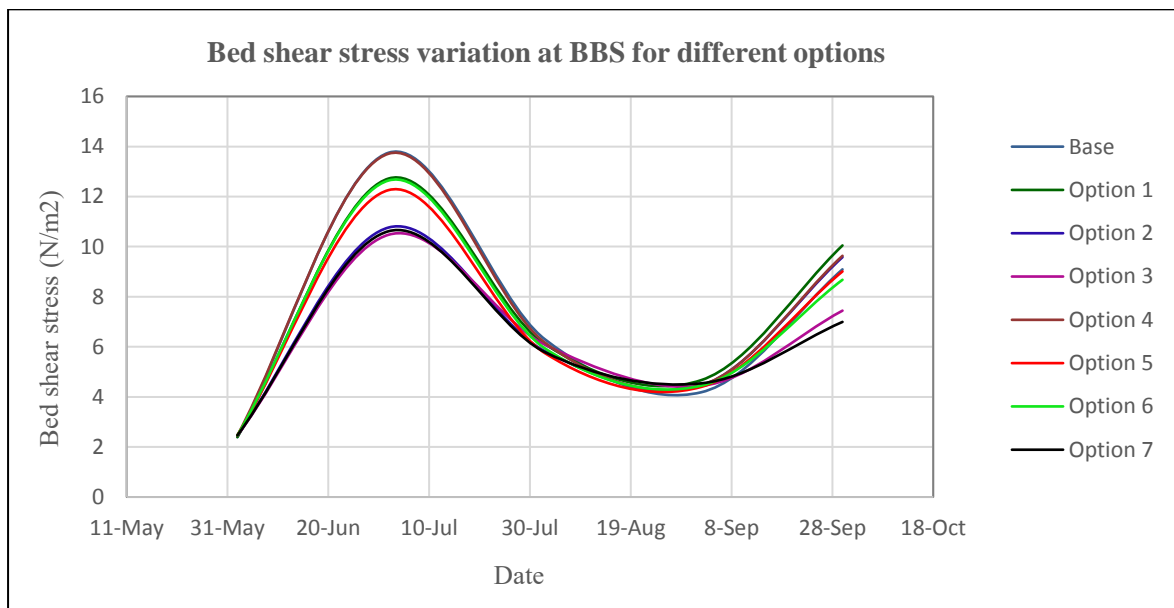


Figure 6.17: Relative comparison of bed shear stress at groyne BBS for different options

6.2.3.1 Bank Line Bed Shear Stress

As like the variation of velocity along the bank line, the bed shear stress variation near the bank has also been observed. This bed shear stresses have been observed along the line near the bank between two consecutive groynes (Figure 6.19). From the observation, it is found that at the base condition the value of bed shear stress ranges from 0.75 N/m² to 1.00 N/m² which is considerable higher than the critical value. Because the average grain size of the river is 0.11 mm and for this grain size, the critical bed shear stress is 0.14 N/m² according to Fischenich formula (Equation 4.1). So, the river bank is susceptible to erosion at normal condition. Also the BWDB has identified this bank as erosion prone area (Figure 5.16). Now for the spacing ratio of the groyne, $S/L = 1.0$, the bed shear stress decreases significantly and belongs to almost zero in some places with a maximum value of 0.025 N/m². With the increasing option, the magnitude of bed shear stress increases and for $S/L = 2.0$, the bed shear stress line is far below from the critical value. But after that the value reaches and crosses the critical line for bed shear stress for $S/L = 3.0$ and if this pattern continues, the more spacing option will increase the bed shear stress as well and reach up to the base condition. So, it is risky in this case, to provide spacing ration more than 2.0. Although the spacing ratio 2.5 may remain below the critical line.

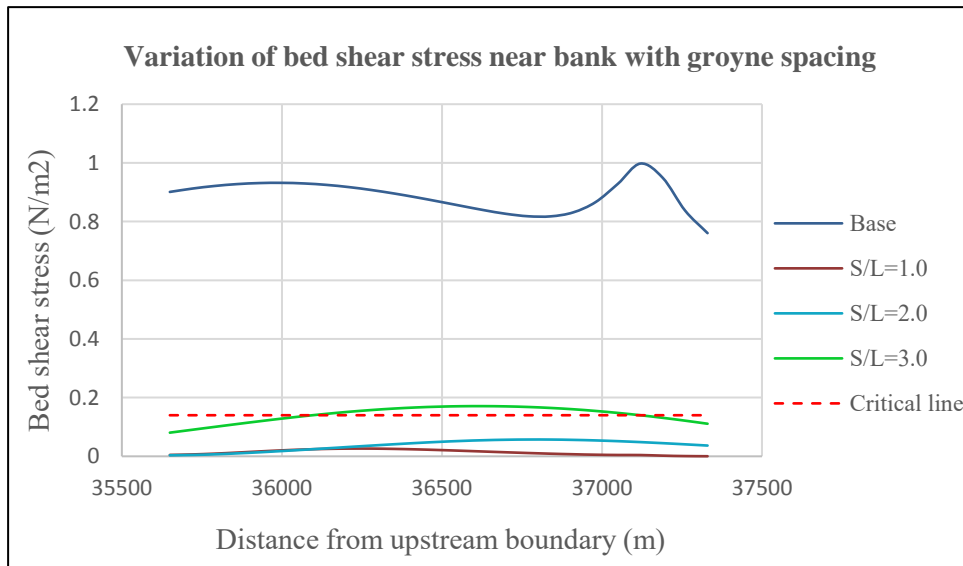


Figure 6.18: Comparison of bed shear stress along the bank line for different spacing of groynes

6.3 Observation of Morphologic parameters

Some sample figures showing the morphologic parameters like total transport, cumulative erosion/sedimentation, cross sections etc. are displayed sequentially to observe the scenarios.

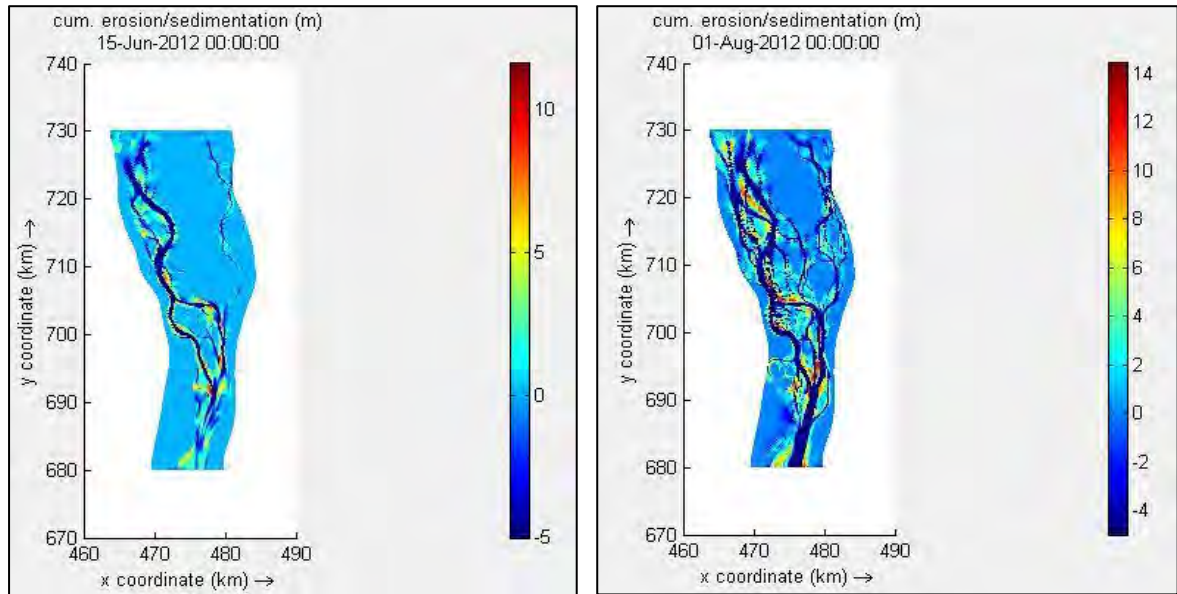


Figure 6.19: Cum. erosion/sedimentation at different dates for 2 groynes with $S/L = 1.5$

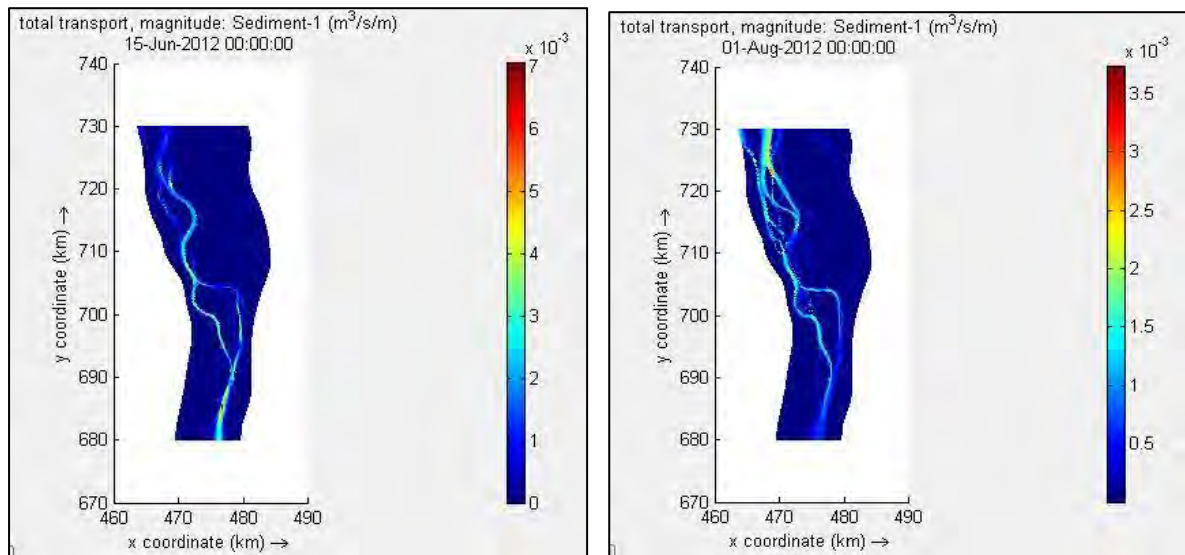


Figure 6.20: Total transport at different dates for 2 groynes with $S/L = 1.5$

6.3.1 Cumulative Erosion/Deposition Curves

From the cumulative erosion/deposition curves at different point for different options it is observed that at the upstream and downstream of the structures, mostly deposition occur after intervention although sometimes it shows erosion. But in case of SHP, there is very little effect of the structures on erosion/deposition. The variation of the sediment at this point is almost zero. This may be due to the distance of the SHP from the intervention point(s). Because the SHP is located at about 8-10 km downstream of the structural intervention point. So the structures has significant role in the vicinity only, not at far upstream or downstream points. Another reason may be due to the problem in model simulation. Because sediment transport is one of the most unpredictable parameters in river analysis. The mathematical model analysis might not always match with the real scenarios. So, there may be a fault of this software of not tracing any movement of sediment at SHP. In case of BBS, the results shows some variation for the months August and September. This deviation might be caused due to the backwater effect of the Bangabandhu Bridge. As the location of the BBS is far downstream, so the effect of these structures on sediment movement has a little quantity.

Option wise cumulative erosion/deposition at specific locations have been plotted and shown in Figure 6.23 to Figure 6.26. The graphs show that the cumulative erosion/deposition has fluctuating behavior from the base condition at maximum points. At SHP, there is very little variation in erosion/deposition. This may be due to the unpredictability of the Jamuna River or this sediment model might have some inefficiencies at that point.

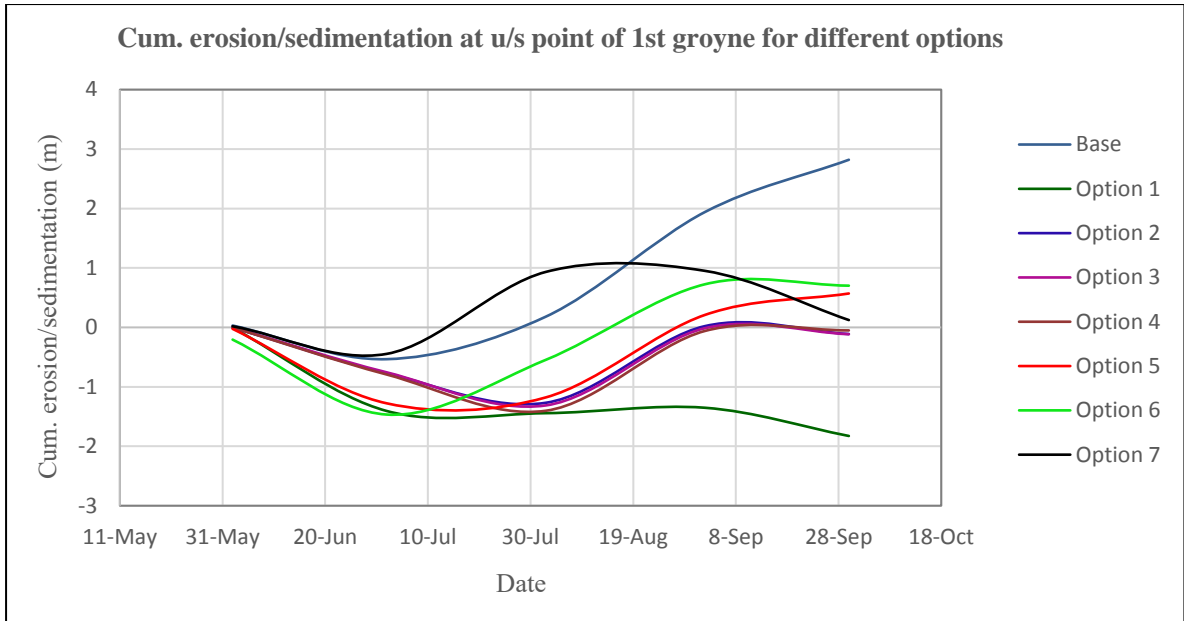


Figure 6.21: Relative comparison of cum. erosion/deposition at groyne u/s for different options

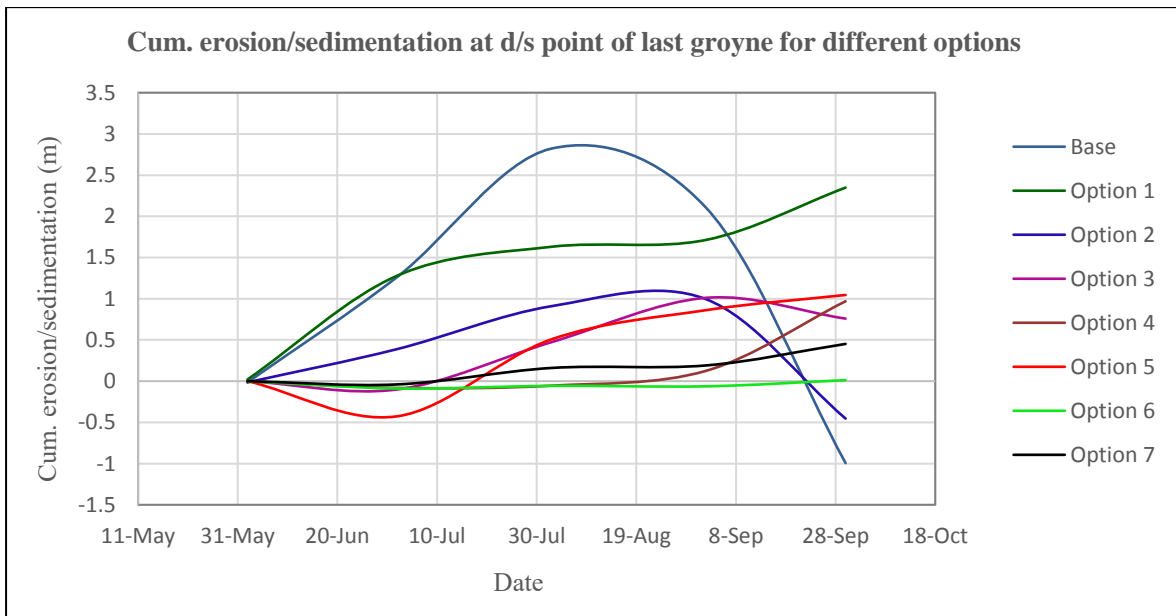


Figure 6.22: Relative comparison of cum. erosion/deposition at groyne d/s for different options

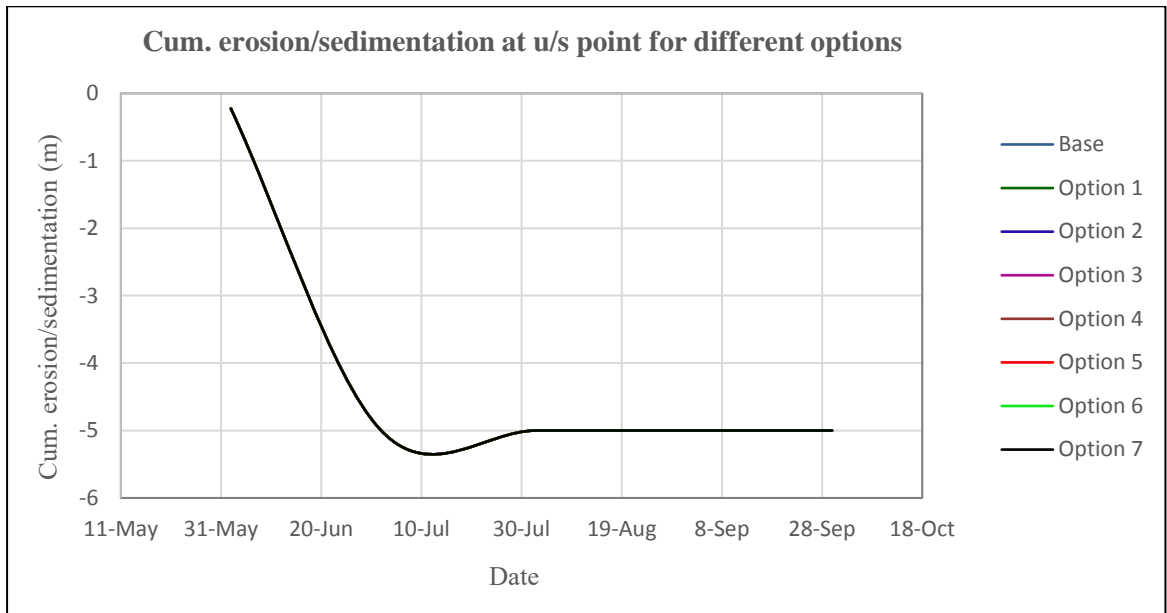


Figure 6.23: Relative comparison of cum. erosion/deposition at groyne SHP for different options

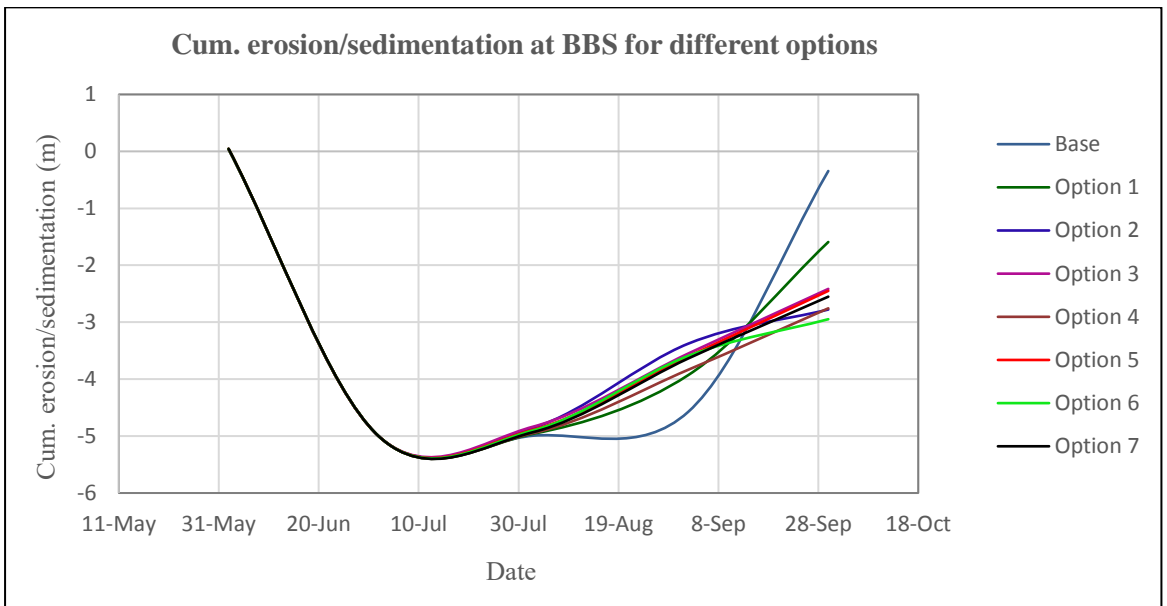


Figure 6.24: Relative comparison of cum. erosion/deposition at groyne BBS for different options

6.3.2 Bed Level Variation at Different Locations

From the previous section the relative variation of cumulative erosion or sedimentation has been observed at four points of interests. Now in this section, the actual bed level variation with respect to base condition at some locations for option 2 has been shown in Figure 6.25. One is along the length of the 1st and 2nd groyne from the right bank up to about 4 km inside the river. These sections are denoted by a-a and c-c. Cross-section of same category at the middle of the two consecutive groynes are denoted by b-b. Another section has been chosen along the river in front of the noses of the groynes which is section 1-1.

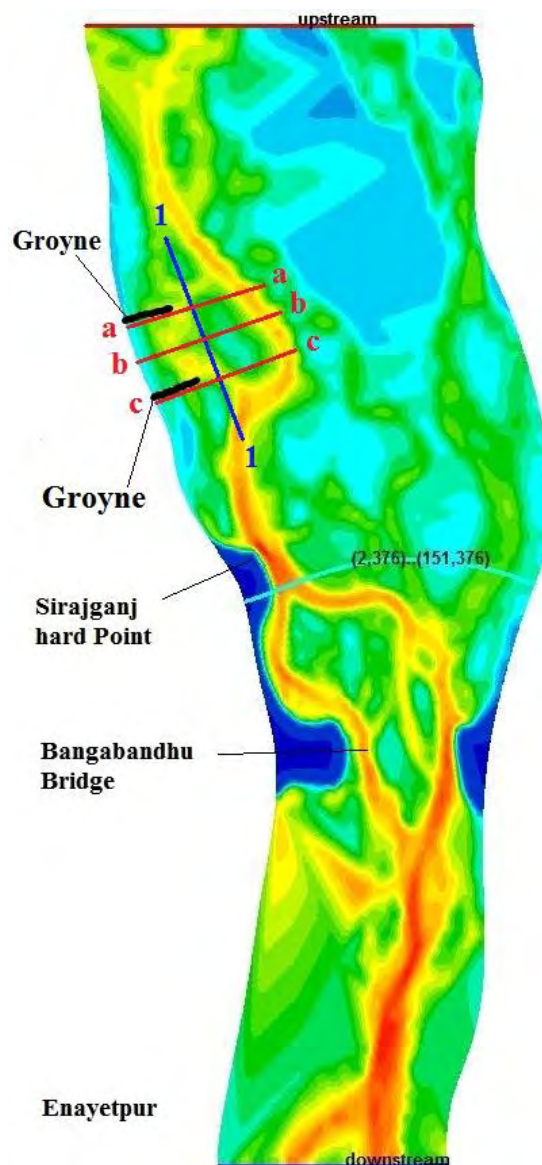
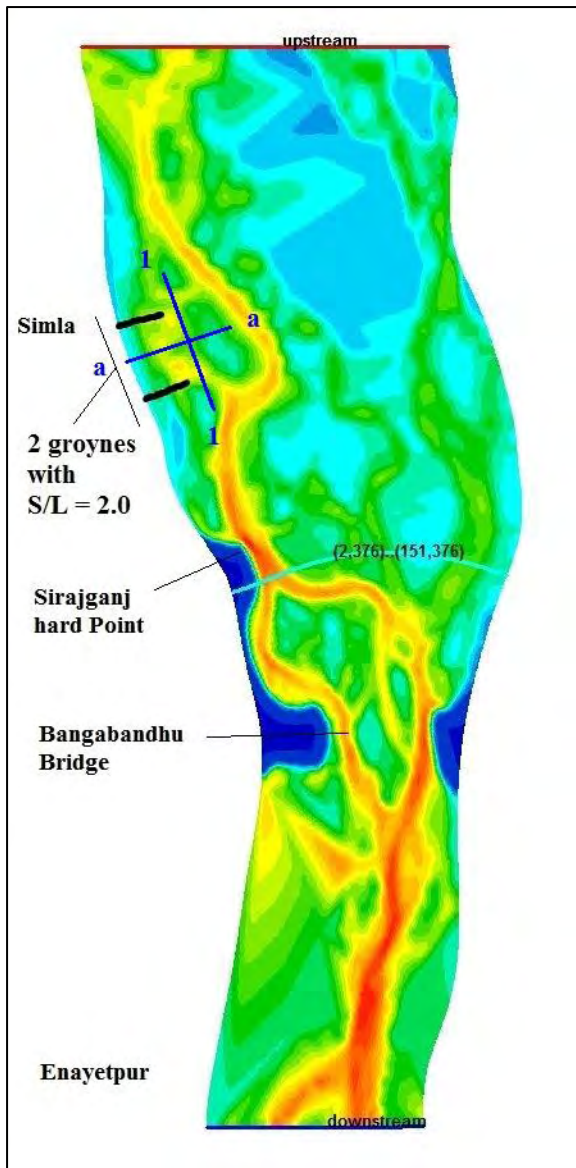
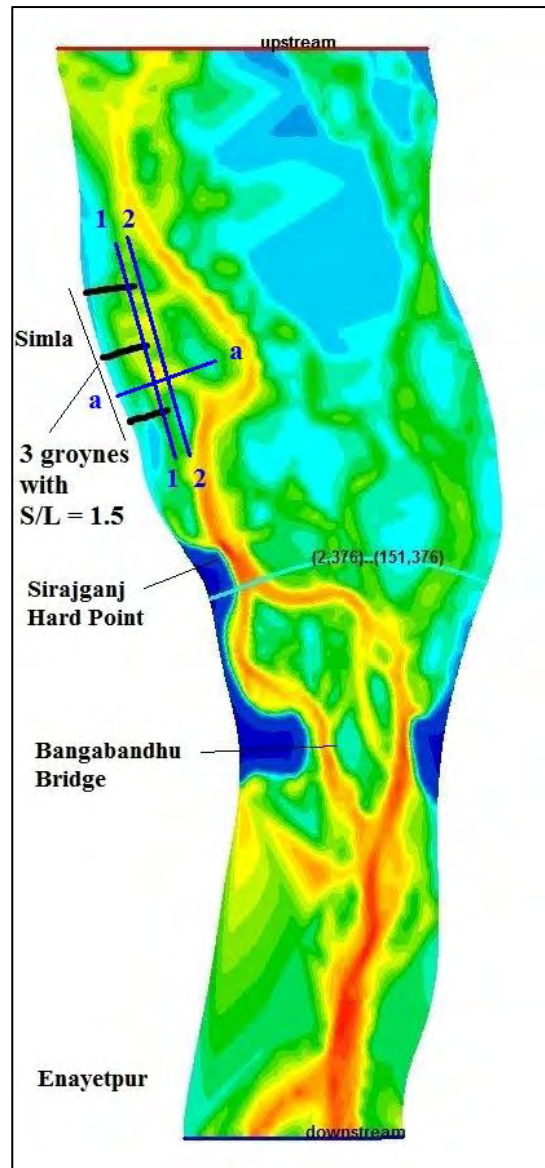


Figure 6.25: Cross-section locations to observe bed level variation across and along the river for option 2



Option 4



Option 6

Figure 6.26: Cross-section locations to observe bed level variation across and along the river for option 4 and 6

Some other sections have been shown for option 4 and option 6 in Figure 6.26. For option 4, the cross section is a-a and long section is 1-1. For option 6, the cross section is a-a and the long sections are 1-1 and 2-2 respectively.

6.3.2.1 Bed Level Variation across the River for Option 2

To observe the bed level variation across the river for section a-a, the Figure 6.27 shows the variation of the bed level along the 1st groyne length from the right bank of the river and extends up to almost 4 km inside the river. From this figure, it is seen that there is major erosion takes place just immediately after the nose of the groyne and after some distances (around 500 m) some deposition occurs. The maximum erosion in this case is -5.25 m which takes place immediately after the nose and maximum deposition is +3.70 m which is located 700 m from the nose. In case of section c-c, shown in Figure 6.28 the result pattern is almost same but the values are different. Here, the maximum erosion is -4.50 m and maximum deposition is +0.74 m.

Comparing these two figures, it can be decided that the erosion/deposition effect is more at the 1st groyne with compared to the 2nd one. Because the value of both erosion and deposition for the 2nd case is lower than the 1st case. Another observation is that for the both cases, the effect of groyne withstands up to 1 km from the nose of the groyne in to the river.

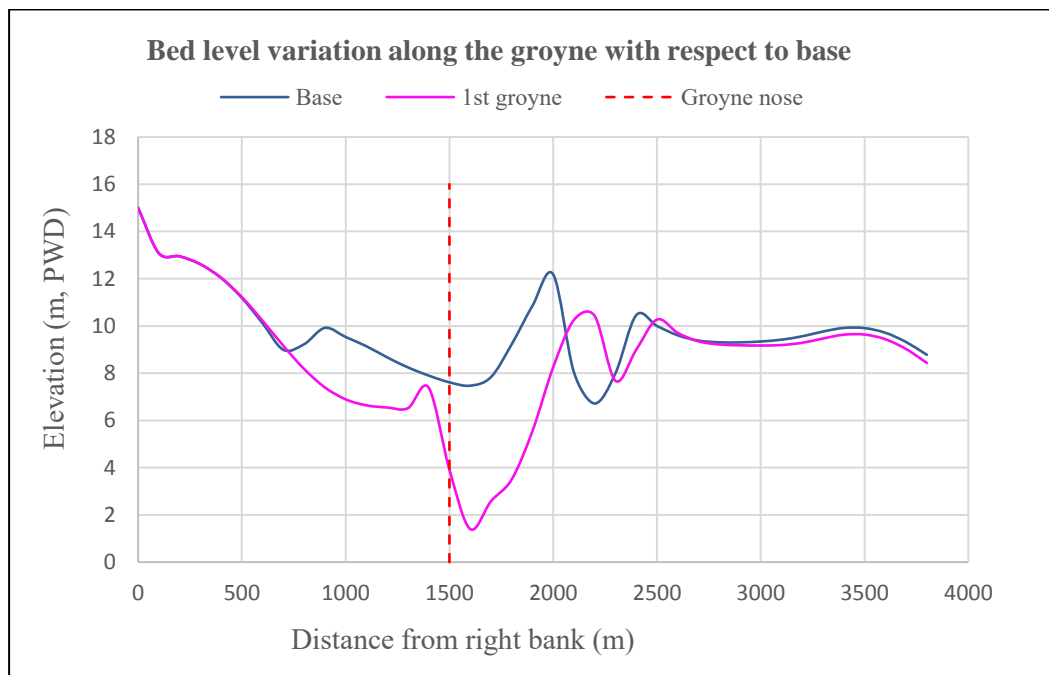


Figure 6.27: Bed level variation along the 1st groyne with respect to base for option 2 (Section a-a)

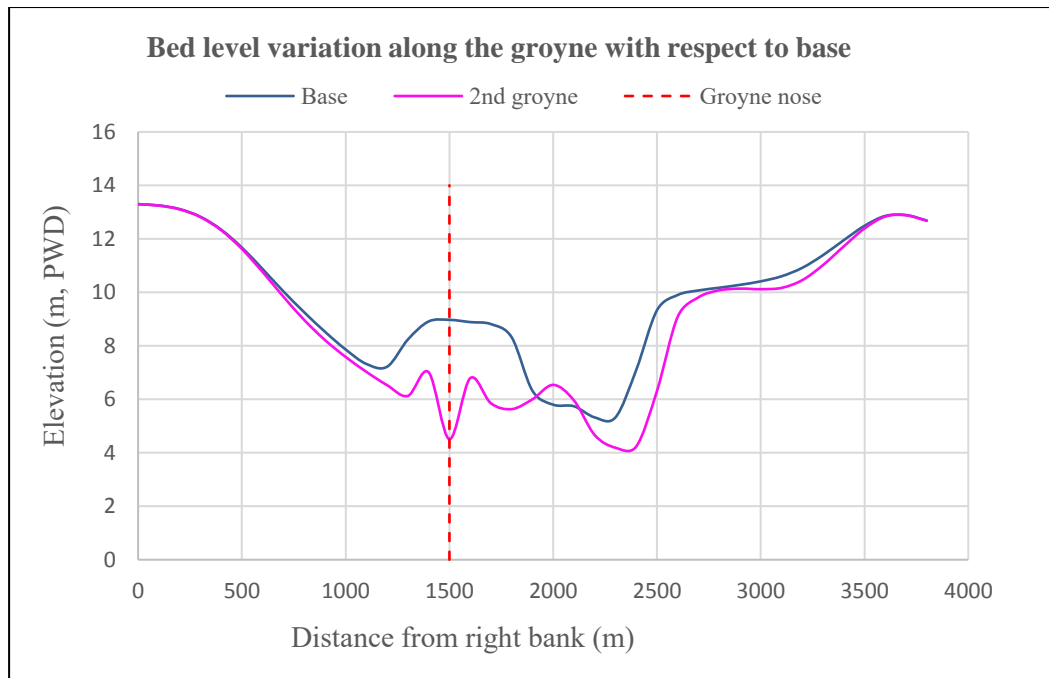


Figure 6.28: Bed level variation along the 2nd groyne with respect to base for option 2 (Section c-c)

At the middle portion between the consecutive two groynes, the effect of groynes are exposed in Figure 6.29. The comparison has been made with respect to base condition and the cross-section extends from the right bank of the river up to around 4 km inside the river.

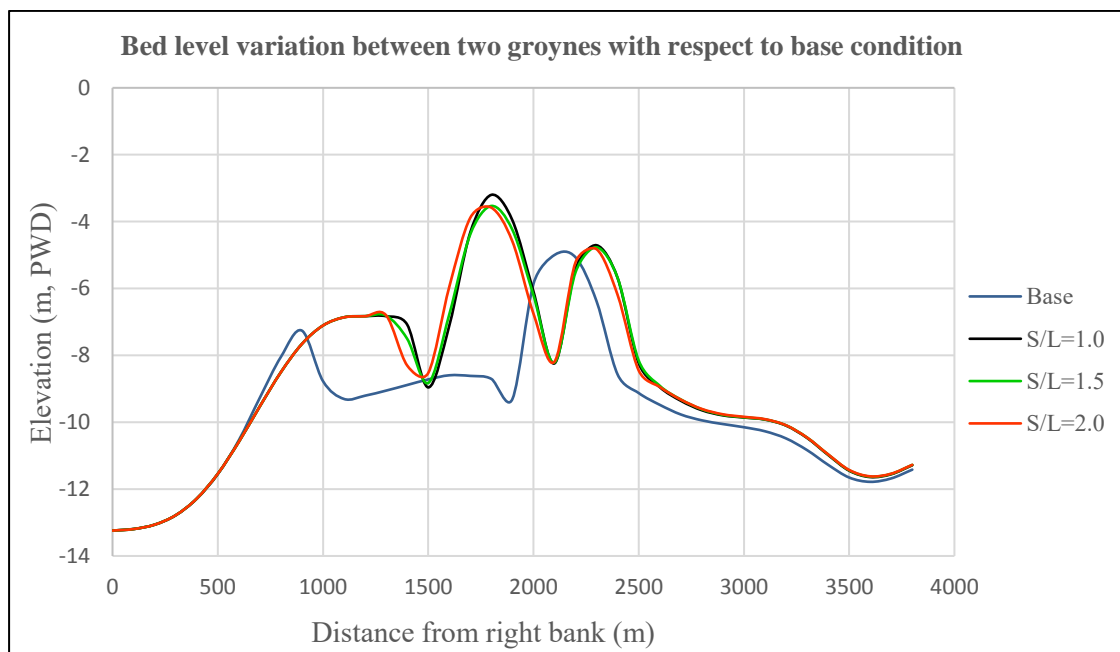


Figure 6.29: Bed level variation between the 1st and 2nd groyne with respect to base for option 2, option 3 and option 4 (Section b-b)

In this case, the comparison has been done for $S/L=1.0$, 1.5 and 2.0 respectively with the base. From the figure it is noticed that major deposition takes place at two locations, one is about 1200 m from the bank the value of which is +2.37 m and another is about 1800 m from the bank and its value is +4.5 m. Maximum erosion takes place at about 2200 m from the bank and the value of erosion is -3.24 m. Here, the noticeable fact is that the variation of bed level among the spacing options is very little. The pattern of this graph is somewhat similar to the previous two cases.

6.3.2.2 Bed Level Variation along the River for Option 2

In case of observing the bed level variation along the river for section 1-1, the Figure 6.30 shows the variation of the bed level along the line extends from 34 km from the downstream boundary up to around 40 km to the north. The line is located in front of the noses of the groynes. Here the groyne spacing is 1.0. From the figure, it is observed that there is huge erosion at the 1st groyne location and surrounding areas and the amount of erosion decreases in case of 2nd groyne with different pattern. And deposition takes place at the downstream of the 2nd groyne. No deposition is in between the two noses of the groynes. The effect of these groynes extends up to 2 km laterally from the nose for both the cases.

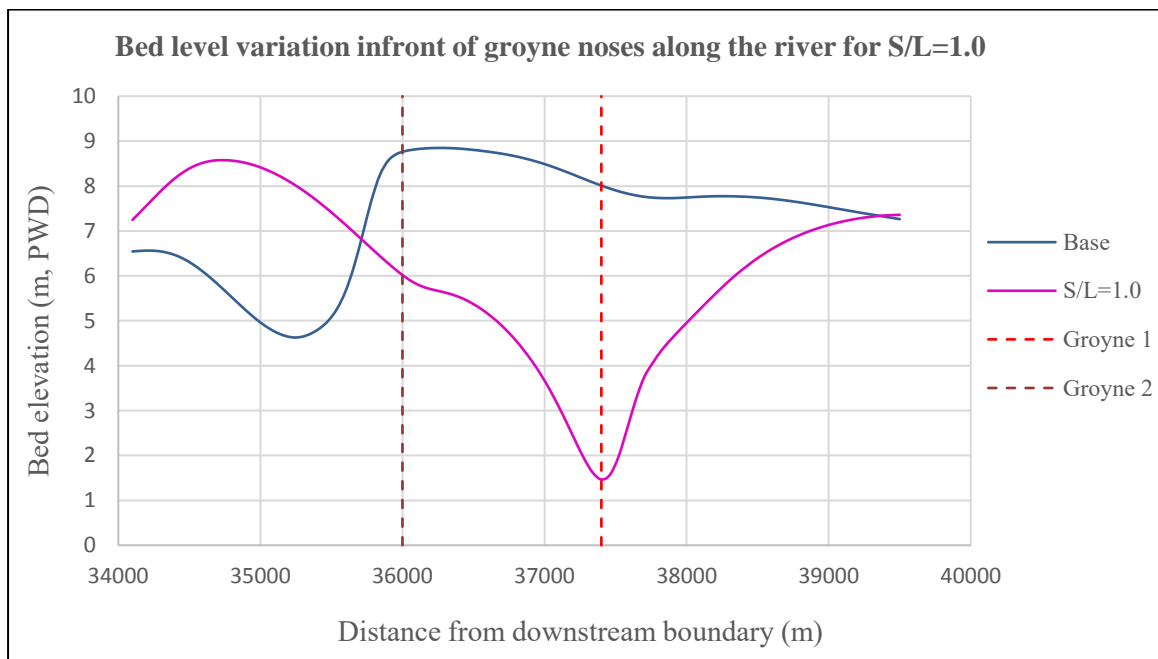


Figure 6.30: Bed level variation along the river in front of the nose of the groynes with respect to base for Option 2 ($S/L = 1.0$) (Section 1-1)

Figure 6.31 is for the same section (Section 1-1) but for different option. Here the S/L ratio is 2.0. From the figure, it is observed that the erosion pattern is almost same at the location of the two groynes with varying values. But the noticeable thing is that the major deposition zone lies between the two groynes which is different from the previous case. A small deposition zone is noticed at the downstream of the 2nd groyne. Here also the effect of these groynes extends up to 2 km laterally from the nose for both the cases.

After comparison of these two graphs, it can be concluded that in case of smaller spacing, there is no deposition between the groyne noses and the major deposition takes place at the downstream of the last groyne. In case of increasing the spacing the deposition zone shifts towards the intermediate locations between the groynes and the erosion zone at the downstream of the last groyne comes to smaller with decreasing deposition values.

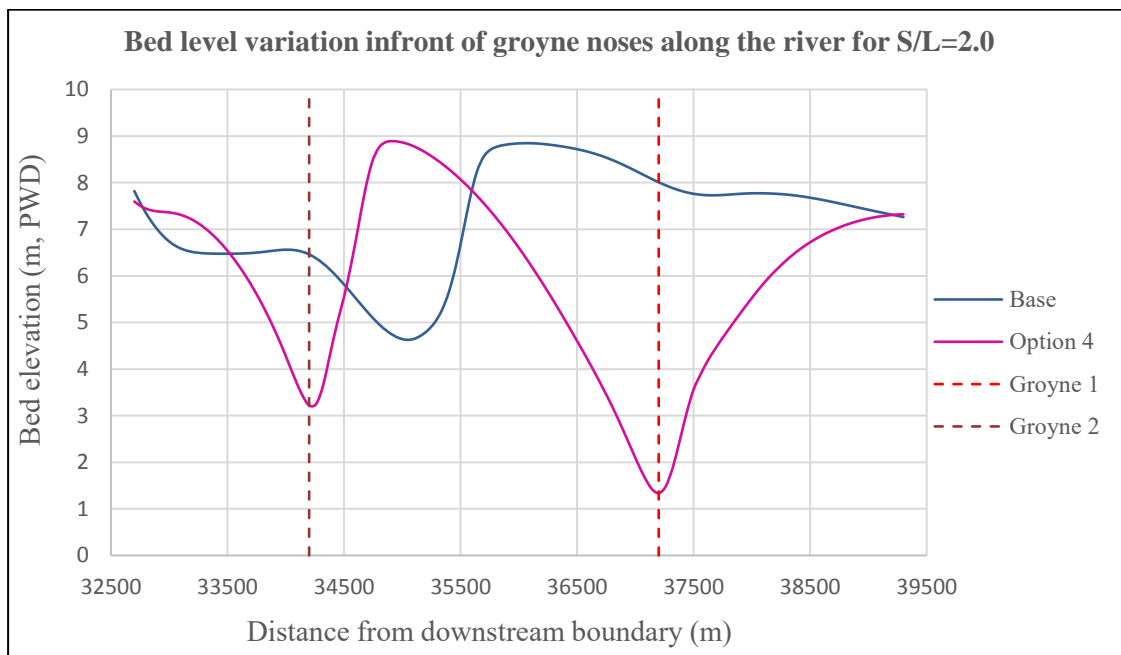


Figure 6.31: Bed level variation along the river in front of the nose of the groynes with respect to base for Option 4 (S/L=2.0) (Section 1-1)

6.3.2.3 Bed Level Variation across the River for Option 4 and Option 6

From the Figure 6.32 and Figure 6.33, it has been observed that mainly deposition takes place between the two groynes for each cases (i.e. section a-a for option 4 and option 6) which is relevant with results of previous several studies. The comparison has been done with respect to base condition across the river.

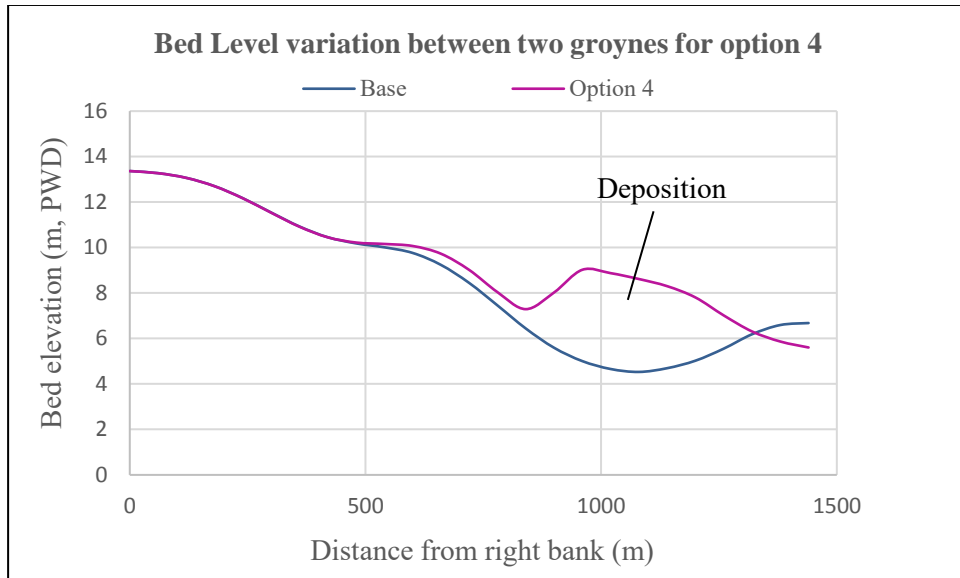


Figure 6.32: Bed level variation between the 1st and 2nd groyne with respect to base for option 4 (Section a-a)

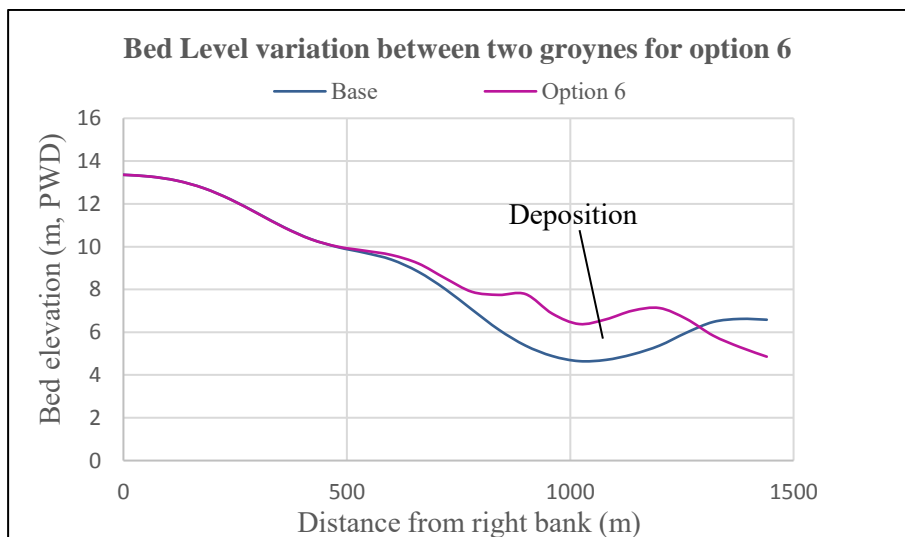


Figure 6.33: Bed level variation between the 2nd and 3rd groyne with respect to base for option 6 (Section a-a)

6.3.2.4 Bed Level Variation along the River for Option 4 and Option 6

In this case, the variation of bed level has been compared with the base condition along the river. Here, Figure 6.34 shows the variation along the line in front of the noses of the groynes for the option 4. The major erosion takes place at the location of the 1st groyne and the value of erosion decreases at the location of the 2nd one and deposition takes place in between the groynes. Here, the maximum erosion is almost -6.0 m and deposition is about +4.0 m.

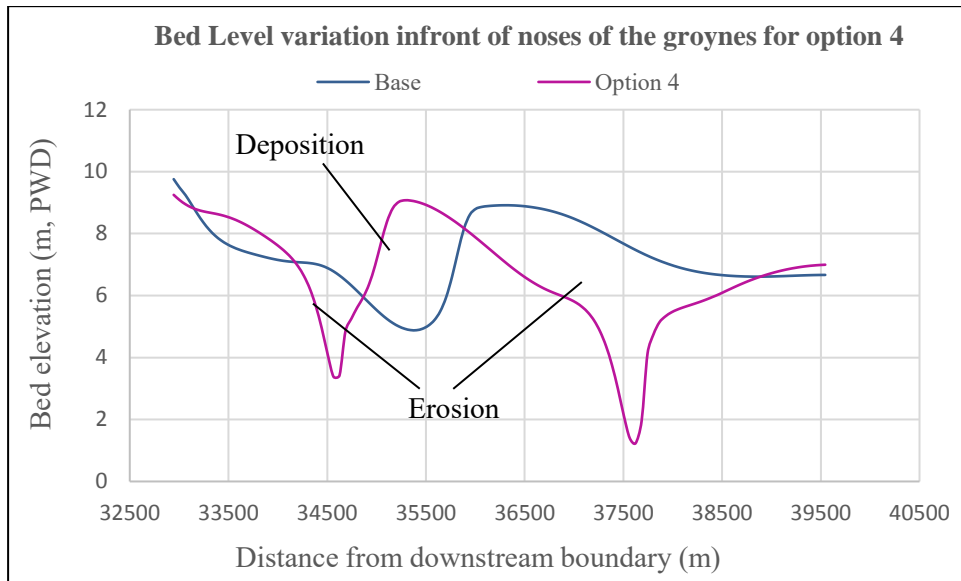


Figure 6.34: Bed level variation along the river in front of the nose of the groynes with respect to base for Option 4 (2 groynes with S/L = 2.0) (Section 1-1)

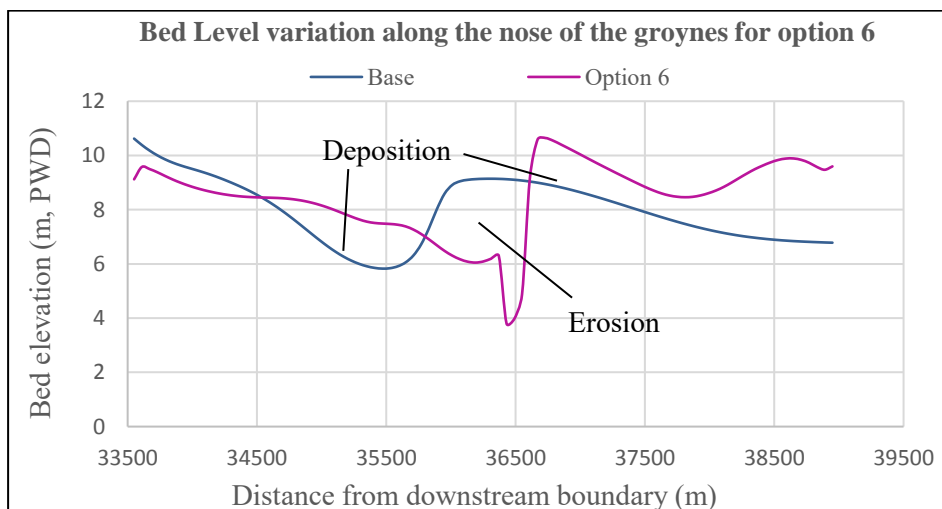


Figure 6.35: Bed level variation along the river along the nose of the groynes with respect to base for Option 6 (3 groynes with S/L = 1.5) (Section 1-1)

Figure 6.35 and Figure 6.36 shows the same circumstances in case of option 6 along the noses of the groynes and along the line in front of the noses of the groynes respectively. For these two cases, the erosion/deposition pattern is almost same with the previous diagrams. From these two cases, the maximum erosion is -5.0 m and deposition is +2.0 m. The effect of the groynes laterally extends up to about 2.0 km from the groyne which is similar to the previous that has been explained in section 6.3.2.2.

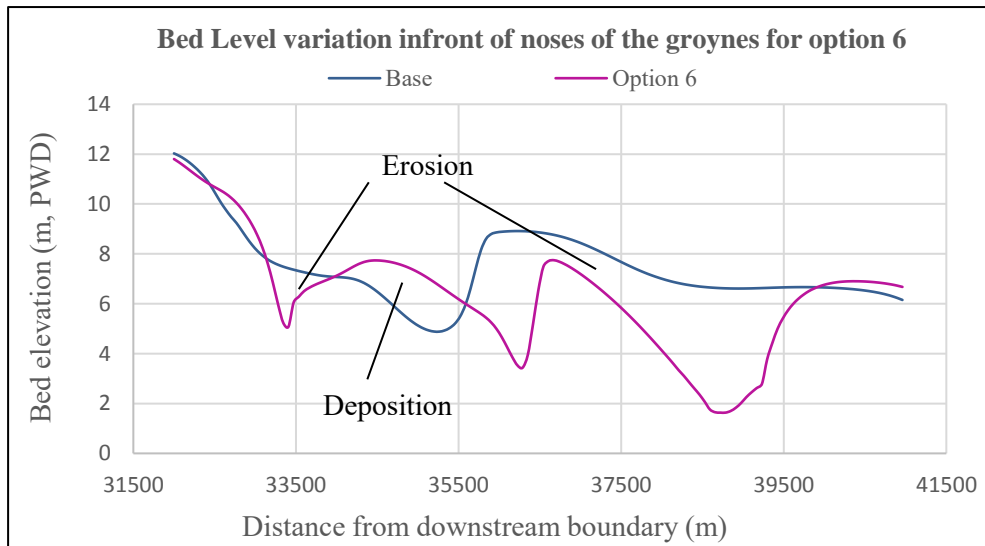


Figure 6.36: Bed level variation along the river in front of the nose of the groynes with respect to base for Option 6 (3 groynes with S/L = 1.5) (Section 1-1)

6.4 Summary of the Results

In order to quantify the response of the river hydrodynamics and morphology for various options at different locations, at first the model has been set up then calibrated and validated subsequently for the both cases (hydrodynamics and morphology). An attempt has been made to compare the results of water level obtained from Delft3D with those of MIKE21C and found satisfactory. Here in this section, model results for the month of July can be assessed as shown in Table 6.1. The remaining results can be seen in Appendix-C. It can be seen from the results that the Jamnua River shows reasonable responses due to the structural intervention at the right bank of the river.

As for example, at upstream of the selected intervention, water level increases about 10.84% and 6.72% for the downstream (Table 6.1, 6.2). This rise of water level may be due to the afflux effect due to the structural intervention(s). The velocity and bed shear stress follow decreasing trend lines at the vicinity of the structures. Similarly the other parameters like velocity, bed shear stress and cumulative erosion/deposition show considerable responses for the selected intervention (options). The changes are +9.92% for velocity, +22.78% for bed shear stress and no erosion/deposition are obtained. At Bangabandu Bridge site (Table 6.4), the water level doesn't change but the velocity follows decreasing trends.

From the velocity vector diagrams, it is observed that the direction of velocity changes and diverted away from the bank with the structural intervention. If the spacing between the groynes increases the vectors enters into the intermediate portions between the groynes forming a curvature shape. And from the bank line velocity and bed shear stress analysis, it is clear that for this reach of the river the spacing ratio more than 2.0 is dangerous because in case of spacing ratio 3.0, the bank line velocity and bed shear stress both cross the critical line.

In case of bed level variation, erosion takes place along the length of the groyne basically in front of nose and deposition occurs more or less 500 m front side of the nose of the groyne. The variation of the middle portion between the groynes shows the similar pattern. In case of lateral variation along the river in front of the groyne nose, the deposition zone shifts towards the intermediate locations between the groynes from the downstream. The effect of groyne extends up to 1 km inside the river and 2 km

laterally from either nose of the groyne.

Thus it can be supposed that to prevent the bank erosion, this kinds of structures with increasing numbers and different spacing provides satisfactory results. Overall, the model results show that it has the capacity to assess responses for various options at the vicinity of the interventions.

Table 6.1: Change of parameters with respect to base condition at u/s for various options (July)

Upstream of structure				
Options	WL (%)	Velocity (%)	Bed shear stress (%)	Erosion/deposition (m)
1 groyne	8.16	-39.78	-60.86	1.54
2 groynes with S/L=1.0	9.32	-46.41	-69.85	-1.16
2 groynes with S/L=1.5	8.53	-30.94	-33.33	3.41
2 groynes with S/L=2.0	9.39	-64.09	-88.76	-4.62
3 groynes with S/L=1.0	8.89	-31.49	-32.40	4.13
3 groynes with S/L=1.5	9.32	-37.02	-50.19	3.96
3 groynes with S/L=2.0	10.84	-31.49	-49.63	-0.20

+ ve means increase/deposition, - ve means decrease/erosion

Table 6.2: Change of parameters with respect to base condition at d/s for various options (July)

Downstream of structure				
Options	WL (%)	Velocity (%)	Bed shear stress (%)	Erosion/deposition (m)
1 groyne	6.58	34.44	66.67	0.00
2 groynes with S/L=1.0	8.16	-16.56	-26.09	0.76
2 groynes with S/L=1.5	7.44	-74.17	-91.30	-2.29
2 groynes with S/L=2.0	6.79	11.92	14.78	-6.00
3 groynes with S/L=1.0	7.15	-84.11	-96.52	2.81
3 groynes with S/L=1.5	6.65	-5.30	-24.64	0.78
3 groynes with S/L=2.0	6.72	-45.70	-44.93	1.93

+ ve means increase/deposition, - ve means decrease/erosion

Table 6.3: Change of parameters with respect to base condition at SHP for various options (July)

Sirajganj Hard Point (SHP)				
Ooptions	WL (%)	Velocity (%)	Bed shear stress (%)	Erosion/deposition (m)
1 groyne	-0.07	1.19	2.95	-5.00
2 groynes with S/L=1.0	0.00	31.35	73.84	-5.00
2 groynes with S/L=1.5	0.14	25.40	58.51	-5.00
2 groynes with S/L=2.0	0.57	13.10	33.33	-5.00
3 groynes with S/L=1.0	1.07	16.27	35.72	-5.00
3 groynes with S/L=1.5	0.93	21.03	48.52	-5.00
3 groynes with S/L=2.0	1.72	9.92	22.78	-5.00

+ ve means increase/deposition, - ve means decrease/erosion

Table 6.4: Change of parameters with respect to base condition at BBS for various options (July)

Bangabandhu Bridge Site (BBS)				
options	WL (%)	Velocity (%)	Bed shear stress (%)	Erosion/deposition (m)
1 groyne	-0.08	-3.83	23.74	-6.00
2 groynes with S/L=1.0	-0.85	-23.96	51.95	6.70
2 groynes with S/L=1.5	-0.85	-67.73	-69.84	5.15
2 groynes with S/L=2.0	-0.08	-24.28	-7.98	-2.10
3 groynes with S/L=1.0	-1.00	-62.94	-50.00	5.90
3 groynes with S/L=1.5	0.15	-37.38	-20.53	2.92
3 groynes with S/L=2.0	0.00	-6.07	28.02	-6.00

+ ve means increase/deposition, - ve means decrease/erosion

Table 6.5: Monthly variation of cum. erosion/deposition at different locations for all the options

Cum. Erosion/Deposition (m)								
u/s								
Date	Base	Option 1	Option 2	Option 3	Option 4	Option 5	Option 6	Option 7
1-Jun	-0.12279	0.001034	-0.05414	-0.06206	-0.06963	0.838351	9.54E-06	-0.21957
1-Jul	-3.38927	1.73075	-1.15469	3.40705	-4.82042	-4.82339	3.27664	-0.20424
1-Aug	-4.99852	1.8153	-1.01404	1.1501	3.2922	2.44095	3.27664	-0.31912
1-Sep	3.14144	4.52101	-4.99971	-4.98486	-4.99994	1.97879	3.27662	-0.28024
30-Sep	-4.9991	1.97102	4.45679	3.76438	3.90919	0.936223	3.27696	-4.99526
d/s								
Date	Base	Option 1	Option 2	Option 3	Option 4	Option 5	Option 6	Option 7
1-Jun	-0.07394	9.54E-07	0.052472	0	9.63E-05	0	0	0
1-Jul	-2.23368	0.00847	0.756154	-0.33232	-4.99733	2.67702	2.46979	1.92763
1-Aug	-1.60298	0.023461	0.820639	2.91779	-5	4.10148	4.14746	0.086869
1-Sep	7.19262	-0.52265	-4.88794	3.44129	-1.74733	5.44723	4.16025	0.356354
30-Sep	5.46633	-0.5785	-4.99955	5.08437	-4.99998	-2.18086	5.55232	2.20797
SHP								
Date	Base	Option 1	Option 2	Option 3	Option 4	Option 5	Option 6	Option 7
1-Jun	-0.82777	-0.82621	-0.85794	-0.85684	-0.85942	-0.85865	-0.85592	-0.85893
1-Jul	-5	-5	-5	-5	-5	-5	-5	-5
1-Aug	-5	-5	-2.85595	-2.85853	-2.85589	-5	-5	-2.85065
1-Sep	-5	-5	-5	-5	-5	-2.22311	-5	-5
30-Sep	-5	-5	-5	-5	-5	-5	-5	-5
BBS								
Date	Base	Option 1	Option 2	Option 3	Option 4	Option 5	Option 6	Option 7
1-Jun	0.696684	0.696303	0.785183	0.786232	0.7864	0.785315	0.785878	0.786103
1-Jul	4.57916	-4.99679	5.29778	5.15313	-2.09781	5.90294	2.9223	-4.99731
1-Aug	6.67965	-4.99956	-5	6.69503	-5	-5	0.221426	1.50671
1-Sep	5.57396	-4.99916	5.83188	2.64203	5.68807	-5	3.4995	5.65976
30-Sep	3.98544	-4.99925	0.626596	1.60514	1.59909	6.77034	7.61095	-2.71065

CHAPTER 7

CONCLUSIONS AND RECOMMENDATIONS

7.1 General

Assessment of river responses for any structural intervention in the braided river like Jamuna River is a complex task. Two-dimensional morphological model has become a useful tool for analyzing the hydrodynamic and morphological behavior of such river. In this study, efforts have been given to assess the river responses due to structural intervention.

7.2 Conclusions

The following concluding remarks can be drawn from the present study-

- i. A two-dimensional mathematical model with Delft3D software has been set up for flow with sediment transport. The model has been calibrated and validated with the reasonable accuracy, thus this model can be available for analyzing the river responses for selected structural intervention.
- ii. Responses of the Jamuna River have been assessed from the model simulations for different options using groyne as a structural intervention. In this study, seven different options with groyne of number such as 1, 2 and 3 with spacing ratio 1.0, 1.5 and 2.0.
- iii. Model results indicate that at upstream of the selected intervention, water level increases about 10.84% and 6.72% for the downstream. In both cases, the reduction of velocity and the bed shear stress is more than 50%.
- iv. For observation, four points were selected among them the effects are considerable at the upstream and downstream of the groyne(s) and for the other two points (e.g. Sirajganj Hard Point and Bangabandhu Bridge Site) the effect is very little due to the long distance.
- v. From the velocity vectors and bank line velocities as well as bed shear stress, it can be decided that for this specific reach of the river, the maximum allowable spacing between the groynes is 2.0 times of its length. Otherwise the bank will be in vulnerable condition due to erosion.
- vi. The bed level variation surrounding the groynes is considerable. The effect of groyne extends up to 1 km inside the river and 2 km laterally from either nose of the groyne. The maximum erosion is -5.25 m and deposition is +3.70 m along the length of the

groyne. In case of lateral section (along the river) the values are -6.0 m and +4.0 m respectively.

- vii. Selected hydrodynamic and morphologic scenarios are extracted from model then interpreted and observed that due to structural intervention, there are significant effects on those variables in case of the selected reach of the Jamuna River.
- viii. Finally, it can be concluded that river bank erosion can be decreased by using the increasing number of such type of transverse structures (groyne) with different spacing and the effect of these types of structures have more influences at the vicinity.

7.3 Recommendations for Further Study

Based on the present study following recommendations can be made for future study-

- i. As Jamuna is an alluvial river in a deltaic region of Bangladesh, so morphological activities are very dynamic in this river. Structural intervention is only fruitful when maintenance is regular.
- ii. In this study a selected reach has been used for analysis. Therefore, effectiveness of the results found in this study should be much better when the other reaches could be included.
- iii. In this study two-dimensional morphological model is used which gives depth average velocity from simulations. Therefore, the prediction of local phenomena like scour at toe level (under water) cannot be properly predicted. 3-D model would be more helpful for such computations.
- iv. Changing the groyne length simultaneously and for more options, the study may give much better results to identify the response of the river.
- v. Comparison with the physical model study is the best way of analysis in this case. So, any mathematical model output need to be verified with the physical model output or field data prior to implementation
- vi. In this study, the structures have been incorporated only one side. Further study may be proceeded by incorporating the structural intervention at the both banks of the river using different options.

REFERENCES

- Abbas, B. G., Mojtaba, G. K. (2009) 'Effect of Groyens Opening Percentage on River Outer Bank Protection', *Journal of Applied Sciences*, 9(12), pp. 2325–2329.
- Ahmad, H. F., Bhat, M. S. and Ahmad, S. (2016) 'One Dimensional Steady Flow Analysis Using HEC- RAS – A case of River Jhelum , Jammu and Kashmir', *European Scientific Journal*, 12(32), pp. 340–350. doi: 10.19044/esj.2016.v12n32p340.
- Ahmed, T. and Hasan, M. Z. (2011) 'A Study on River Bank Protection Works and Flooding of Sirajganj Town'. Bangladesh University of Engineering and Technology, Bangladesh.
- Alam, S. and Matin, M. A. (2012) 'Application of Delft3D Mathematical Model in the river Karnafuli For Two-Dimensional simulation', in 1st International Conference on Advances in Civil Engineering 2012 (ICACE 2012), CUET, Chittagong, Bangladesh, pp. 12–14.
- Alam, S. and Matin, M. A. (2013) 'Application of 2D morphological model to assess the response of Karnafuli River due to capital dredging', *Journal of Water Resources and Ocean Science*, 2(3), pp. 40–48. doi: 10.11648/j.wros.20130203.13.
- Alauddin, M. (2011) 'Morphological Stabilization of Lowland Rivers by using a Series of Groynes'. Nagoya University, Japan.
- Ali, A., Mynett, a. E. and Azam, M. H. (2007) 'Sediment Dynamics in the Meghna Estuary, Bangladesh: A Model Study', *Journal of Waterway, Port, Coastal, and Ocean Engineering*, 133(August), pp. 255–263. doi: 10.1061/(ASCE)0733-950X(2007)133:4(255).
- Ali, M. M. (2004) 'Hydrodynamic Simulation of the River Jamuna'. Bangladesh University of Engineering and Technology, Dhaka.
- Best, J. L. *et al.* (2003) 'Three-Dimensional Sedimentary Architecture of a Large, Mid-Channel Sand Braid Bar, Jamuna River, Bangladesh', *Journal of Sedimentary Research*, 73(4), pp. 516–530. doi: 10.1306/010603730516.
- Best, J. L. *et al.* (2007) 'The Brahmaputra-Jamuna River , Bangladesh'.
- Briere, C., Giardino, A. and Van der Werf, J. (2011) 'Morphological Modeling of Bar Dynamics With Delft3D: the Quest for Optimal Free Parameter Settings Using an Automatic Calibration

Technique', Coastal Engineering Proceedings, 1(32), p. 60. doi: 10.9753/icce.v32.sediment.60.

Churuksaeva, V. and Starchenko, A. (2015) 'Mathematical modeling of a river stream based on a shallow water approach, Procedia - Procedia Computer Science'. Elsevier Masson SAS. doi: 10.1016/j.procs.2015.11.024.

Coleman, J. M. (1969) 'Brahmaputra River: channel processes and sedimentation', Sediment. Geol., 3(129-239).

Dani, B. A. *et al.* (2013) 'An investigation of the use of groynes as a means of riverbank erosion protection', (March).

Dargahi, B. (2004) 'Three-dimensional flow modelling and sediment, transport in the River Klarälven', Earth Surface Processes and Landforms, 29(7), pp. 821–852. doi: 10.1002/esp.1071.

Elias, E. P. L. *et al.* (2001) 'Hydrodynamic Validation of Delft3D with Field Measurements at Egmond', Coastal Engineering 2000, pp. 2714–2727. doi: 10.1061/40549(276)212.

FAP1 (1991) 'River Training Studies of the Brahmaputra River'.

FAP2 (1992) 'North West Regional Study'.

FAP21/22 (2001) "Bank protection and river training (AFPM) pilot project," Final project evaluation report, Volume I, WARPO, Ministry of water resources, Government of People's Republic of Bangladesh., I, p. 2001.

FAP24 (1996) 'Morphological processes in the Jamuna River', Special Report No. 24, River Survey Project, Prepared for Water Resources Planning Organization (WARPO), Dhaka, Bangladesh.

Garg, S. K. (2005) 'Irrigation Engineering & Hydraulic Structures'. 19th edn. Khanna Publishers. doi: 10.15713/ins.mmj.3.

Goodell, C, Warren, C. (2006) 'Flood Inundation Mapping using HEC-RAS'.

Haque, A. Z. M. S. (2018) 'Hydrodynamic and Morphological Analysis of New Dhaleswari River Offtake using Mathematical Model'. Bangladesh University of Engineering and Technology.

Hassanzadeh, Y. (2012) 'Hydraulics of Sediment Transport', Hydrodynamics - Theory and

Model, (1984). doi: 10.5772/25982.

Hjulström, F. (1935) 'Studies of the Morphological Activity of Rivers as Illustrated by the River Fyris', PhD Thesis, Geological Institute Upsala.

Hongwei, Z., Xuehua, Z. and Bao'an, Z. (2009) 'System Dynamics Approach to Urban Water Demand Forecasting', Transactions of Tianjin University, 15(1), pp. 70–74. doi: 10.1007/s12209.

Hoque Mollah, T. and Ferdaush, J. (2015) 'Riverbank Erosion, Population Migration and Rural Vulnerability in Bangladesh (A Case Study on Kazipur Upazila at Sirajgonj District)', Environment and Ecology Research, 3(5), pp. 125–131. doi: 10.13189/eer.2015.030502.

Ivanova, O. and Ivanov, M. (2016) '1-D Mathematical Modelling of Flood Wave Propagation', 53, pp. 139–144. doi: 10.3303/CET1653024.

Kolmogorov, A. N. (1942) 'Equations of turbulent motion of an incompressible fluid', IZV Akad. Nauk. USSR, Ser. Phys., 6, pp. 56–58.

Lesser, G. R. *et al.* (2004) 'Development and validation of a three-dimensional morphological model', Coastal Engineering, 51(8-9), pp. 883–915. doi: 10.1016/j.coastaleng.2004.07.014.

Manual, D.-F. U. (2013) 'Simulation of multi-dimensional hydrodynamic flows and transport phenomena, including sediments', 3.15.30932.

Matin, D. M. A. (2016) 'An overview of River Bank Protection in Bangladesh'. Bangladesh University of Engineering and Technology.

Matsuda, I. (2004) 'River Morphology And Channel Processes', Encyclopedia of Life Support Systems (EOLSS), p. 12.

Morianou, G. G. *et al.* (2015) '2D Simulation of Water Depth and Flow Velocity using the MIKE 21C Model', in, pp. 3–5.

Moriasi, D. N. *et al.* (2007) 'Model Evaluation Guidelines for Systematic Quantification of Accuracy in Watershed Simulations', American Society of Agricultural and Biological Engineers, 50(3), pp. 885–900.

Mosselman, E. (2006) 'Bank protection and river training along the braided Brahmaputra-Jamuna River, Bangladesh.', Braided Rivers: Process, deposits, ecology and management. Special

Publication No. 36 of the International Association of Sedimentologists., pp. 278–287. doi: 10.1002/9781444304374.ch13.

Musfequzzaman, M. (2012) ‘Study of Hydro-Morphological Impact of Dredging in Selected Reach of the River Jamuna using Two-Dimensional Morphological Model’, MSc. Engg. Thesis, Department of Water Resources Engineering, BUET, Dhaka, T-261(July).

Nicholas, A. P. (2013) ‘Modelling the continuum of river channel patterns’, *Earth Surface Processes and Landforms*, 38(10), pp. 1187–1196. doi: 10.1002/esp.3431.

Noor, F. (2013) ‘Morphological Study of Old Brahmaputra Offtake using Two-Dimensional Mathematical Model’. Bangladesh University of Engineering and Technology, Dhaka.

Pal, P. K., Rahman, A. and Yunus, A. (2017) ‘A Study on Seasonal Variation of Hydro-Morphodynamic Parameters of Jamuna River’, 6(6), pp. 307–311.

Prandtl, L. (1945) ‘Uber ein neues formelsystem fur die ausgebildete turbulenz (On a new formation for fully developed turbulence)’, Report of Academy of Sciences, Gottingen, Germany, pp. 6–19.

Rahman, M., Mahmud, F. and Uddin, M. N. (2012) ‘Effect of Sand Bars on Failure of Bank Protection Work along Large Sand Bed Braided River Key words’, 6th International Conference on Scour and Erosion, 6, pp. 469–476.

Richardson, E. V., Stevens, M. A., Simons, D. B. (1975) ‘The design of spurs for river training’, in 16th IAHR Congress, São Paulo, Brazil, pp. 382–388.

Roy, B. (2015) ‘A Study on Hydrodynamic and Morphological Behavior of Padma River using Delft3D model’, BSc. Engg. Thesis, Department of Water Resources Engineering, BUET, Dhaka, T-759(September).

Saleh I.Khassaf, Awad, A. M. (2015) ‘Mathematical Modeling of Unsteady Flow for AL- Kahlaa Regulator River’, 05(02), pp. 9–20.

Schiavi, E.Flower, A.C., Diaz, J. I., Munoz, A. I. (2008) ‘Mathematical Analysis of a Model of River Channel Formation’, 165, pp. 1–20. doi: 10.1007/s00024-004-0394-3.

Schumm, S. A. (1969) ‘River Metamorphosis’, *Journal of the Hydraulic Division, Proc. of the*

ASCE, 95(HY1), pp. 255–273.

Schumm, S. A. (1985) ‘Patterns of alluvial rivers’, *Annual Review of Earth and Planetary Sciences*, 13, pp. 5–27.

Schuurman, F., Kleinhans, M. G. and Middelkoop, H. (2016) ‘Network response to disturbances in large sand-bed braided rivers’, *Earth Surface Dynamics*, 4(1), pp. 25–45. doi: 10.5194/esurf-4-25-2016.

Timbadiya, P. V, Patel, P. L. and Porey, P. D. (2011) ‘Calibration of HEC-RAS Model on Prediction of Flood for Lower Tapi River , India’, 3(November), pp. 805–811. doi: 10.4236/jwarp.2011.311090.

Uddin, M. N. and Rahman, M. (2012) ‘Flow Processes into the Scour Hole around the Bank Protection Works’, 1(3).

Urmi Laz, O. and Navera, U. K. (2018) ‘Application of Delft3D Mathematical Model in the Jamuna River for Two-Dimensional Simulation’, in 4th International Conference on Civil Engineering for Sustainable Development (ICCESD 2018), pp. 1–7.

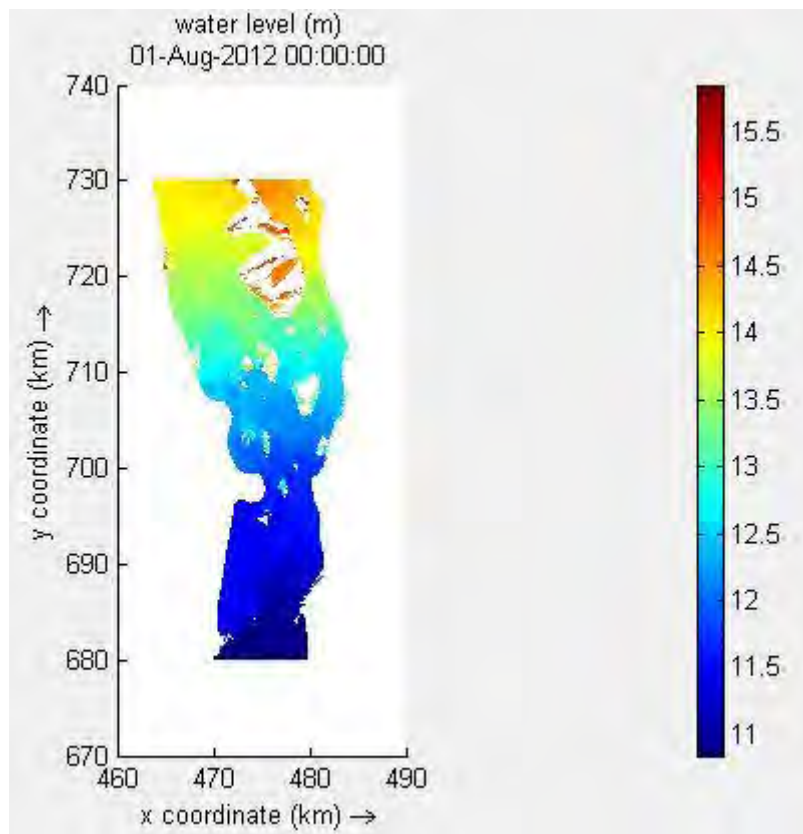
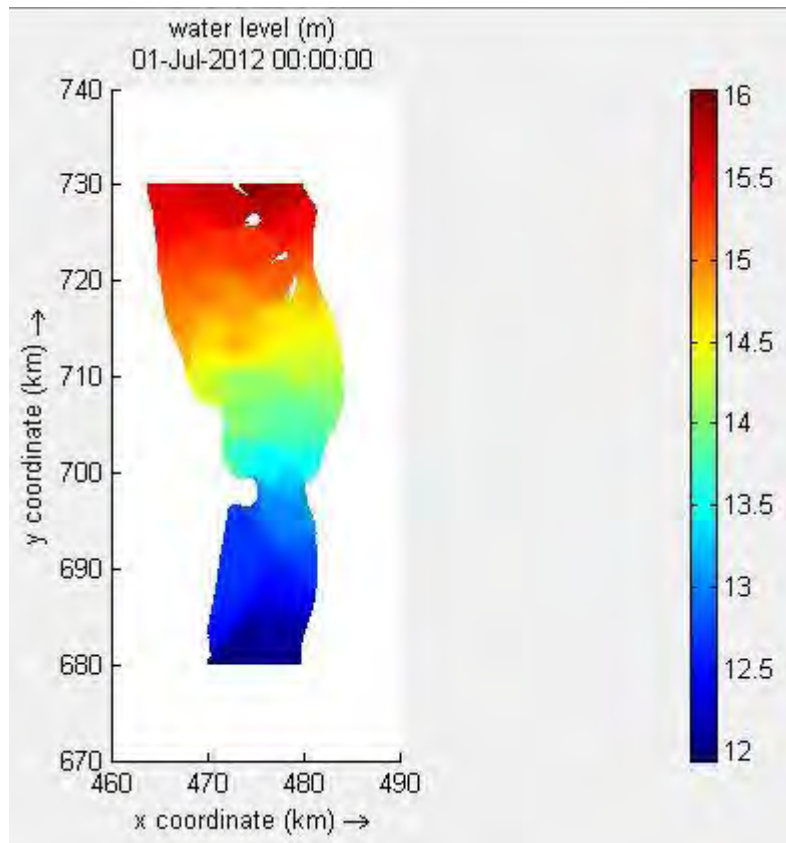
Urmilaz, O. (2012) ‘Morphological Assessment of a Selected Reach of Jamuna River by using Delft3D Model’, MSc. Engg. Thesis, Department of Water Resources Engineering, BUET, Dhaka, T-269(December).

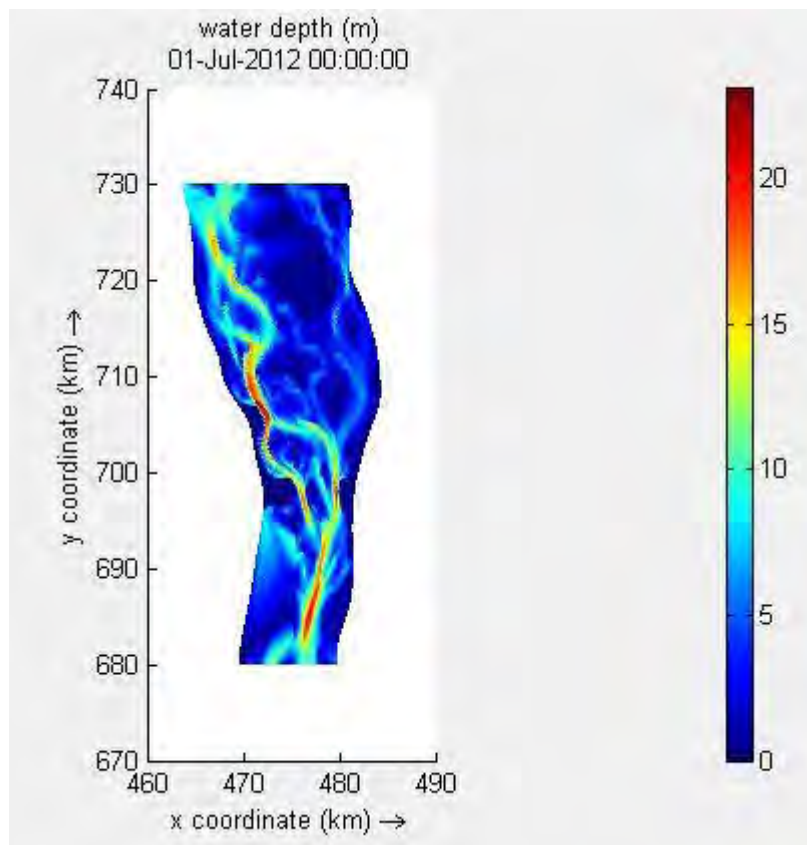
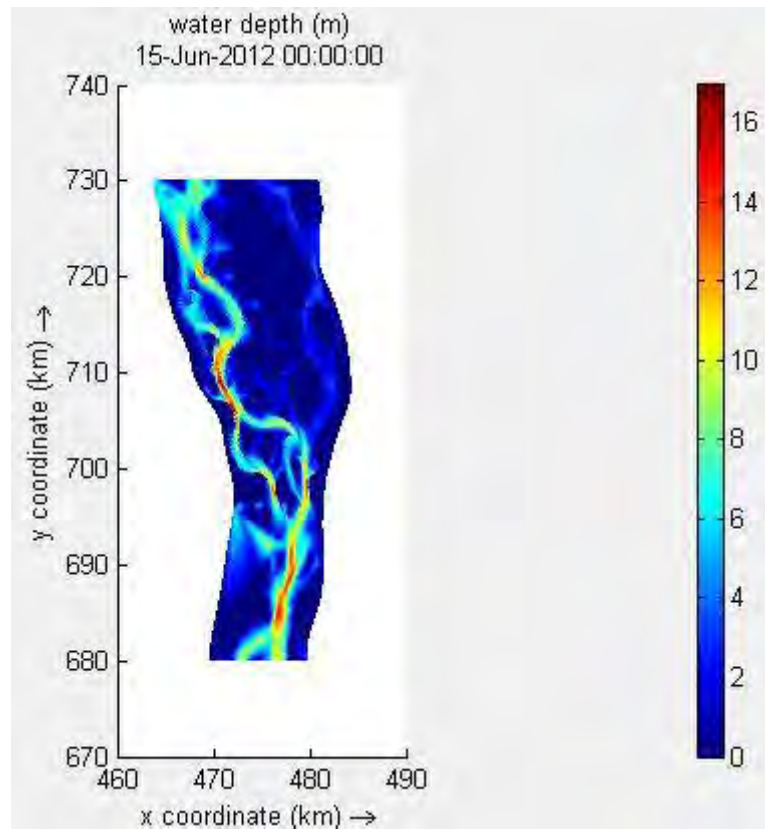
Yang, H., Lin, B. and Zhou, J. (2015) ‘Physics-based numerical modelling of large braided rivers dominated by suspended sediment’, *Hydrological Processes*, 29(8), pp. 1925–1941. doi: 10.1002/hyp.10314.

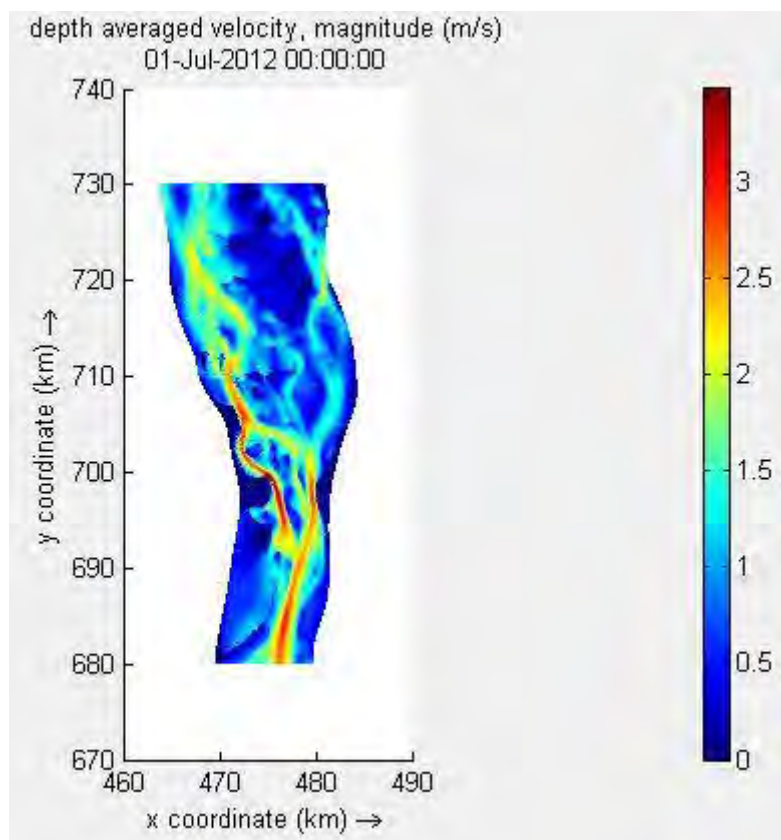
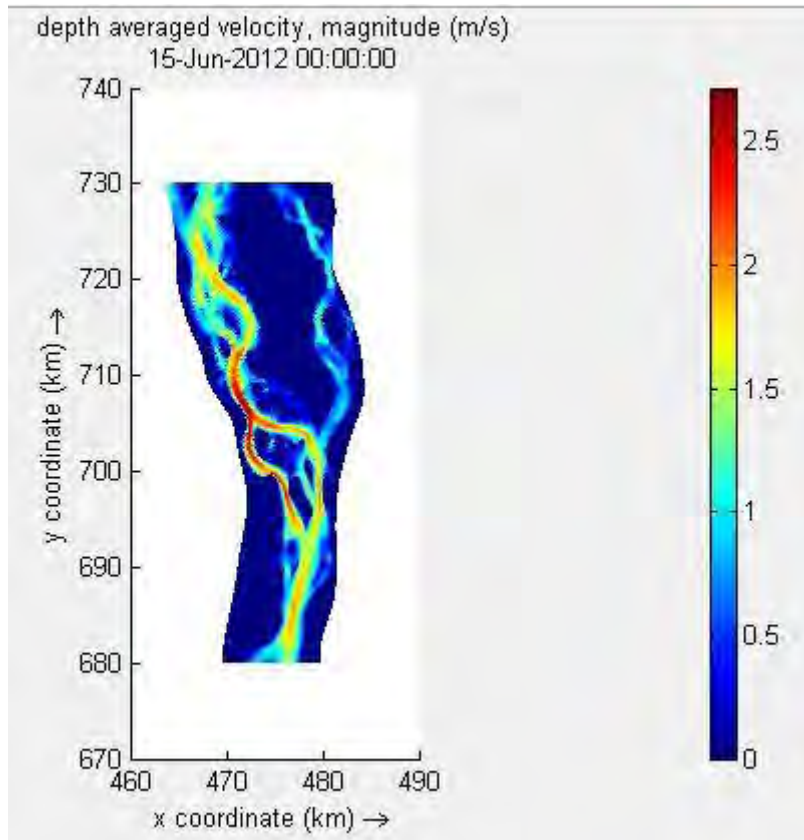
Zijl, F. (2002) ‘On the effect of non-hydrostatic simulation on buoyant jets’. Delft University of Technology.

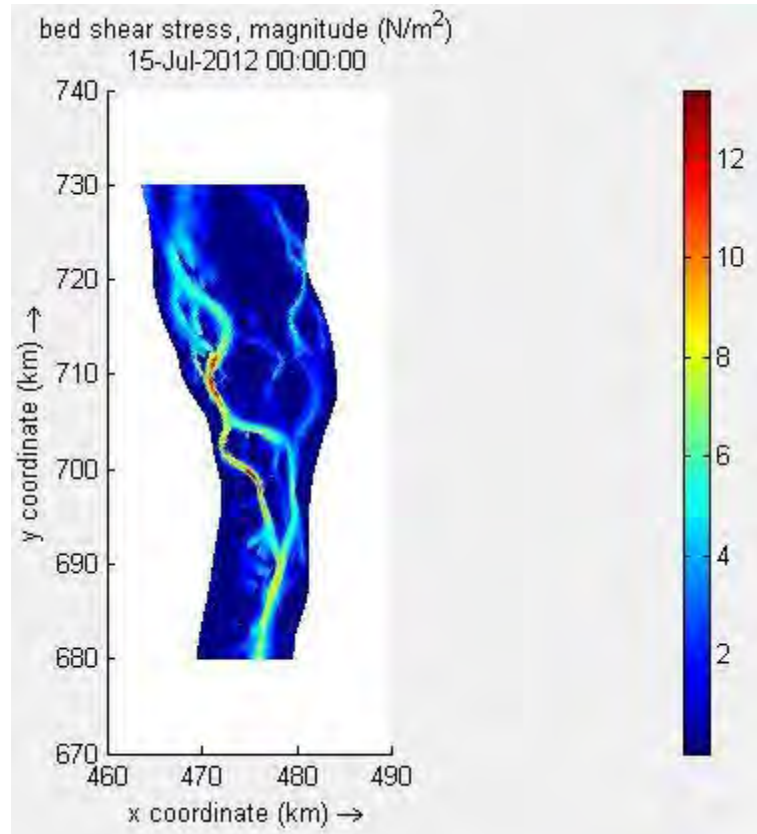
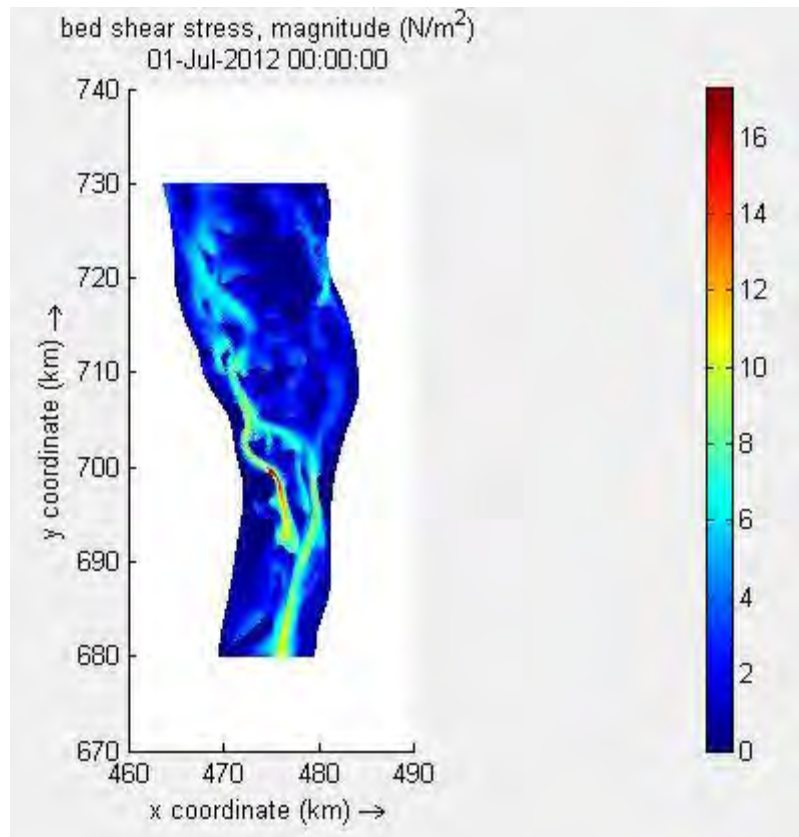
APPENDIX-A

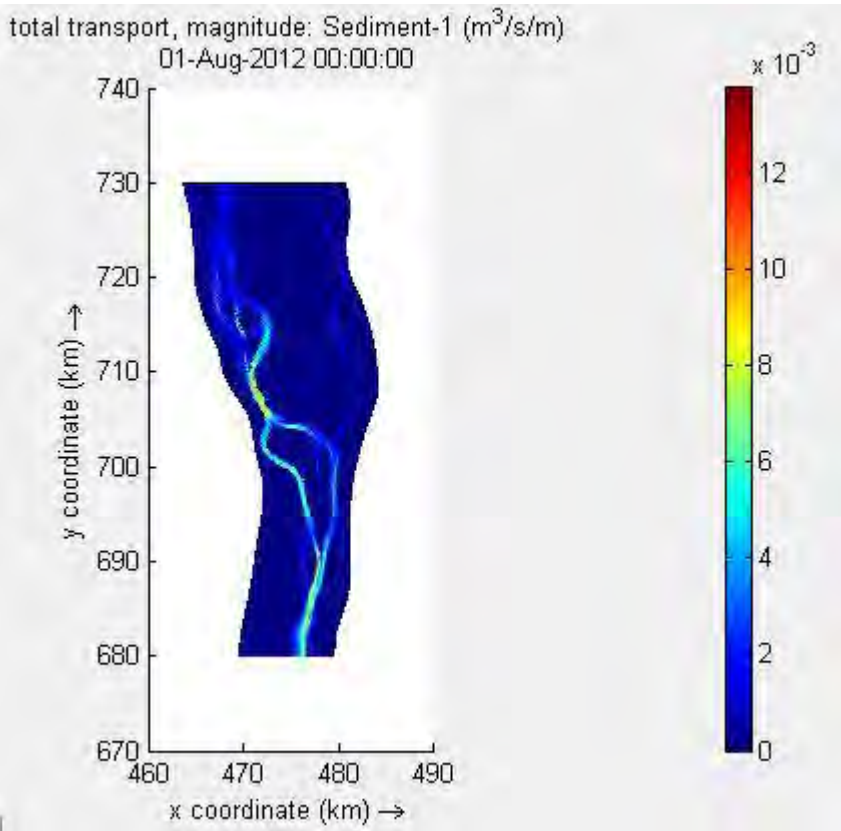
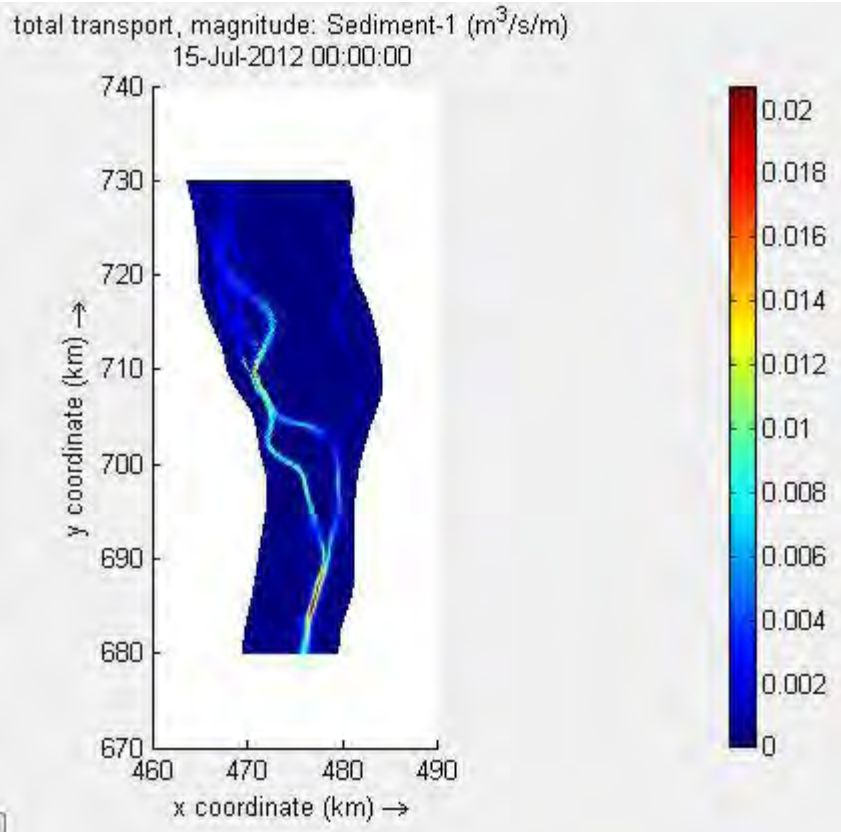
Model output for different parameters

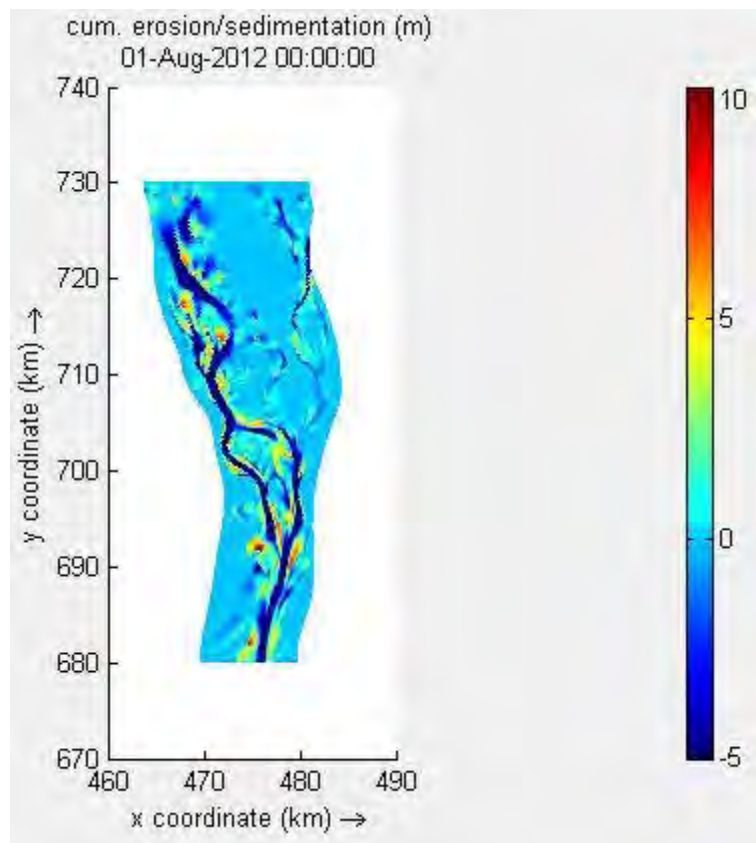
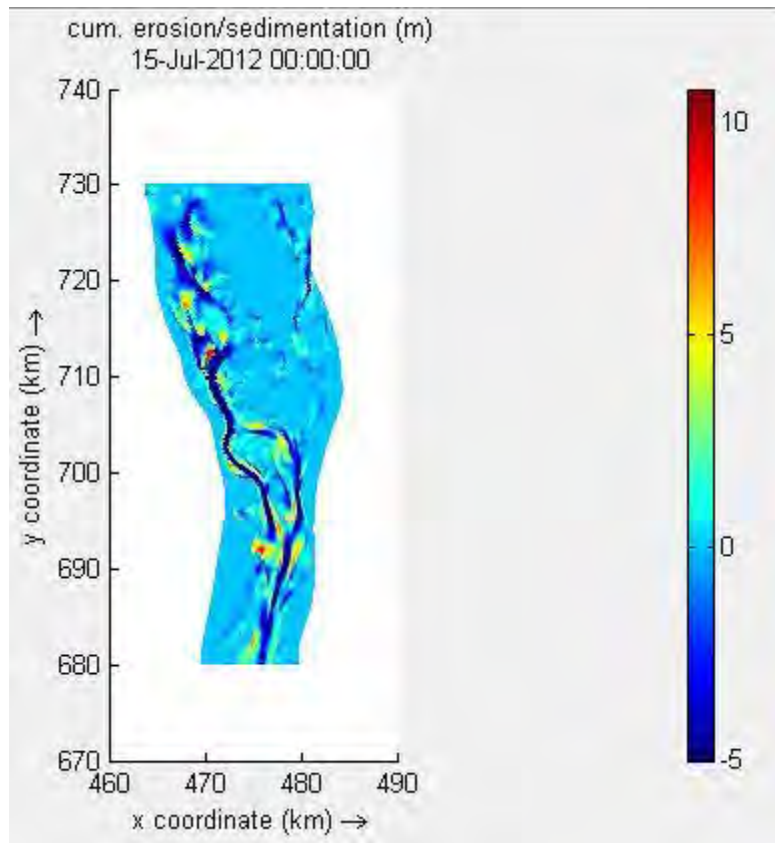






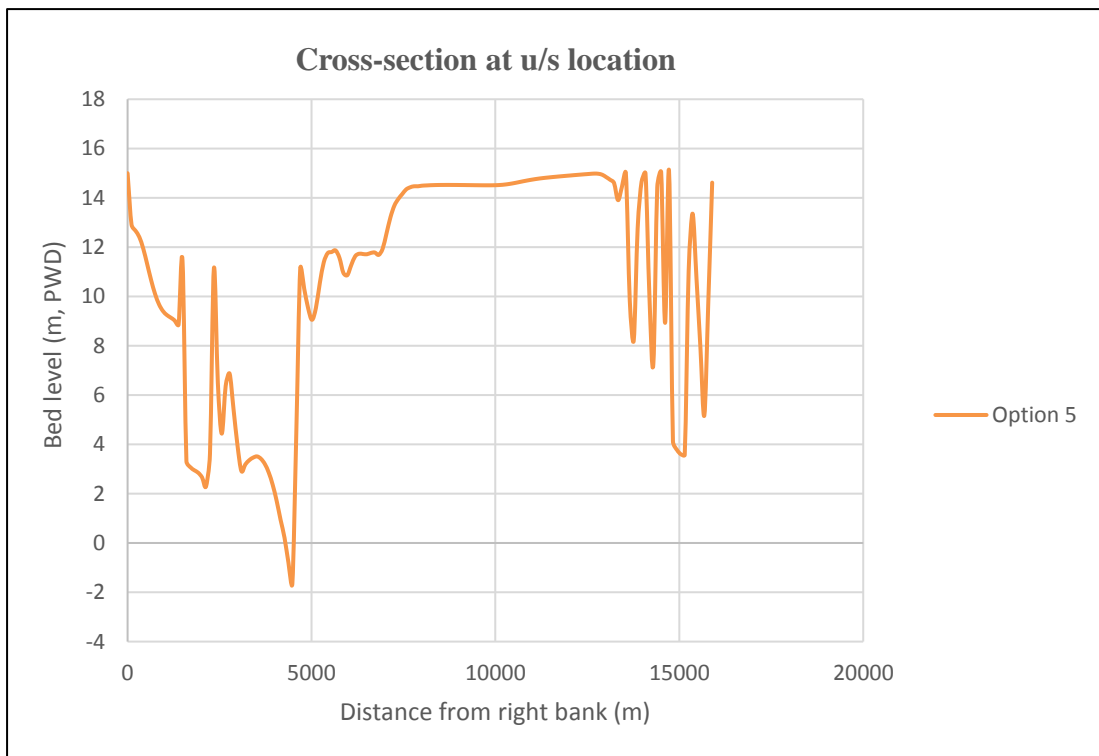


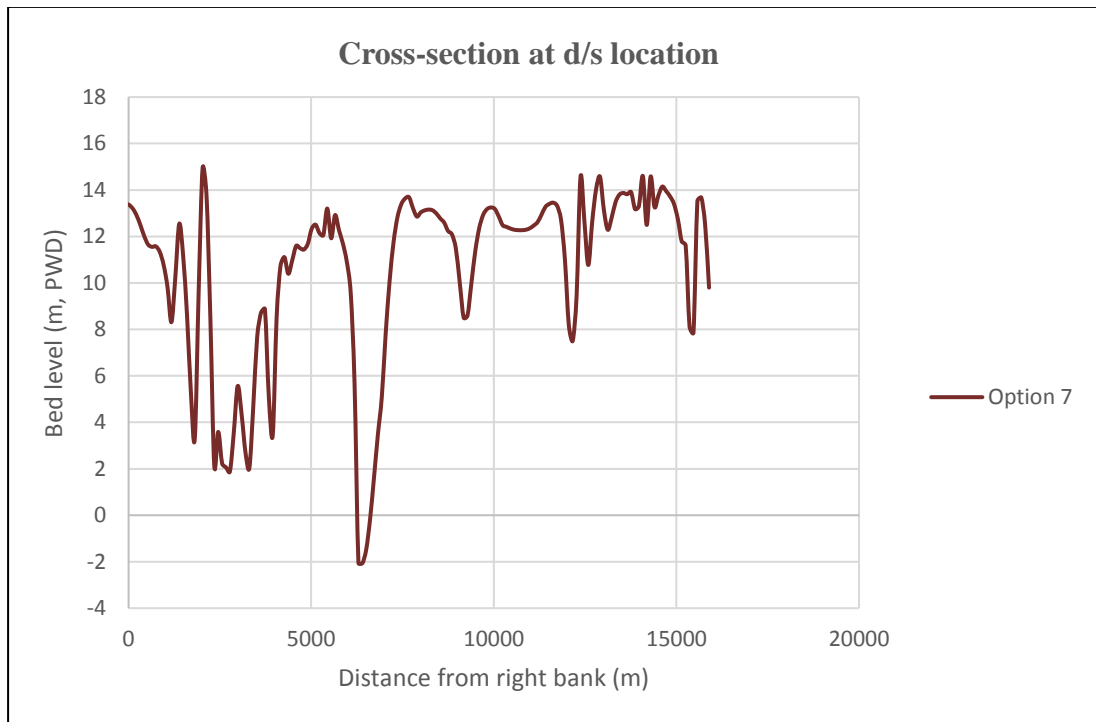


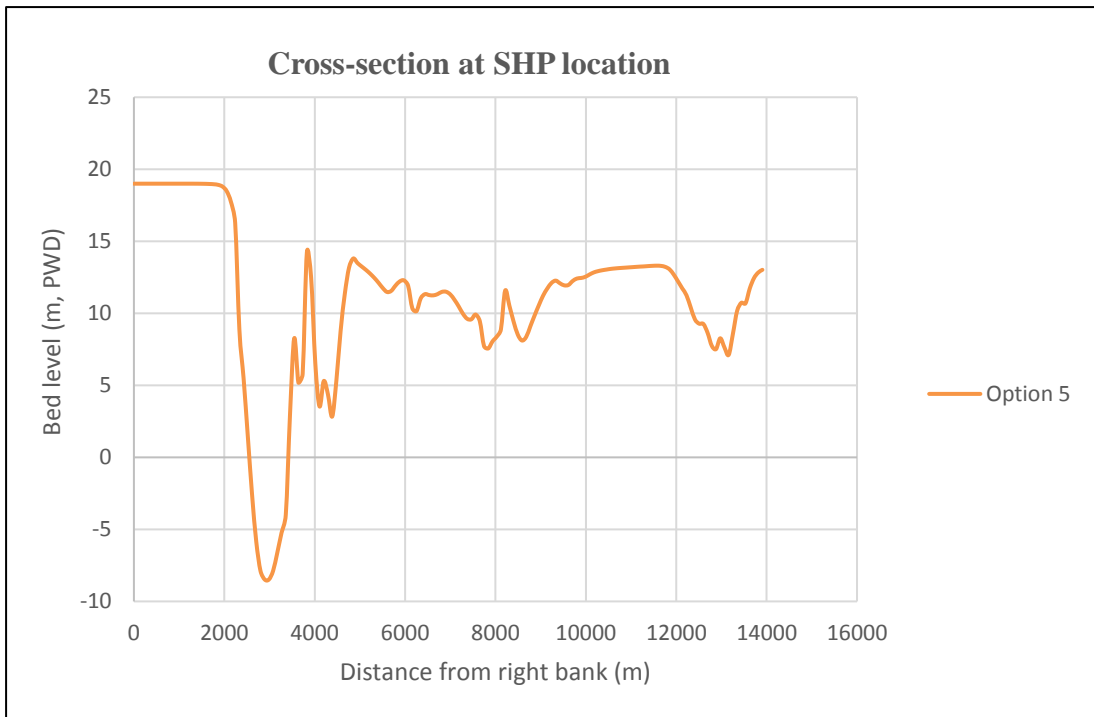
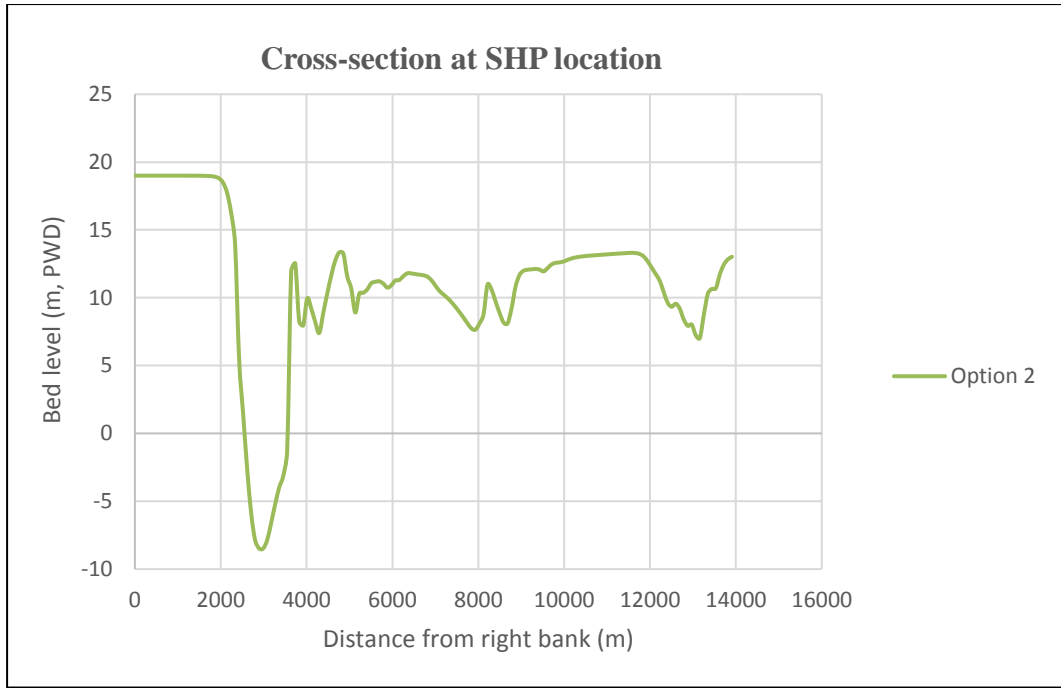


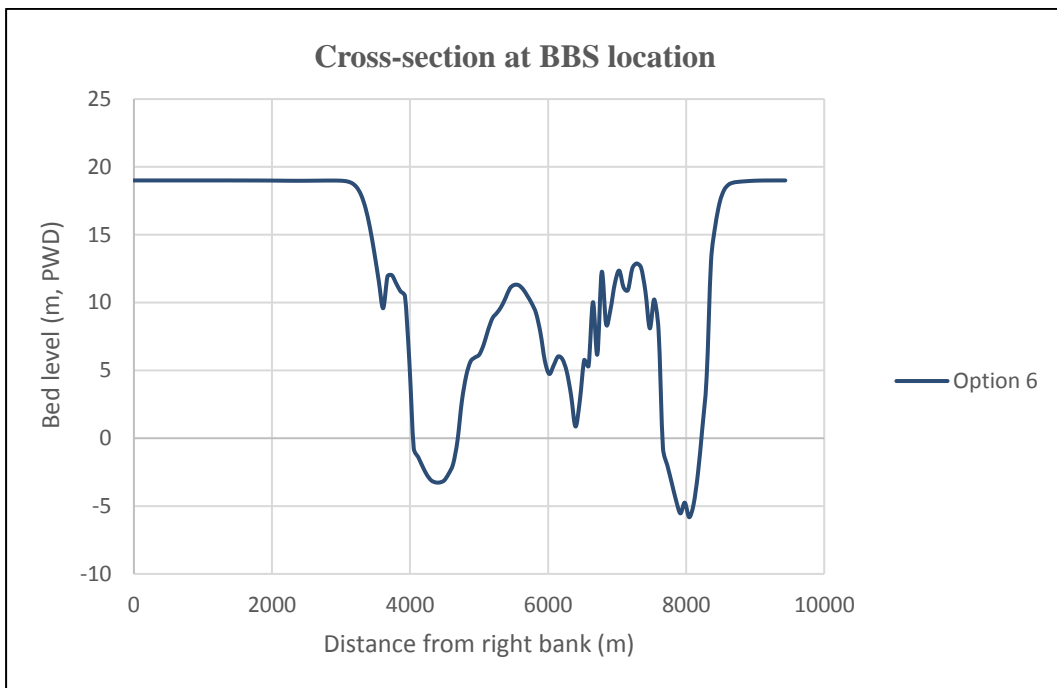
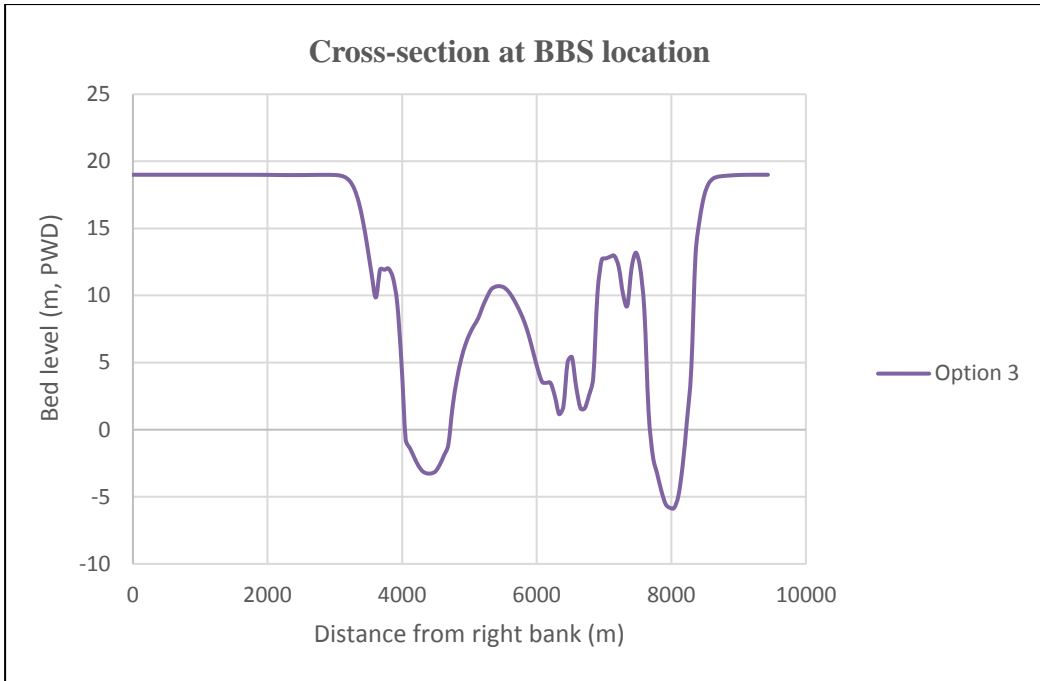
APPENDIX-B

Model simulated cross-sections at different locations









APPENDIX-C

Model output in tabular forms for various option simulations

For option 1 at 1st July

Parameters	SHP	BBS	1u/s	1nose	1d/s
Water level (m)	13.98	12.99	14.97	14.8	14.75
Depth average velocity (m/s)	2.55	3.01	1.09	2.08	2.03
Depth average discharge (m ³ /s)	3550.77	2293.74	108.12	2560.05	2578.76
Instantaneous discharge (m ³ /s)	76658.65				
Bed shear stress (N/m ²)	7.32	12.72	2.09	5.83	5.75
Bed level (m)	-8.48	0.49	8.7	0.74	2.85
Cum. Erosion/sedimentation (m)	-6	-6	1.54	-4.99	-3.78

For option 2 at 1st July

Parameters	SHP	BBS	1u/s	1nose	1st middle	2u/s	2nose	2d/s
Water level (m)	13.99	12.89	15.13	15.08	15.02	15.02	14.99	14.97
Depth average velocity (m/s)	3.31	2.38	0.97	1.7	0.02	0.51	1.97	1.26
Depth average discharge (m ³ /s)	4739.8	259.79	867.19	2945.26	16.79	194.27	2874.63	1050.81
Instantaneous discharge (m ³ /s)	76616.64							
Bed shear stress (N/m ²)	12.36	15.62	1.61	3.76	0	0.57	5.21	2.55
Bed level (m)	-8.48	10.79	7.13	0.66	7.7	9.97	1.68	6.96
Cum. Erosion/sedimentation (m)	-6	5.7	-1.16	-4.95	0.01	4.25	-6	0.76

For option 3 at 1st July

Parameters	SHP	BBS	1u/s	1nose	1d/s	1st middle	2u/s	2nose	2d/s
Water level (m)	14.01	12.89	15.02	15.01	14.94	14.95	14.94	14.91	14.87
Depth average velocity (m/s)	3.16	1.01	1.25	1.68	0.12	0.04	0.62	1.47	0.39
Depth average discharge (m ³ /s)	4534.51	117.2	451	2638.6	36.65	14.92	147	1130.73	191.38
Instantaneous discharge (m ³ /s)	76726.77								
Bed shear stress (N/m ²)	11.27	3.1	3.56	3.82	0.04	0	0.93	3.07	0.3
Bed level (m)	-8.48	10.64	11.69	1.88	10.01	11.25	12.65	3.5	9.73
Cum. Erosion/sedimentation (m)	-6	6.15	3.41	-3.74	3.11	4.76	6.43	-0.55	2.29

For option 4 at 1st July

Parameters	SHP	BBS	1u/s	1nose	1st middle	2u/s	2nose	2d/s
Water level (m)	14.07	12.99	15.14	15.1	15.03	14.97	14.86	14.78
Depth average velocity (m/s)	2.85	2.37	0.65	1.77	0.37	1	2.01	1.69
Depth average discharge (m ³ /s)	4104.22	1134.72	901.43	3096.38	165.05	314.89	2683.4	1945.54
Instantaneous discharge (m ³ /s)	76846.41	76846.41						
Bed shear stress (N/m ²)	9.48	9.46	0.6	4.09	0.25	0.26	5.1	3.96
Bed level (m)	-8.48	3.29	3.47	0.62	10.06	10.06	1.14	2.61
Cum. Erosion/sedimentation (m)	-6	-2.1	-6	-6	3.13	3.13	-6	-6

For option 5 at 1st July

Parameters	Water level (m)	Depth average velocity (m/s)	Depth average discharge (m ³ /s)	Bed shear stress (N/m ²)	Bed level (m)	Cum. Erosion/ sedimentation (m)
SHP	14.14	2.93	4230.24	9.65	-8.48	-6
BBS	12.87	1.16	91.9	5.14	11.39	5.9
1u/s	15.07	1.24	649.49	3.61	11.12	4.13
1nose	15.07	1.25	1637.58	2.26	3.21	-4.2
1d/s	15	0.41	564.7	0.24	2.84	-4.82
1st middle	15	0.01	5.07	0	7.75	0
2u/s	15	0.69	219.33	1.08	12.13	4.62
2nose	14.96	1.96	3164.15	5.04	0.87	-6
2d/s	14.96	0.73	234.65	1.19	11.95	6.27
2nd middle	14.94	0.06	39.24	0.01	8.75	0.66
3u/s	14.92	0.8	128.64	1.79	13.32	6.85
3nose	14.88	1.82	2404.67	4.81	1.7	-2.96
3d/s	14.83	0.24	93.18	0.12	10.73	2.81

For option 6 at 1st July

Locations	Water level (m)	Depth average velocity (m/s)	Depth average discharge (m ³ /s)	Bed shear stress (N/m ²)	Bed level (m)	Cum. Erosion/ sedimentation (m)
SHP	14.04	3.05	4396.23	10.56	-8.48	-6.6
BBS	13.02	1.96	491.96	8.17	8.41	2.92
1u/s	15.13	1.14	500.46	2.66	11.23	3.65
1nose	15.07	1.86	2659.77	4.84	3.05	-4.99
1d/s	15.02	-0.08	58.75	-0.02	2.78	-4.51
1st middle	15.01	-0.08	21.53	-0.01	10.36	3.28
2u/s	15.02	-0.56	328.83	-0.58	9.49	3.25
2nose	14.96	1.87	2965.6	4.56	-0.67	-6
2d/s	14.97	1.49	1107	2.2	5.96	0.04
2nd middle	14.97	1.08	377.64	2.43	11.34	2.03
3u/s	14.91	1.02	302.32	2.27	11.66	2.47
3nose	14.85	1.83	1876.98	4.77	3.7	-4.56
3d/s	14.76	1.43	385.42	2.6	10.79	-0.78

For option 7 at 1st July

Parameters	Water level (m)	Depth average velocity (m/s)	Depth average discharge (m³/s)	Bed shear stress (N/m²)	Bed level (m)	Cum. Erosion/ sedimentation (m)
SHP	14.23	2.77	4009.32	8.73	-8.48	-6
BBS	13	2.94	1933.18	13.16	0.49	-6
1u/s	15.34	1.24	930.81	2.69	9.04	0
1nose	15.25	1.93	3038.47	5.05	2.53	-6
1d/s	15.18	0.21	124.56	0.09	10.7	1.49
1st middle	15.18	0.01	6.95	0	10.55	0.12
2u/s	15.15	1.16	1394.7	1.96	4.32	-2.79
2nose	15.02	2.32	3559.53	7.1	1.23	-6
2d/s	14.97	1.16	913.03	2.26	7.61	1.68
2nd middle	14.96	0.23	219.57	0.09	4.24	-4.29
3u/s	14.96	0.79	455.87	1.08	8.22	-2
3nose	18.41	2.26	2411.68	7.79	3.46	-6
3d/s	14.77	0.82	94.22	1.9	13.25	1.93